Aus dem Institut für Humangenetik

der Universität Würzburg

Vorstand: Professor Dr. med. Thomas Haaf

The effects of paternal age on DNA methylation of developmentally important genes in human and bovine sperm

Inauguraldissertation

zur Erlangung der Doktorwürde der

Medizinischen Fakultät

der

Julius-Maximilians-Universität Würzburg

vorgelegt von

Andreas Prell

aus Marburg

Würzburg, August 2023

Referent: Prof. Dr. Thomas Haaf

Korreferentin: Prof. Dr. Helga Stopper

Dekan: Prof. Dr. Matthias Frosch

Tag der mündlichen Prüfung: 20.12.2023

Der Promovend ist Arzt.

Table of contents

1 Introduction 1

1.1 Epigenetic key modifications 4

1.2 DNA methylation 5

1.2.1 Basic principles 5

1.2.2 Establishment and erasure 5

1.2.3 Biological functions 7

1.3 Crosstalk of epigenetic mechanisms 9

1.4 Epigenetic reprogramming 9

1.5 Male ageing 10

1.6 Transgenerational epigenetic inheritance 12

1.7 Genes of interest 14

1.8 Aims of this study 19

2 Material and Methods 20

2.1 Material 20

2.1.1 Ethics approval and consent 20

2.1.2 Reagents and equipment 20

2.1.3 Human sperm samples for pyrosequencing 22

2.1.4 Human foetal cord blood (FCB) samples 22

2.1.5 Human sperm samples for genotyping 23

2.1.6 Human sperm samples for Bisulphite Sequencing 23

2.1.7 Bovine sperm samples 24

2.2 Methods 24

2.2.1 Sperm Purification 24

2.2.2 Sperm DNA isolation 25

2.2.3 Blood DNA isolation 25

2.2.4 Bisulphite conversion 26

2.2.5 Sample amplification 27

2.2.6 Gel visualisation 28

2.2.7 DNA quantification 28

2.2.8 Bisulphite-converted Pyrosequencing 29

2.2.9 Deep Bisulphite Sequencing (DBS) 34

2.2.10 Data processing and analysis 39

3 Results 41
3.1 Pyrosequencing results of 10 human and 4 bovine candidate loci 41
3.2 Comparison of conserved CpG sites between human and bovine sperm 46
3.2.1 Identification of conserved CpG sites between human and bovine sperm 46
3.2.2 Comparison of human and bovine sperm methylation in conserved regions 48
3.2.3 Age effects on human and bovine sperm methylation in conserved regions 49
3.3 Transgenerational epigenetic inheritance 51
3.3.1 Genotyping results of FCB samples 52
3.3.2 Methylation levels in FCB 55
3.3.3 Parental influence on FCB DNA methylation 55
3.4 Haplotype-dependent allele specific DNA methylation 57
4 Discussion 58
4.1 Validation of candidate loci via Pyrosequencing 58
4.1.1 Direction of age-associated methylation changes 59
4.1.2 Putative functional consequences of age-associated methylation changes 60
4.2 Species comparison 61
4.2.1 Species-specific DNA methylation levels in conserved regions 62
4.2.2 Species-specific age effects on DNA methylation in conserved regions 63
4.3 DNA methylation on a single allele level 64
4.3.1 Transmission to the next generation 64
4.3.2 Haplotype-dependent DNA methylation 65
4.4 Strengths and limitations 66
4.5 Future perspectives 67
5 Summary 69
6 References 72

1 Introduction

In 1940, the development biologist Conrad H. Waddington was the first to summarize "the interactions of genes with their environment, which bring the phenotype into being" under one common term that we still use today: "Epigenetics". Ever since, the meaning of the term "epigenetic" was repeatedly amended by different authors and is not used uniformly. Generally admitted epigenetic features comprise histone modifications, small regulatory RNAs, and the probably best-studied epigenetic mark and the subject of this study: DNA methylation. In a demographic context, especially the interrelationship between DNA methylation and the ageing process has social and economic relevance: In recent years, a demographic transformation has occurred in several Western countries with social and economic factors such as the achievement of career goals and financial stability postponing family formation and leading to a clear trend of delayed parentage[1]. From a medical point of view, the offspring of elder parents have an increased risk for impaired medical conditions such as diabetes[2], autism[3], schizophrenia[4], and some forms of cancer[5]. However, only a decent fraction of this disease susceptibility can be explained by DNA mutations or single nucleotide polymorphisms. Instead, epigenetic mechanisms including DNA methylation might account for a larger portion of disease susceptibility than initially expected.

To address this issue, especially germ cells appear as an interesting focus of research. Traditionally, impaired medical conditions that originate from advanced parental age were mainly assigned to female senescence. Obviously, the shrinking ovarian reserve and augmenting oocyte aneuploidy rates are made responsible for impaired fertility, miscarriages, and chromosome disorders such as Down syndrome[6]. However, several researchers discovered that the same applies to the developmental potential of sperm from ageing men. Contrary to popular opinion, the sperm does not only deliver the paternal DNA, but also impinges on the development potential and disease susceptibility of the resulting offspring through its methylation pattern[7-9]. Obviously, the sperm epigenome as the ultimate result of the male germline reprogramming process is exposed to a variety of conditions during its formation, including stochastic and environmental terms as well as individual premises such as infertility, paternal diet, and notably paternal age. Indeed, paternal age has a greater influence than maternal age on rare monogenic conditions[10] and

increases the risk for neurodevelopmental disorders such as autism, bipolar disorder, and schizophrenia[11]. This is insofar not surprising as the quantity of spermatogonial cell divisions augments from around 35 times at adolescence to more than 800 times at the age of 50 years[10]. Assuming that the error rate of the copying process to the daughter cells is around 10 to 100-fold higher for the epigenome than for the genome[12], epimutations make up a considerably larger portion of the mutational burden in spermatozoa from elder males than DNA mutations. Some of these age-dependent methylation changes are highly consistent between different individuals and have been extensively studied in the human[8,13,14] and bovine[15,16] sperm methylomes. Numerous epigenetic clocks based on linear regression models have been established to successfully predict age from human sperm methylation data[13,17]. Genetic regions containing CpGs undergoing age-related sperm methylation changes are commonly referred to as age-dependent differentially methylated regions (age-DMRs). In humans, these age-DMRs aggregate nearby genes participating in the regulation of embryogenesis and neuronal development. This suggests that the ageing sperm methylome might influence the offspring's development potential and elevate its life-long risk of disease[13]. Indeed, a few age-DMRs in the paternal sperm have been proven to persist transgenerationally[7,18,19] and might contribute to the development of complex diseases by impairing key epigenetic checkpoints in cell differentiation during embryogenesis[20].

Previous experiments by Bernhardt *et al.* conducted in our lab used a method called reduced representation bisulphite sequencing (RRBS) in human and bovine sperm samples to detect new age-DMRs in the respective species. RRBS is a form of whole genome sequencing that focuses on the fraction of the genome where most of the DNA methylation occurs. Here, they identified more than 1500 age-DMRs in the human epigenome that have already been published as "Age-related methylation changes in the human sperm epigenome". Equipollent results in bovine sperm are assembled in a lab intern candidate list that remains unpublished yet (July 2023).

A primary goal of this study was to use a different methodical approach in an independent cohort to increase the trustworthiness of our RRBS results. We therefore applied Pyrosequencing to target several age-DMRs in developmentally important genes from our human and bovine sperm RRBS studies. Selection of the candidate genes relied on

the location of the CpG sites in regulatory units (Promoter, CTCF binding), the p-value in RRBS, the presence of a SNP, and evolutionary conservation between humans and bulls.

Notably, for most of the highly selected target CpGs of different epigenetic clocks, it remains an enigma whether they are a mere epiphenomenon or if they exercise a functional role in the ageing process[21]. To fathom this issue, we investigated in a second experiment, whether the observed paternal age effect on DNA methylation has been evolutionarily conserved at orthologous CpG sites in bovine and human sperm. Suchlike findings have been reported for repetitive elements such as 28s and 18s rDNA that display a positive correlation between the donor's age and the level of sperm DNA methylation in several different mammalian species[22]. If the same effect also exists in single-copy genes, this finding will emphasize the role of DNA methylation as part of a preserved epigenetic hallmark. In this case, filtering for age-related epigenetic markers in the same direction in two or more species could increase the power of identifying genes, pathways, and potential common mechanisms susceptible to paternal ageing. If not, age-DMRs could represent a species-specific response to different environmental factors as part of the initiation and maintenance of species boundaries over an evolutionary period[23]. We therefore used Pyrosequencing to decipher whether CpGs that were subject to a paternal age effect in one species also showed a paternal age effect at evolutionarily conserved CpG sites in the sperm epigenome of the other species.

Finally, we used Deep Bisulphite Sequencing in human foetal cord blood (FCB) samples to investigate whether there is any transgenerational transmittance for some of these epigenetic marks from the paternal sperm to the offspring's somatic epigenome, providing a direct mechanism between the paternal age and impaired health conditions in the offspring.

1.1 Epigenetic key modifications

Epigenetic modifications comprise regulatory RNAs, histone modifications, as well as DNA methylation. All these epigenetic marks work in a complex interplay and shall therefore be delineated shortly. A separate chapter is devoted to DNA methylation, as it is the most prominent epigenetic modification in this study and is therefore discussed in a more detailed manner.

Regulatory non-coding RNAs

Not less than 75% of the human genome is transcribed into RNA, still, protein-coding sequences make up not more than 3% of the entire human genome[24]. Small RNAs are a group of non-coding RNAs (ncRNAs) that extend to 17–22 nucleotides in length. Among others, they comprise the well-known microRNA (miRNA), small nuclear RNA (snRNA), and small interfering-RNA (siRNA)[25]. These ncRNAs are not translated into proteins but regulate gene expression and control several biological functions by post-transcriptional gene silencing (siRNA), recruitment of chromatin-modifying complexes, alteration of chromatin conformation (siRNA and miRNA), and degradation of specific mRNAs (miRNA)[26]. Evidence insinuates that at least one-third of all biological processes are controlled by miRNAs[27] including the implication of ncRNAs in the development of several types of cancer[28,29].

Histones

Histone modifications, DNA methylation, and microRNAs work in a complex interplay to regulate transcription activity. The eukaryotic DNA is tightly packaged with histone proteins that allow the widespread DNA strands to fit into the narrow nuclear compartment. Therefore, several histone proteins, two each of H2A, H2B, H3, and H4, aggregate to build up the basic unit of chromatin in the form of an octamer. The specific amino acids are post-translationally modified by chemical reactions that include methylation, acetylation, citrullination, ubiquitination, and phosphorylation[30] among many others. These modifications determine how the DNA strands are packaged and regulate transcription activity by either facilitating or precluding access for transcription factors and polymerases to the DNA. Histone modifications that lead to a rather loose chromatin structure, such as acetylation generally promote transcription, whereas histone

modifications such as deacetylation compress the DNA structure and reduce transcription activity.

1.2 DNA methylation

1.2.1 Basic principles

DNA methylation describes the addition of a methyl group to the fifth position (C-5) of the cytosine ring[31]. In humans, DNA methylation is restricted to a CpG dinucleotide context[32]. These CG dinucleotides do not appear haphazardly across the entire human genome but agglomerate in so-called CpG islands (CGIs)[33]. Although the term "CpG island" is not uniformly used, it is generally considered a region with a length greater than approximately 200 bp, and a CG content greater than expected compared to the entire human genome[34,35]. Excluding repetitive sequences, the number of CpG islands in the human genome amounts to approximately 25,000 CpG islands[34]. About 50% of them are embedded in gene promoters. Conversely, more than two-thirds of all gene promoters collocate with a CGI[36], turning it into the most frequent promoter type in the human genome[37]. CpG islands are predominantly unmethylated in somatic tissues, only 10% of the CpG islands are methylated.

Interestingly, CpG nucleotides occur at only a minor fraction of the expected frequency of 4.41% by multiplying the fraction of cytosines and guanines (0.21×0.21). This phenomenon is named CG suppression[34] and can be explained as follows: Spontaneous deamination of unmethylated Cytosine results in uracil residues, a mutation that is pinpointed and repaired by the base excision repair (BER) machinery of the cell. In contrast, when methylated CpGs undergo the equipollent deamination reaction, T residues are formed that are generally not recognized by cellular repair mechanisms.

1.2.2 Establishment and erasure

Maintenance and establishment of DNA methylation patterns are implemented by members of a whole family of enzymes that are referred to as DNA methyltransferases (Dnmts). In humans, the DNMT family comprises four members that fall into three groups: the maintenance methyltransferase DNMT1, the de novo methyltransferases DNMT3A, DNMT3B, and the regulatory DNMT3L[38-40]. These enzymes catalyze the addition of a methyl group from *S*-Adenosyl methionine (SAM) to the cytosine ring, resulting in 5-Methylcytosine (5mC). Despite their structural resemblance, they have

different expression patterns and perform distinct functions[41,42]. DNMT1 preserves preexistent methylation marks in emerging daughter cells during replication by identifying hemi-methylated DNA and then translating the methylation pattern to the newly synthesized DNA strand[43,44]. Unlike DNMT1, DNMT3A and DNMT3B have a higher affinity for unmethylated CpGs[45] and are in charge of *de novo* DNA methylation during early embryonic development[46]. DNMT3L lacks proper catalytic activity but increases the affinity of the *de novo* methyltransferases to S-Adenosyl methionine (SAM)[47,48]. Cooperation among different DNMTs is for example essential during the methylation of repetitive elements[49].

Although several different biochemical reactions have been proposed to reverse 5mC to its unmodified state, the exact process of DNA demethylation is still controversial. Two principal strategies have been suggested that can be divided into either passive or active:

Passive: Inhibition of the active Dnmt1 during cell replication permits the newly synthesized strand to remain unmethylated. The global methylation level is thereby passively reduced after each cell division cycle.

Active: In contrast, active DNA demethylation is achieved by a variety of successive enzymatic reactions that revert 5mC to a blank cytosine[50,51]. 5mC is susceptible to chemical modifications from both, the amine as well as the methyl sites. Hence, two main mechanisms of successive demethylation have been proposed: Modification of the amine group by the activation-induced cytidine deaminase/apolipoprotein B mRNA-editing enzyme complex (AID/APOBEC) results in a guanine-thymine mismatch that is spotted and repaired by the base excision repair (BER) pathway[52]. Another possible active DNA demethylation mechanism is implemented by the ten-eleven translocation (Tet) enzymes. They catalyze a series of biochemical modifications of 5mC. 5mC is oxidized to 5-Hydroxymethylcytosine (5hmC)[53] and processed in stepwise oxidation to 5-formyl-cytosine (5fC) and further to 5-carboxy-cytosine (5caC)[53,54]. Finally, thymine DNA glycosylase (TDG) mediates the removal of the modified residue through the BER pathway, and the apyrimidinic site is filled with a naked cytosine[53,55,56].

If 5hmC, 5fC, and 5caC solely function as intermediates in DNA demethylation or if they exert their own functional roles is still controversial. However, several observations emphasize that especially 5hmC is its own epigenetic mark and exerts important functions

in the regulation of DNA demethylation and gene expression. Supporting this idea, it was observed that 5-hmC levels are most abundant in brain tissues, where around 1% of all cytosines are 5-hmC[57,58]. Here, its levels are positively correlated with gene expression[59]. 5hmC is further hypothesized to be a key player in the preservation of pluripotency in embryonic stem cells (ESCs)[60].

1.2.3 Biological functions

Gene expression: The importance of DNA methylation in shaping gene expression is still not entirely unveiled. Generally, it may impinge on transcription in two ways: Principally, the methyl group itself might sterically encumber the docking of transcription factors to the gene[61]. Second, and supposedly more relevant, methylated DNA interacts with proteins exhibiting a methyl-CpG binding domain (MBDs) that recruit auxiliary proteins, including chromatin remodelers such as histone deacetylases. These proteins subsequently modify histones, thereby forming compact, inactive chromatin. Yet, the effect size of DNA methylation on transcription activity hinges very much on the genetic region where it occurs: In the human genome, around 10% of the CpG methylation sites are embedded in gene promoters. Here, DNA methylation keeps transcription factors outside the gene promoters, impedes transcription factor binding, and changes chromatin into a closed structure[62]. Therefore, higher methylation levels in promoters are commonly correlated with lower levels of downstream gene expression[63-65]. For example, cancer-specific hypermethylation of CGIs that reside in promoter regions of certain tumour suppressor genes can stably silence gene expression, and thereby lead to uncontrolled tissue proliferation and tumour growth. Interestingly, DNA methylation in gene bodies appears to exert different functions: In dividing cells, DNA body methylation is positively correlated with gene expression[32,66-68]. Contrarily, in slowly dividing and non-dividing tissues, especially the brain, gene body methylation does not enhance transcription[69] or is even negatively correlated with gene expression[70]. To date, there is no plausible explanation for this putative paradox.

Specific biological functions: DNA methylation does not only act as a regulator of gene expression but also exerts further essential sideline functions in the development of the organism. These key features of epigenetic modifications include X-chromosome inactivation, genomic imprinting, and the silencing of transposable elements. The human genome, for example, comprises three main classes of transposable elements that together

account for more than 45% of the human DNA[49]. These elements are able to change their position within the genome and have the capability to alter gene control in the host organism[71]. If expressed, these elements have putative genotoxic effects, as their insertion can cause genomic rearrangements and DNA mutations[72]. Therefore, most of these elements are stably repressed by DNA methylation[73] or by mutations induced by the deamination of 5mC[74] to repress their harmful potential[49].

Imprinting: Genomic imprinting describes the epigenetic phenomenon of differing allele expression depending on the sex of the transmitting parent (monoallelic expression)[75]. These epigenetically imprinted patterns, including DNA methylation as well as histone modifications undermine the genomic reprogramming events during early embryogenesis. So far, as many as 228 imprinted genes have been reported in humans[76]. A famous theory to explain the origin of imprinting rests upon the parental conflict hypothesis (Haig and Westoby, 1989) suggesting that genomic imprinting emerges from a parental conflict. In this conflict, maternally and paternally expressed genes exert opposing functions during early development because of sexual antagonism. Accordingly, paternally expressed genes would aim to enhance growth by retrieving maternal nutrients to optimize the offspring's development, whereas maternally expressed genes aim to preserve maternal resources for further gestation by limiting foetal growth. The importance of correct imprinting is emphasized by the findings that abnormal imprinting is implicated in a multitude of diseases, such as Wilms tumour[77] or overgrowth disorders such as Beckwith-Wiedemann-Syndrome[78].

X-chromosome inactivation: Another important physiological function of epigenetic modifications is the inactivation of X-chromosomes. This term describes the process of silencing one of the two X-chromosomes by conversion into a transcriptionally inactive structure called Barr body. This process is often referred to as dosage compensation and is indispensable to depleting the potentially toxic effects of double-expressed X-linked genes. The inactivation is mediated by the binding of the non-coding Xist-RNA[79,80] to the randomly selected X-chromosome. This, in collaboration with additional factors, leads to deacetylation of histones and DNA methylation of promoters, turning chromatin into a silent state[81,82].

1.3 Crosstalk of epigenetic mechanisms

To not evoke the impression that the three presented forms of epigenetic modifications stand for themselves and are functionally independent, a prominent example of "epigenetic crosstalk" shall shortly delineate their complex interrelation: Indeed, DNA methylation, histone modifications, and microRNA (miRNA) interplay with each other to regulate transcription. It was already mentioned that proteins endowed with a methyl-binding domain can recruit histone deacetylases to remove activating histone modifications and consequently silence gene transcription. However, not exclusively can DNA methylation be translated into chromatin structure, but the reverse can also occur: Methylation of Lysin (H3K4me) is a well-studied epigenetic mark associated with either high[83] (H3K4me2 and H3K4me3) or low (H3K4me0) gene expression levels[84]. The regulatory Dnmt3L communicates with the N-terminus of histone H3 if H3K4 is unmethylated[85]. This finding indicates that Dnmt3L functions as a sensing element for H3K4 methylation[86]. If the respective site lacks methylation, Dnmt3L itself initiates DNA methylation by recruiting the de novo methyltransferase Dnmt3a[86]. Though, if the histone modification H3K4 trimethylation (H3K4me3) is present, it encumbers the binding of Dnmts to H3 histone tails and in this manner impedes methylation[85,87]. Along with that, a strong negative relationship is observed between DNA methylation and the level of H3K4me in different tissues[88,89]. These findings are interesting insofar as CpG islands contain specifically high levels of H3K4me3 [90]which gives a possible explanation of how CpG islands can be kept in a hypomethylated state[91].

Taken together, the interplay of different epigenetic key players is complex, yet exists. Therefore, when interpreting studies implying only one epigenetic mark, it is essential to consider epigenetic crosstalk to correctly evaluate results and their functional consequences.

1.4 Epigenetic reprogramming

DNA methylation is an essential epigenetic feature that ensures that cells are correctly shaped according to their destined lineages. Still, it also represents a challenge to sexual reproduction, where the development of the embryo occasionally requires a totipotent state of the epigenome[92]. Therefore, DNA methylation undergoes two pivotal waves of

genome-wide reprogramming at different developmental stages: first during gametogenesis and the second during early embryogenesis.

Embryonic cells that are chosen to become germ cells assemble in the embryo's germinal ridge. Here, these cells undergo epigenetic reprogramming in two successive demethylation events: first, passive demethylation leads to a loss of nearly the entire DNA methylation layer by replicative dilution[93] except for X-inactivation-associated marks in females, certain germ cell-related genes, and imprinted loci. The latter are therefore erased in a second event by an active process[94] and subsequently remethylated based on the sex of the transmitting parent[94]. A wave of genome-wide re-methylation takes place during germ cell development. In the male germline, further epigenetic changes will occur during spermatogenesis to refine the hydrodynamic shape of the spermatozoa and protect the paternal genome from oxidative stress. This is achieved by a genome-wide exchange of histones by the intermediate transition nuclear proteins and subsequently by protamines, resulting in a tightly packaged chromatin structure.

After fertilization, a second wave of epigenetic reprogramming is required to ensure totipotency for subsequent cell-specific differentiation. Thereby, the paternal genome is actively demethylated, while demethylation of the maternal genome follows in a passive way[95]. Notably, imprinted marks escape this second reprogramming event and are stably maintained during each replication cycle. In order to re-establish the specific methylation patterns required for stage and tissue-specific development, a wave of re-methylation takes place between the two-cell and blastocyst stages.

1.5 Male ageing

Various socioeconomic and secular factors have led to a clear trend of delayed parentage in developed countries. In Germany, the average age of fathers at the birth of their first child has increased by an average of 3.6 years since 1991[96]. Nonetheless, the impact of ageing on males, especially on the male germline, has historically received far less attention compared to female senescence. Increasing paternal age elevates the incidence of certain medical disorders, including schizophrenia, bipolar disorders, autism, and childhood leukaemia in the progeny[97]. It has as well been shown to cause certain single-gene and chromosomal defects in sperm[10,98]. The term “paternal age effect” is used to

subsume the multiple biological effects of the father's age on the sired child, and, amongst others, reflects genetic and epigenetic changes in the male germline.

Genetics of ageing in the male germline

Considering that spermatogenesis persists until senescence, one can easily hypothesize that the sperm of elder men is endowed with a huge number of de novo genetic changes[99], elevating the mutational load in the sperm of older males. As a simplified illustration, one can assume that spermatogonial stem cells undergo mitotic replication every 16 days[100], thus resulting in approximately 200 mitotic cell divisions in a 20-year-old and more than 600 divisions in a 40-year-old male[101]. Now considering a germline mutation rate of around 1.2×10^{-8} mutations per nucleotide per division[102] and expecting pathogenetic changes to account for 1-2% of this mutational burden, 4-8 novel pathogenic mutations might occur over a 20-year lifespan[103]. Accumulating errors in mismatch repair mechanisms might exponentially enhance this process[103]. Accordingly, some researchers report a doubling of sperm mutations every 16.5 years[102]. Indeed, specific point mutations occurring in the paternal germline are causal for a few well-studied congenital disorders. For example, point mutations in fibroblast growth factor receptor 2 (*FGFR2*) can provoke Apert syndrome, mutations in *FGFR3* result in achondroplasia[100].

Epigenetics of ageing

During each cell division, the daughter cells must be endowed not only with the correct DNA sequence but also with the accurate epigenetic pattern of the parental cell. However, as the error ratio of the copying process is around 10 to 100-fold higher for the epigenome than for the genome[12], ageing sperm cells acquire considerably more epigenetic than DNA sequence changes. Indeed, ageing is concomitant with progressive changes in several epigenetic hallmarks, including the accumulation of histone variants, changes in chromatin accessibility[104], disruption of heterochromatin[105-107], deregulated expression or activity of miRNAs[108,109] and altered DNA methylation patterns. Nonetheless, epigenetic mechanisms underlying ageing are complex, and the extent or even the direction of these changes differs between cells, tissues, and species[110,111]. Principally, this effect may occur in two main patterns: overall, as a result of environmental influences or spontaneous stochastic errors[112] during the maintenance of epigenetic marks, interindividual patterns of baseline DNA methylation become more and more divergent. This phenomenon is

often referred to as "epigenetic drift"[113] and results in incalculable mosaicisms in the methylomes of ageing individuals[114]. Contrarily, some age-associated methylation changes occur in consistent regions of the genome and are highly reproducible between individuals. These DNA methylation patterns can predict chronological age in a variety of tissues[115] and are referred to as epigenetic clocks[116, 117].

Interestingly, human sperm methylation differs strikingly from patterns of DNA methylation in somatic tissues: While somatic cells undergo a global decline in DNA methylation levels[118] with a strong tendency towards site-specific hypermethylation, preferentially at CGI promoters[119], human sperm exhibits a global increase in methylation levels but reveals demethylation in regions known to be impacted by ageing. Furthermore, age-related methylation changes in sperm cells are often more extensive than those in somatic tissues: the mean fractional methylation variation in sperm amounts to around 0.3% per year in hypermethylated and a bit less in hypomethylated regions, whereas the annual change in DNA methylation in somatic cells is generally not more than 0.15%[8]. Importantly, sperm DNA methylation alterations observed with paternal age do not occur arbitrarily but appear to be enriched in developmentally important gene sets[120].

1.6 Transgenerational epigenetic inheritance

The heritable component of many widespread human medical conditions is extensive, with genetically complex traits such as schizophrenia showing up to 80% heritabiliy[121] or autism with even 90%[122]. However, multitudinous genome-wide association studies repeatedly failed to explain this heritability sufficiently[123-125]. Apparently, underlying genetic variants including DNA mutations or single nucleotide polymorphisms do not account for more than 10% of the inheritance of complex traits[126,127]. This phenomenon is generally referred to as "missing heritability". Epigenetic mechanisms along with complex genetic interactions and rare genetic variants are methodically missed by common DNA sequence-based analysis and are supposed to be a key element in illuminating the observed discrepancy[128].

Several studies have shown that exposure to a huge variety of factors, including maternal metabolism and physiology[129,130], nutritional supplements[131,132], xenobiotics[133,134], maternal and paternal behaviours[135], and viruses[136], can lead to epigenetic changes of the host genome and can potentially be transmitted to subsequent generations even without

persistent exposure. A famous example comprises children born during the Dutch Hunger Winter from 1944 to 1945. Here, maternal undernourishment during gestation led to increased obesity rates and less DNA methylation of the IGF2 gene in the respective female offspring[137]. Still, it was a long-time assumption that, in contrast to the female germline, epigenetic changes in the male germline have no impact on the embryonic development or disease susceptibility of the progeny. This imbalance can possibly be explained by the want of known transfer mechanisms of epigenetic modifications between the father and his offspring. Several arguments have been commonly used to defend this hypothesis and shall shortly be scrutinised[138]:

1. During spermatogenesis, nearly a whole layer of "epigenetic data" drops away when histones are replaced by alkaline protamines. This process is essential to transform spermatozoa into a small and fast messenger of DNA, but it also precludes transcription[139]. Still, the replacement of histones by protamines is incomplete with 5-15% of histone-bound DNA being retained at imprinted loci, miRNA, developmental transcription factors, and signalling molecules loci[140]. Accordingly, the preserved histone marks might be a crucial factor in passing epigenetic information to the zygote and consecutively influence the progeny[140].

2. Concerning DNA methylation, researchers generally assumed that epigenetic marks are entirely cleared and re-established afresh during embryogenesis. However, a variety of specific loci in the epigenome have been found to undermine methylation reprogramming mechanisms. That is to say, the erasure of the epigenetic landscape is incomplete and not restricted to the case of imprinted genes and some repetitive elements[7,92,141]. Interestingly, age-associated methylation alterations in the male germline are significantly enriched in regions escaping histone replacement[8] and functionally enriched at genes expressed in the brain and controlling neural development[142].

3. Unlike the mother, the father of course does not provide a direct environment for the development of the child during pregnancy, which might have led to the assumption that fathers might only play a minor role in epigenetic inheritance. Still, impacts of environmental clues such as diets or mental stress on the paternal phenotypes could be mediated by sperm RNAs, especially microRNAs (miRNAs) and tRNA-derived

small RNAs (tsRNAs)[143]. Indeed, spermatozoan RNA transcripts are able to prevent histones from being replaced by protamines[144], thus putatively enabling selective gene activation in the embryo[139].

In summary, it is well known that a child's risk of suffering from diseases such as autism and schizophrenia increases with advanced paternal age[145] at the time of conception and that ageing implies epigenetic aberrations in the male germline. Furthermore, possible transfer mechanisms for epigenetic alterations to future generations do exist. Accordingly, further understanding of the epigenetics of the male germline is helpful to ascertain the effect of paternal age on embryogenesis and the development potential of the offspring.

1.7 Genes of interest

The following chapter is supposed to give a short overview of the genes and regions of interest analysed in this study. Although per se no direct link between the DNA methylation level of the analysed CpGs and functional consequences on gene expression can be established, it shall at least give a short impression of possible implications of the observed age effects. Some genes are discussed in a more detailed way than others as they represent important (epi-)genetic key regulators (*MBD3*, *EEF1A2*) or are well-studied players in disease development (*CHD7*, *LMNA*). General information on taxonomy, genomic location, expression data, molecular function, and involved pathways is taken from the websites genecards.org, uniprot.org and the National Library of Medicine[146].

BEGAIN

The human *BEGAIN* gene encodes the brain-enriched guanylate kinase-associated protein. It is specifically expressed in brain tissues and was shown to interact with the postsynaptic density (PSD)-95/SAP90[147], a synaptic membrane-associated guanylate kinase[148] attached to the postsynaptic membrane[149]. Many proteins in the PSD are involved in the regulation of synaptic functions.

EEF1A2

The *eEF1A2* gene "encodes an isoform of the alpha subunit of the elongation factor-1 complex (eEF1A)"[150] that catalyzes the docking of aminoacyl tRNAs to the A-site of the

80s ribosome during protein biosynthesis[151]. EEF1A is an extremely copious molecule making up around 3% of the total cellular protein[152]. Despite being encoded by separate loci, the isoforms eEF1A1 and eEF1A2 are around 98% similar[153,154]. Unlike the nearly ubiquitous expression of eEF1A1, eEF1A2 expression is only detectable in cells of the brain, spinal cord, heart, and skeletal muscle[155,156]. Besides its role in translational elongation, eEF1A exerts a multitude of sideline functions separate from protein synthesis[157]: For the EEF1A complex implications in protein degradation[158,159], cellular apoptosis[160], nucleocytoplasmic trafficking,[161] and multiple aspects of cytoskeletal regulation[162] have been observed, witnessing its significance in diverse cellular events. The A2 subunit is further considered a proto-oncogene as it is known to enhance tumour growth in different types of cancer such as ovarian[154] and breast tumours[154] as well as prostate cancer[163]. In addition to the enhancement of tumour growth, to date several de novo mutations of *EEF1A2* have been found in model organisms, causing severe neurological deficits such as epilepsy[164] and global development delay[165].

HDAC11

Histone deacetylase 11 (HDAC11) plays an important role in the regulation of cellular events by catalysing the removal of an acetyl group from lysine residues[166]. Furthermore, it is important for cell cycle progression and developmental events. Notably, it is overexpressed in several cancers[167] where it is supposed to be associated with longer disease-free survival[168].

LMNA

This gene encodes the LMNA protein, also known as Lamin A/C of the lamin family. It builds up the matrix of the core lamina that underlies the inner nuclear membrane, and is therefore essential for the stability of the cell[169]. Mutations in the LMNA gene are causal for diseases called laminopathies. Among the most prominent ones are Hutchinson-Gilford progeria syndrome, Emery-Dreifuss muscular dystrophy, and Charcot-Marie-Tooth disease[170].

MBD3

Basically, two different models exist explaining how DNA methylation exerts an effect on transcriptional activity. One is the direct interference of Methyl-caps with the binding sites of transcription factors[171], as is the case for the transcription factors c-Myc[172], NF-kB[173]m and CREB[174]. The second approach is the recruitment of chromatin remodelling or corepressor complexes by proteins that specifically bind to methylated cytosines and convey the crosstalk between methylation and the chromatin structure. In vertebrates, different classes of methyl-CpG binding proteins have been identified, including the Kaiso-like proteins, SRA domain-containing proteins, and the MBD family, amongst them MBD3. The whole MBD family is endowed with a methyl-CpG-binding domain[175]. However, unlike the other family members, MBD3 lacks methylated DNA binding capacity but instead has a high affinity to hydroxy methylated DNA[176]. MBD3 is a subunit of the Mi2/NuRD corepressor complex[177]. This complex combines ATP-driven chromatin remodelling and protein deacetylase activity and herewith regulates gene expression. MBD3 is crucial for bridging the remodelling and core histone deacetylase subcomplexes[177]. Several researchers suggest a protective role for MBD3 in tumour development. In pancreatic cancer tissues MBD3 expression was lower in tumour than in non-tumour tissues. Here, lower MBD3 levels were associated with significantly lower survival compared to patients with higher levels[178].

NFKB2

NFKB2 is a subunit of the transcription factor complex nuclear factor-kappa-B p100 (NFkB). It is expressed in various tissues and is crucial for immunoactivity[179]. It can be activated by a multitude of stimuli, such as cytokines and oxidant-free radicals[180]. Inadequate activation is associated with several inflammatory disorders such as rheumatoid arthritis[181], peptic ulcer[182], lung fibrosis[183], and malignant processes such as Hodgkin lymphoma[184]. Contrarily, complete, and sustained inhibition of NF-kappa-B has been linked to insufficient immune cell development, as emphasized by the finding that NFKB2 has been identified as a molecular cause of common variable immunodeficiency (CVID)[185,186].

PAK1

This gene encodes a member of the serine/threonine protein kinases and takes part in intracellular signalling pathways, cytoskeleton reorganization, cell adhesion, and nuclear signalling[187]. Abnormal activation is observed in a wide variety of medical conditions, including cancer[188,189], inflammation[190], and viral infections[191].

PRKAR2A

In humans, the *PRKAR2A* gene encodes the cAMP-dependent protein kinase type II-alpha regulatory subunit. cAMP is an important signaling molecule in charge of a variety of cellular functions. cAMP induces the cAMP-dependent protein kinase, which then transmits the signal by phosphorylation of sundry target proteins[192]. PRKAR2A may mediate membrane association by interacting with various A-kinase anchoring proteins such as the MAP2 kinase and dictating the localization of the cAMP-dependent protein kinase. It further "regulates protein transport from endosomes to the Golgi apparatus and the endoplasmic reticulum"[193]. In accordance with its function as a regulatory subunit, PRKAR2A deficient mice showed a predisposition to hematopoietic malignancies such as rare diffuse large B cell lymphomas[194].

PRAM1

This gene in humans encodes the PML-RARA-regulated adapter molecule 1. The gene is particularly expressed in peripheral blood leukocytes and bone marrow[195]. The expression of this gene is stimulated by retinoic acid and, as the name implicates, is repressed by PML-RARalpha, a fusion protein of the retinoic acid receptor-alpha (RARalpha) and the promyelocytic leukaemia protein (PML)[196]. This results in the expression of a hybrid protein with altered functions, for instance by blocking transcription and differentiation of granulocytes[197], and can be found in 95% of all cases of acute promyelocyte leukaemia (PML)[198].

PTK2B

The gene product is a cytoplasmic tyrosine kinase participating "in calcium-induced regulation of ion channels and activation of the map kinase"[199] signalling pathway[200]. It is crucial for the regulation of neuronal activity, humoral immune response, and

cytoskeleton reorganization[201]. It is further supposed to participate in the pathogenesis of Alzheimer's disease[202].

RASGEF1C

This gene encodes a guanine-nucleotide releasing factor, involved in small GTPase-mediated signal transduction[203]. Interestingly**,** RASGEF1C was found to be differentially methylated at single positions in the temporal gyrus between Alzheimer patients and controls[204].

RPL6

The RPL6 gene encodes a component of the 60S subunit (60S ribosomal protein L6) of the ribosome. As for most ribosomal proteins, multiple processed pseudogenes of RPL6 can be found throughout the genome[205]. Besides the well-studied participation in ribosome assembling, the ribosome-independent implications of ribosomal proteins are getting more attention, for example in DNA damage response[206] and immunosurveillance[207]. Potential disease implications include gastric cancer[208] and Parkinson's disease[209] in the case of RPL6.

SPIB

SPIB encodes the transcription factor Spi-B. SPIB forms part of the SPI subfamily of ETS transcription factors, one of the largest families of transcription factors[210]. SPIB is expressed in plasmacytoid dendritic cells and B-cells[211]. SPIB binds to a purine-rich sequence, the PU box, that can act as a lymphoid-specific enhancer and is therefore essential for the development of plasmacytoid dendritic cells[212].

1.8 Aims of this study

To give a short impression of the constructive approach of this study, Figure 1 illustrates the three successive main experiments.

	Project 1	**Project 2**	**Project 3**
	Validation of 10 candidate genes in 94 human sperm and 4 genes in 36 bovine sperm samples via Pyrosequencing	*Species comparison in conserved regions between human and bovine sperm via Pyrosequencing*	*Transmission to the next generation via DBS in 24-38 FCB samples for 3 genes*
Homo sapiens	*BEGAIN* *EEF1A2* *LMNA* *MBD3* *NFKB2* *PRAM1* *PRKAR2A* *RASGEF1C* *RPL6* *SPIB*	*CHD7* *HDAC11* *PAK1* *PTK2B*	*BEGAIN* *EEF1A2* *SPIB*
Bos taurus	*CHD7* *HDAC11* *PAK1* *PTK2B*	*RPL6*	

Figure 1: Constructive approach of the study subdivided into three experiments:

Project 1: 10 human and 4 bovine genomic loci were selected from a lab intern candidate list based on Reduced representation bisulphite sequencing (RRBS) and validated for age-dependent differentially methylated regions (age-DMRs) via Pyrosequencing.

Project 2: 1 human (*RPL6*) and 4 bovine (*CHD7*, *HDAC 11*, *PAK1*, *PTK2B*) genes that had shown an age effect in Project 1 were now searched for an age effect in the complementary species, again via Pyrosequencing. The corresponding genomic region was previously identified by the publicly available nucleotide BLAST tool from the website www.ensembl.org.

Project 3: Deep Bisulphite Sequencing (DBS) in 24-38 human foetal cord blood samples (FCB) was performed to decipher whether the age-dependent methylation changes observed for *BEGAIN*, *EEF1A2*, and *SPIB* (Project 1) are transmitted to the next generation.

2 Material and Methods

2.1 Material

2.1.1 Ethics approval and consent

The methylation study of human foetal cord blood and human and bovine sperm was approved by the Ethics Committee of the Medical Faculty of the University of Würzburg (AZ- 117/11 and 212/15). Written informed consent was obtained from all human contributors.

2.1.2 Reagents and equipment

All reagents and equipment that were used during the experiments were purchased from different manufacturers and are listed below in Table 1.

Table 1: Reagents and equipment

CHEMICALS	**Producer**
10x DNA Protect Buffer with Mg_2Cl	Invitrogen
4 M Acetic Acid	
6x loading Dye	Thermo Fisher
Agarose, universal	VWR Life Science
Ampuwa water	Fresenius KABI
Aqua ad iniectabilia	Berlin Chemie
Bisulphite Solution	Qiagen
BoviPure®	Nidacon
BoviDilute®	Nidacon
Buffer BD	Qiagen
Buffer BL	Qiagen
Buffer BW	Qiagen
DNA Protect Buffer	Qiagen
Elution Buffer	Qiagen
Ethanol absolut	Chemikalien Scheller
Fast Start DNA Taq Polymerase	Roche
Gene Ruler DNA 100bp ladder mix	Thermo Fisher
HD Green plus DNA stain	INTAS Science imageing
Isopropanol	
NaOH pellets	Carl ROTH
NEBNext Multiplex Oligo's	Illumina
PCR Grade Nucleotide Mix (dNTPs)	Roche
PureSperm® 40/80/90	Nidacon
Pyromark Binding Buffer	Qiagen
Pyromark Annealing Buffer	Qiagen
PyroMark Gold Q96 CDT	Qiagen
Streptavidin sepharose beads	GE Healthcare
Tris Molecular biology grade	Applichem GmbH
EQUIPMENT	
Biosphere Filter Tips	Sarstedt

4titude® 96 well plate	Brooks Life Sciences
AirPore™ Tape sheet	Qiagen
Biometra waterbath TS1 Thermo Shaker	AnalytikJena
Centrifuge	Eppendorf
Centrifuge ThermoTM scientific HERAEUS FRESCOTM 17	Thermo Fisher Scientific
Collection tube	Qiagen
Gloves	Carl Roth
Illumina Index primer rack	Illumina
Janus® automated workstation	PerkinElmer
MiSeq™	Illumina
Multichannel reagent reservoir	Integra
Nanodrop 2000c	Thermo Fisher Scientific
Nexus gradient flexlid Thermal cycler	Eppendorf
Non-skirted 96 well plate	Hartenstein
Pipettes (10 µl, 20 µl, 100 µl, 200 µl, 1000 µl)	Eppendorf
PyroMark Q96 HS Plate	Qiagen
PyroMark Q96 MD	Qiagen
Pyromark Q96 Work Station	Qiagen
Pyromark Vakuum Prep Tool 60-0236	Qiagen
QUali PCR tubes	Kisker Biotech Gmbh & CoKG
Qubit fluorometer	invitrogen™
Reaction tubes (0.2 ml, 1.5 ml, 2.0 ml, 20 ml) Safe Lock	Eppendorf
Spin column	Qiagen
Tape stripes (8 strip flat caps)	SARSTEDT
Thermo Shaker TS-100	Peqlab Biotechnologie GmBH
UV bench Model 300	Airclean Systems
Vortex Genie 2	Scientific industries
Water bath	Gesellschaft für Labortechnik mbH
Wash buffer	1.21 g Tris, 1l dH_2O, pH=7.6
50x TAE buffer	242 g Tris, 100 mL 0.5 M EDTA (pH 8), 57.1 mL acetic acid, 1000 mL dH2O)
Denaturation buffer	8 g NaOH, 1 l dH_2O
KITS	
FlexiGene® DNA-Kit (250)	Qiagen
Agilent High sensitivity DNA Kit	Agilent
DNeasy Blood and Tissue kit	Qiagen
EpiTect® Fast 96 DNA Bisulphite Kit	Qiagen
EpiTect® Fast DNA Bisulphite Kit (50)	Qiagen
Qubit™ dsDNA BR Assay System Kit	Thermo Fisher Scientific
SOFTWARE	
Agilent 2100 Expert Software	Agilent
Amplikyzer	Sven Rahmann
FluorChem HD 2	Cell Biosciences, Inc
NanoDrop 2000/2000c	Thermo Scientific

Pyromark Assay Design 2.0	Qiagen
Pyro Q CpG 1.0.9	Biotage
SPSS Statistics 26	IBM
WEBSITES	
bisearch.enzim.hu	
ensembl.org	
uniprot.org	
genecards.org	

2.1.3 Human sperm samples for pyrosequencing

All human sperm samples for the methylation analysis were gathered by the Fertility Centre "Kinderwunschzentrum" in Wiesbaden from excess material, subsequently pseudo-anonymized, and finally stored at -80°C. Further purification was achieved with the density gradients PureSperm 80 and 40. To adjust for the contributor's fertility as a possible confounding factor, mostly normozoospermic sperm samples were used. Furthermore, information about the father, such as weight, height, BMI, and semen parameters according to the criteria of the World Health Organization[213] was gathered (Supplementary Table 1 in the appendix). Key characteristics of the sperm cohort used to validate age-DMRs via Pyrosequencing are shown in Table 2.

Table 2: Human sperm cohort parameters for Pyrosequencing

(kg=kilogram, m=meter, ml=millilter, SD=standard deviation, yr=years)

Parameter	Mean ± SD [range]
Sample size	94
Normozoospermia	90
Donor's Age (yr.)	39.3±5.94 [29.4-71.7]
BMI (kg/m^2)	25.6±2.92 [18.9-31.8]
Sperm Concentration (Million/ml)	84.5±45.77 [15-260]

2.1.4 Human foetal cord blood (FCB) samples

All analysed FCB samples were gained from neonates conceived through either in vitro fertilisation (IVF) or intracytoplasmic sperm injection (ICSI) and were collected by collaborating obstetric clinics throughout Germany. Most contributors were of central European descent. Informative samples for Deep Bisulphite Sequencing (DBS) were selected by genotyping a whole cohort of samples via Pyrosequencing. Finally, only heterozygous samples with homozygous fathers for the respective single nucleotide

polymorphism (SNP) were used for DBS. On the grounds of clarity, only these samples are represented in Table 3. More detailed information is provided in Supplementary Tables 2 and 3 in the appendix.

Table 3: Human FCB cohort parameters

(cm=centimeter, g=gram, ICSI=Intracytoplasmatic sperm injection, IVF= In vitro fertilization, SD=standard deviation, yr=years)

Parameter		**Average±SD [range]**
Sample size		80
Gender	Male	37
	Female	35
Treatment	IVF	20
	ICSI	42
Birth mode	Spontaneous	31
	section	24
	vacuum	9
Birth weight (g)		3202.7±578 [2090-4950]
Length (cm)		51.2±2.38 [45-57]
FCB pH		7.25±0.1 [6.9-7.43]
Age father (yr.)		38.76±5.01 [30-51.46]
Age mother (yr.)		34.68±3.51 [25-42]

2.1.5 Human sperm samples for genotyping

To identify which of the two alleles in the heterozygous FCB samples was of paternal origin, the sperm samples of the corresponding father also had to be genotyped for the respective SNP. A cohort comprising all sperm samples from the fathers was provided by the collecting obstetric clinics and is depicted in Supplementary Table 4 in the appendix. This cohort is different from the one mentioned in 2.1.2.

2.1.6 Human sperm samples for Deep Bisulphite Sequencing

As DBS was performed with a throughput of 48 MIDs per run and only a few FCB samples fulfilled the criteria, the DBS run was filled up with heterozygous sperm samples to validate the observed age effect in a second method and to gain further insights on ageing effects on a single read level. Therefore, for each gene (BEGAIN, EEF1A2, and SPIB), a young (<40 years) and an old (>40 years) cohort of heterozygous sperm samples was designed whose characteristics are shown in Table 4. More detailed information is provided in Supplementary Table 5 in the appendix.

Table 4: Human sperm cohort parameters for DBS

(SD=standard deviation, yr=years)

Gene	Age (yr.) Mean± SD [range]	
	Young	Old
BEGAIN	28,70±1,63 [26,8-30,57]	47,27±1,12 [45,56-48,59]
EEF1A2	33,78±4,14 [28,08-39,98]	43,19±3,2 [40,25-48,28]
SPIB	33,47±2,66 [30-39,8]	43,59±2,94 [40,49-49,83]

2.1.7 Bovine sperm samples

For all experiments commercially available bovine sperm samples (Masterrind) were used. The samples were obtained from 15 different high-performance breeding bulls (Bos taurus) at different ages of their lifespan. From nine bulls, samples at young age (<3 years), middle age (3–6 years), and old age (>6 years) were available. Bull sperm samples were purified by BoviPure and BoviDilute (Nidacon) according to the manufacturer's protocol. The characteristics of the cohort are shown in Table 5. More detailed information is provided in Supplementary Table 6 in the appendix.

Table 5: Characteristics of the bovine sperm cohort

(nr=number, yr=years)

Parameters	Mean ± SD [range]
Sample size	36
Bulls (nr.)	15
Donor's Age (yr.)	4.81±3.11 [0.7-12.3]

2.2 Methods

Several researchers have contributed to the sperm and blood cell isolation, purification, and bisulphite conversion processes of different samples over a longer period. They have all given their consent to the further use of their work in this study.

2.2.1 Sperm Purification

Human sperm

The freshly thawed swim-up sperm fraction was purified by silane-coated silica density gradients PureSperm 40/80. Therefore, 2 mL of the lower layer of PureSperm 80 was pipetted into a 15 mL glass tube, and 2 mL of the upper layer PureSperm of 40 was applied on top of it. 1.5 mL of liquefied semen was added, followed by a centrifugation step at

300 x g for 20 minutes. The resulting pellet contained the purified spermatocytes in the form of about 4-6 mm 80 fractions.

Bovine sperm

Here, purification was achieved by using a combination of BoviPure and BoviDilute. Mixing 200 µL BoviPure and 300µL BoviDilute resulted in 40 fractions, whereas 80 fractions were obtained by blending 400 µL BoviPure and 100 µL BoviDilute. 250 µL of semen was layered on top of 500 µL of each fraction in a 1.5 mL tube. Subsequently, the tubes were centrifuged at 300 x g for 15 minutes. The supernatant was discarded and only the pellet containing the purified spermatocytes remained.

2.2.2 Sperm DNA isolation

300 µl buffer (stock consisting of 5 ml of 5 M NaCl, 5 ml of 1 M Tris-HCl (pH 8), 5 ml of 10% SDS (pH 7.2), 1 ml of 0.5 M EDTA (pH 8), 1 ml of 100% β-mercaptoethanol and 33 ml of dH_2O) was mixed with the purified sperm. After adding 100 µl of proteinase K (20 mg/ml), the samples underwent 2 hours of incubation at 56˚C under mild agitation. Afresh 20 µl proteinase K was supplemented and incubation was pursued for 2 h at 56˚C. Afterwards, the sperm DNA was processed further using the DNeasy Blood and Tissue kit according to the manufacturer's protocol ("Purification of Total DNA from Animal Tissues (Spin-Column Protocol)"). Therefore, the lysate was blended with 400 µl each of Buffer AL and ethanol (96-100%). Gradually, the solution was pipetted into the provided DNeasy Mini spin columns and centrifuged at 13,300 x g for 1 min, the resulting flow-through was discarded from the collection tubes. Two subsequent washing steps with 500 µl of Buffer AW1 and Buffer AW2 were carried out. Next, 100 µl Buffer AE was layered onto the dry DNeasy membrane, submitted to 1 min of incubation at room temperature, and finally eluted by centrifuging at 13,300 x g for 1 min. Genomic DNA was frozen at -80°C until further use.

2.2.3 Blood DNA isolation

For the isolation of foetal cord blood DNA, the FlexiGene kit was applied according to the manufacturer's protocol "Isolation of DNA from 100–500 µl Whole Blood". After quickly thawing the foetal cord blood samples in a water bath at 37°C, 500 µl of blood was blended with 1250 µl of the supplied buffer FG1 in a 2 ml centrifuge tube. Two successive

centrifugation steps were performed for 1 min at 10,000 x g and the supernatant was discarded. The dry DNA pellet was subsequently resuspended in 250 µl of a mix of Buffer FG2 and Qiagen Protease and incubated for 5 min at 65 °C. The whole solution was mixed with 250 µl isopropanol causing the DNA to precipitate. Two cleaning steps with 70% ethanol were carried out guaranteeing the evaporation of all liquid residues that could potentially interfere with further reaction steps. Finally, the dry pellet was resuspended in 200 µl buffer FG3 and left overnight at room temperature.

2.2.4 Bisulphite conversion

The overall aim of this study was to identify age-dependent methylation marks in human and bovine sperm and the generated offspring. As the methylation patterns cannot be identified if proceeding directly to PCR after DNA isolation, bisulphite conversion was performed to convert the DNA into a form that allows for preserving the methylation pattern of each sample. This method is based on the deamination of non-methylated cytosines to uracil by bisulphite solution, whereas methylated and hydroxy-methylated CpGs remain unaffected. For bisulphite conversion of whole 96 plates, the EpiTect® Fast 96 DNA Bisulphite Kit was used, for smaller sample sizes the EpiTect® Fast DNA Bisulphite Conversion Kit was employed using the respective protocols consisting of a bisulphite conversion step followed by a clean-up. For sperm samples, a 500 ng DNA approach was selected, whereas 1000 ng was used for FCB. The reaction mix was set up as shown in Table 6, mixed thoroughly, and incubated in a thermal cycler with a heated lid according to the protocol shown in Table 7. The following clean-up steps of the two protocols differ in some steps. Exemplarily, the clean-up procedure for the EpiTect® Fast 96 DNA Bisulphite Kit is now described: Upon completion of the bisulphite treatment, 310 µl buffer BL, 250 µl ethanol (96-100%) and the entire bisulphite reaction product were pipetted into each well of a provided EpiTect 96 plate. The whole solution was vortexed and centrifuged for 1 min at 5800 x g at room temperature, followed by a wash step with 500 µl buffer BW and a subsequent incubation at room temperature with 250 µl buffer BD for 15 min. Two further wash steps with 500 µl buffer BW each and one wash step with 250 µl ethanol (96-100%) were carried out, followed by an ultimate centrifugation for 15 min at 5800 x g. Finally, the samples were eluted with 70 µl buffer EB each by centrifugation at 5800 x g for 1 min and stored at -20°C until further use.

Table 6[214]: Reaction setup for bisulphite conversion according to the manufacturer's manual (www.qiagen.com)

*(ng=nanogram, µg=microgram, * The combination of DNA and RNase-free water must total 20 µl, ˆ DNA solution and RNase-free water must total 40 µl)*

	Volume (µl)	
Component	Samples with high concentration (1 ng – 2 µg)	Samples with low concentration (1–500 ng)
DNA	Variable* (maximum 20 µl)	Variableˆ (maximum 40 µl)
RNase-free water	Variable*	Variableˆ
Bisulphite Solution	85	85
DNA Protect Buffer	35	15
Total	140	140

Table 7: Thermal cycler programme for bisulphite conversion

(min=minute, ∞=indefinite)

Step	**Duration**	**Temperature**
Denaturation	5 min	95°C
Incubation	20 min	60°C
Denaturation	5 min	95°C
Incubation	20 min	60°C
Hold	∞	20°C

2.2.5 Sample amplification

For all utilized samples, amplification of the region of interest was achieved via polymerase chain reaction (PCR) in a non-skirted PCR plate. All primers were designed for bisulphite-converted DNA with Pyromark assay design 2.0 software and are shown in Tables 11-14. The specific annealing temperature required for each gene was previously identified by gradient PCR. Table 8 shows the reagent setup for a 1 µl sample. The standard cycler programme is depicted in Table 9.

Table 8: Reagent setup for standard PCR

(dH2O=distilled water, dNTP=deoxynucleoside triphosphate, bscDNA=bisulphite converted DNA, mM= millimolar, µl=microliter)

Reagent	Amount for 1µl bscDNA
dH2O	18.3 µl
10x PCR Buffer with MgCl2	2.5 µl
dNTPs (10 mM)	0.5 µl
Forward Primer (10 pmol/ml)	1.25 µl
Reverse Primer (10 pmol/ml)	1.25 µl
FastStart Taq DNA polymerase	0.2 µl

Table 9: Thermal cycler conditions for standard PCR

(X=variable)

Temperature	**95°C**	**95°C**	**X°C**	**72°C**	**72°C**	**4°C**
Duration	5min	30s	30s	1min	5min	Hold
Cycles			35			

2.2.6 Gel visualisation

To ensure specific and successful amplification of the targeted sequence, gel electrophoresis was performed after each PCR run. Therefore, 4 µl of PCR product was mixed with 6 µl 1x loading dye, applied on a 1.5% agarose gel, and run for 20 minutes at 150 volts in an electrophoresis chamber with 1x TAE buffer. The correct base-pair length of the bands was verified by comparing it to a 100bp gene ruler DNA ladder under ultraviolet light.

2.2.7 DNA quantification

Depending on the experiment and the expected DNA concentration, different techniques of DNA quantification were used and are now presented individually.

Nanodrop

The Nanodrop was used for DNA quantification on the eve of bisulphite conversion. Therefore, a 1 µl droplet of genomic DNA was pipetted on the Nanodrop 2000/2000c spectrometer after blanking with the respective buffer and measured twice. The mean of both measurements was considered for further experiments. A 260/280 ratio of 1.8 and a 260/320 ratio of 2.0 were considered pure DNA.

Qubit fluorometer

To obtain more dedicated concentration results in Deep Bisulphite Sequencing, the Qubit dsDNA BR Assay System kit was used. Therefore, the kit was thawed at room temperature, and for each sample 199 µl Buffer and 1 µl Quant-IT reagent were mixed. 10 µl 100 and 0 standard and 2 µl of the sample were adjusted to a total volume of 200 µl in Qubit tubes using buffer and reagent mix, vortexed for 3 seconds,

and incubated at room temperature for 2 minutes, avoiding exposure to light, and finally measured after gauging the photometer with the standards. Again, all samples were measured twice, and the average concentration was considered for further experiments.

Bioanalyzer

To verify the correct fragment length after the second PCR in DBS and to determine the molarity of each sample, the PCR product was applied on a Bioanalyzer Chip according to the Bioanalyzer protocol using the High Sensitivity DNA Reagent kit. Therefore, reagents were allowed to equilibrate to room temperature and subsequently 9 µl gel-dye mix, 5 µl DNA marker, 1 µl ladder, and 1 µl sample were pipetted into the respective wells. The whole chip was vortexed for 60 s at 2400 rpm in the IKA vortex mixer and run in the Agilent 2100 Bioanalyzer.

2.2.8 Bisulphite-converted Pyrosequencing

General principles

Pyrosequencing with the Pyromark Q96 MD is a reliable and time-saving technique to determine the DNA methylation status of a maximum throughput of 96 samples per run. However, its application is restricted to short stretches of DNA of preferably not more than 100bp. Therefore, it is not convenient to identify new candidate regions, but is a

fortiori helpful to validate previously determined regions of interest. In contrast to DBS, which gives a result on a single allele level, Pyrosequencing generates a mean methylation value for each sample. To identify DNA methylation levels, the targeted amplicon sequence must undergo bisulphite conversion prior to the sequencing run. Upon bisulphite conversion, methylated cytosines remain unaffected, while unmethylated cytosines are deaminated to uracil. Pyrosequencing relies on the detection of light triggered by the release of pyrophosphate during the incorporation of the nucleotides. An enzyme called ATP-Sulfurylase converts this pyrophosphate into ATP, providing energy that is used by the enzyme luciferase to oxidise luciferin to oxyluciferin. That last reaction provokes a light emission that is finally interpreted by a camera and displayed as a peak on the computer. Here, the size of the peak corresponds to the number of incorporated nucleotides. An enzyme called apyrase finally eliminates the unincorporated dNTPs.

Application

In this study, bisulphite pyrosequencing was performed for two different purposes: Previous experiments in our lab based on an epigenome-wide sequencing technique (RRBS) had identified novel age-associated DNA methylation loci in human and bovine sperm. We selected 10 human age-DMRs from this list to become validated in a cohort of 94 human and 4 bovine age-DMRs to be replicated in a cohort of 36 bovine sperm samples. We further compared the methylation levels of these 2 species at corresponding CpG sites. Second, pyrosequencing was used to genotype FCB samples and the sperm of their corresponding fathers by targeting an informative SNP nearby the analysed CpG sites, allowing precise differentiation of the paternal and maternal alleles in heterozygous FCB samples required for DBS.

Procedure

Prior to sequencing with the PyroMark Q 96MD, the PCR product was prepared in a specific manner: amplified DNA was captured on sepharose beads, secondly washed to remove unbiotinylated strands, and subsequently denatured to enable the annealing of the sequencing primer. Therefore, in the first step, 70 µl of Master Mix 2 (Table 9) was mixed with 10 µl of the PCR-product in a PCR plate to ensure the binding of the sepharose beads to the biotin-cap of the PCR primers. The amplicons that had now attached to the beads were then captured via suction on small pins in the PyroMark Q96 vacuum workstation,

while all residual fluids were subducted. The amplicons were washed in 70 % ethanol, then placed in Denaturation Buffer and finally cleaned in wash buffer for another 5-10 s. Vacuum and suction were turned off to place the beads into the previously prepared PyroMark Q96 well plate containing Master Mix 1 (Table 10). Subsequent incubation for 2 min at 80°C ensured optimal conditions for the binding of the sequencing primers to the PCR product. The whole plate was inserted into the PyroMark 96 MD pyro-sequencer along with a previously defined amount of enzyme, substrate, and nucleotides.

Pyrosequencing data was generated by the Pyro Q CpG software. A respective pyrogram was earned for each run and average methylation data for each CpG was acquired in text format and ultimately converted into Excel files. Samples with insufficient sequencing quality indicated by red colour were excluded from further analysis.

Table 10: Reagent setup for Pyrosequencing

Reagent	**Amount per 10 µl PCR product**
Master Mix 1	
Annealing Buffer	11.5 µl
Sequencing Primer	0.5 µl
Master Mix 2	
dH2O	40 µl
Binding Buffer	28 µl
Sepharose beads	2 µl

Table 11: PCR and Pyrosequencing primers for 10 different human amplicons

*(A.T.=Annealing temperature, Nr=number of CpGs, *=biotin cap)*

Gene	Primer	Sequence (5´-3´)	A.T.	Nr
Human *BEGAIN*	forward	GTTTTGTTTTTTAGGGGTTAATGAGGA	60°C	
	reverse*	AAATCTCCAACAAACCTCTTCTCTAT		
	sequencing 1	GGGTTAATGAGGAAAATTTTT		2
	sequencing 2	AGGTTATTTTTAGTAGAATGG		5
	Sequencing 3	AGTTTTGTTATGGAAGTTT		2
Human *EEF1A2*	forward*	GGGGAGAGATGGTTATTGTTTTTTA	58°C	
	reverse	CTCCACCTAACACTTACTAAACT		
	sequencing 1	ACTATTCTAAATTCCTAATCTAAAC		3
	sequencing 2	AAACCCCCACCTCCC		3
Human *LMNA*	forward	TAGGAGGTTGAGATAGGAGAATTGTT	60°C	
	reverse*	ACCTAACTCTCCAAACCTTAAAAACTT		

	sequencing 1	AGATAGGAGAATTGTTTGAA		2
	sequencing 2	AGTTGTAGTGAGTTTAGAT		1
Human *MBD3*	forward	GGAGTTTGAGATTAGGTTGATTTAATAT	58°C	
	reverse*	ACAAACATCCACACCTCATAA		
	sequencing 1	GAGGTAGGAGAATTATTTGA		2
	sequencing 2	GATGATATTATTGTATTTTTGTTTG		3
Human *NFKB2*	forward	GGAGGAAGGTTTTGTTTATTTTTTTTTAGT	60°C	
	reverse*	TTTACCCCTCCCTCCATCAATAC		
	Sequencing 1	AGGTTTTGTTTATTTTTTTTTAGTT		3
Human *PRAM1*	forward	AGGTTGGGAGAATTTTTTTAGTTTATTA	60°C	
	reverse*	ATCCTTCCATACCCCTTCTATATATT		
	sequencing 1	TGGAATTTTGTTTTGATGT		2
	sequencing 2	TTTTTTAGTTTATTAAATTTAGGT		3
Human *PRKAR2A*	forward	AGTGGTATGATTTTGGTTTATTGTAA	61°C	
	reverse*	CTAAACAAAATAAACACCCTACCTC		
	sequencing 1	AGTGTTGGGATTATAGG		3
	Sequencing 2	GGTTAATTTTTGTATTTTTAGTAGA		1
	sequencing 3	TTTTTTAAGTAGTTGGGATTATAGA		4
Human *RASGEF1C*	forward	GGGAGGGTATAGTGTATTTGTGT	62°C	
	reverse*	CCTCCATCCACAAAAAACTCCTTAAT		
	Sequencing 1	GGTGAGGAAGGTGGT		3
Human *RPL6*	forward	GTAATTGTTATAAAATTAGTTGGTGGTGA	60°C	
	reverse*	TCCAATTTACAATCCCCACATC		
	Sequencing 1	AGTTGGTGGTGATAAGAA		4
Human *SPIB*	forward	GGTTTTTAGGGTTTAGTTTGTTTTTGAGA	60°C	
	reverse*	ACCCTACTTTAAAACTCCCAATTATT		
	sequencing 1	GGTTTATTTTTATATTTTTAGTAG		2
	sequencing 2	GAGTAATTTTGTTGTTTTAGTT		3

Table 12: PCR and Pyrosequencing primers for 4 different bovine amplicons

*(A.T.=Annealing temperature; *=biotin cap)*

Gene	Primer	Sequence (5´-3´)	A.T.	CpGs
Bovine *CHD7*	forward	GGGTAGGGTTATTTTTTATATTTGT	58°C	
	reverse*	TTTCCCTAACTCAAACCCTCTTA		
	sequencing 1	GGTTATTTTTTATATTTGTAGTAGT		3
	sequencing 2	GTAGTATGGTTAGTTATAGT		2
Bovine *HDAC11*	forward	TGGGTTGTAGGGAGTAGAT	58°C	
	reverse*	CCAACCCAACTATACCAACA		
	sequencing 1	GTTGTAGGGAGTAGATGTA		2
	sequencing 2	GAGGTTGATTATTTTGTTTTATT		2
	Sequencing 3	GGTTTAGGAAGGTTATGTT		7
Bovine *PAK1*	forward	ATGTTTTAGGGTGGGTTAGTATTAT	60°C	
	reverse*	CAACCCCAAAACTAAACCTTTACT		
	sequencing 1	GGGTGGGTTAGTATTATT		6
	sequencing 2	GATATTTAGGTTTTATT		5
Bovine *PTK2B*	forward	GGGTTTTGGGGGGTTTTTA	60°C	
	reverse*	AAATAAACTCACACCCATCATTTC		
	sequencing 1	GGGGGGTTTTTAGGT		3

	sequencing 2	GGTTTAGGGTTTTAGATA		3
	Sequencing 3	GGTTAGGATTAGTATAT		2

Table 13: Checking for evolutionary conservation; PCR and Pyrosequencing primers

*(A.T.=Annealing temperature; Nr=number of CpGs, *=biotin cap)*

Gene	Primer	Sequence (5´-3´)	A.T.	Nr
Human *PAK1*	forward	GGTATTATTTGGTGGGGAAGGTTAG	62°C	
	reverse*	CCAAAAACCCAACCCAACTAAATC		
	sequencing 1	GGGGAAGGTTAGTTT		5
	sequencing 2	GGGTATTTATAAGGTTTTTGTTTT		3
Human *CHD7*	forward	GGTTTATTTTTTGTTGTGGTTGATTAT	60°C	
	reverse*	ACCCCAAAACTATTCAAATACCA		
	sequencing 1	ATGTTGTTGTATGGAAAAATT		1
	sequencing 2	GGTTTTGTGTAGGGG		5
Human *PTK2B*	forward	TTTGGGGTTATGAGGTATGTG	60°C	
	reverse*	CTACTAATACCACCACCATAAACTCTA		
	sequencing 1	GTTGTTTTTGTAGGATTGTAAT		1
	sequencing 2	GGATGTTTGGGGTGT		5
Human *HDAC11*	forward	GGGGGATTTTTTATATTTTTTAGGAAATT	58°C	
	reverse*	CCCAACTATACCAACATATACCAAAAACA		
	sequencing 1	AAATTGATTATTTTGTTTTATTT		1
	sequencing 2	GTTTATGAAGGTGATGTTGTA		5
Bovine *RPL6*	forward	AGTTGGTGGAGATAAGAATGG	60°C	
	reverse*	TAAACCCCAAACTCACTATCCT		
	sequencing 1	AGATAAGAATGGTGGTAT		2

Table 14: Genotyping primers for 3 different amplicons

(A.T.=Annealing temperature, SNP=single nucleotide polymorphism)

Gene	Primer	Sequence (5´-3´)	A.T./ SNP
Human *BEGAIN*	forward	TTGTTGGAGAATTTAGTTTAGAGTTAG	60°C rs7141087
	reverse	ACACCCAACAAACTTAACCTAC	
	sequencing 1	AACCCAAAAAATCCAAATA	
Human *EEF1A2*	forward	GGTAGGTTGGGTTAGAGTT	60°C rs1757693
	reverse	TCCTCCTTCCTCAAACTAAAACA	
	sequencing 1	GGATTTTTATAGGGATAGATAG	
Human *SPIB*	forward	ATGGGATTTTTGTAGTTAGTGTT	60°C rs11084013
	reverse	ACTACAACCTCTACCTCCTAAATT	
	sequencing 1	TGTTTTGAAATTTTTAGTTATTGG	

2.2.9 Deep Bisulphite Sequencing (DBS)

General principles

Deep Bisulphite Sequencing is a more elaborated and revealing NGS-based technique to measure DNA methylation levels. In contrast to Pyrosequencing, it allows recognition of DNA methylation in longer stretches of DNA up to 400bp and detection of the methylation status at a single molecule level. Thus, it fits well with the question of this study, whether the observed methylation changes in the male germline detected in Pyrosequencing are also affecting the next generation.

Application in this study

In this study, Deep Bisulphite Sequencing was performed on the Illumina MiSeq Platform. The NEBNext Multiplex Oligos kit for Illumina (Dual Index Primers Set 1) was used to endow each sample with a unique barcode. The BisPCR^2 protocol for targeted bisulphite sequencing[215] was adjusted to sequencing amplicons on the Illumina MiSeq system. DBS was performed on bisulphite-converted DNA of human foetal cord blood and sperm samples that were previously genotyped by pyrosequencing of an informative SNP in order to clarify if the observed age effects in human sperm detected by Pyrosequencing are transmitted to the next generation. The analysed genes were BEGAIN, EEF1A2 and SPIB. Only heterozygous foetal cord blood samples with homozygous fathers for the respective SNP were used allowing specific correlation of the methylation level of the paternal allele in FCB with the paternal age. Since 48 MIDs were used in our run, the unused MIDs were filled with heterozygous sperm samples to delineate age effects between young and old sperm at single-allele resolution. The amplification primers for the respective genes are shown in Table 15.

Table 15: DBS primers for 3 different amplicons

(A.T.=Annealing temperature; Nr=number of CpGs)

Forward Primer Overhang: 5'-ACACTCTTTCCCTACACGACGCTCTTCCGATCT-3'

Reverse Primer Overhang: 5'-GTGACTGGAGTTCAGACGTGTGCTCTTCCGATCT-3'

Gene	Primer	Sequence (5´-3´)	AT	Nr
Human *BEGAIN*	forward	TAGTAAGTTTTTTTTTGTTGGAGTTT	60°C	14
	reverse	ACAAAAACCCTATATTCTCACCAAAACAC		
Human *EEF1A2*	forward	GGGAGAGATGGTTATTGTTTTTTAT	60°C	15
	reverse	ACCCCAAAATAACTTCTATCCTCTT		
Human *SPIB*	forward	AGATGGGATTTTTGTAGTTAGTG	60°C	16
	reverse	CCTAATCTCCCAACCTCTCA		

Procedure

Library preparation

As the first step of library preparation, a gene-specific standard PCR was carried out. All gene-specific primers were supplied with a 5‘overhang for annealing of the barcoding primers that contained the multiplex identifiers (MID) in the final amplification step. PCR was performed with 2 µl of bisulphite converted DNA of each FCB and sperm sample following the standard protocol described in Table 7. Correct and gene-specific amplification was verified via gel electrophoresis for 12 min at 170 volts. Subsequently, all samples were bead cleaned up by a robot using the Janus Automatic Workstation with 75% Ethanol, Elution Buffer, and 0.7 Agencourt AMPure XP beads. After measuring the DNA concentration of each sample with the Qubit dsDNA BR Assay System kit, 3 µl of each sample was diluted to a concentration of 0,2 ng/µl with EB buffer. Subsequently, 3 µl of all samples from different amplicons with the same MID were pooled together, and a manual solid phase reversible immobilization (SPRI) bead clean-up was performed twice for each pool in order to remove potential primer dimers and unbound nucleotides: In the first purification step, 50 µl product from the first PCR was mixed with 40 µl Agencourt AMPure beads giving a 0.8 ratio. The whole mix was incubated at room temperature for 15 minutes outside and 5 minutes on the magnet. After removing the clear phase by pipet, the retained beads were cleaned with 200 µl 75% ethanol, followed by 30 seconds of incubation and once again the rejection of the clear phase. Dry beads were then eluted in 40 µl Elution Buffer, incubated for 2 min outside the magnet, and

subsequently dried for 5 min onto the magnet. 40 µl of the clear phase containing the PCR product were eluted in a new 1,5 ml tube.

Now, this PCR product was used for a final amplification with Illumina barcoding primers, enabling easy differentiation of each sample after sequencing. Figure 2 gives a graphical impression of the two successive PCRs. Therefore, all reagents were set up according to Table 16 using different combinations of index primers for all 48 MIDs. Touchdown PCR cycler conditions are depicted in Table 17. The mapping of the sample ID and the corresponding index primer pair is illustrated in Table 18. The index primer sequence is shown in Table 19. Amplification was again followed by a manual bead clean-up as previously described. Successful amplification was verified via Bio-Analyzer according to the Agilent High Sensitivity DNA Kit Quick Start Guide and information on the molarity of each sample was taken from the programme. All pools were diluted to a concentration of 4000 pM with EB Buffer and combined into one final pool containing all 48 MIDs.

Table 16: Reagent setup for PCR with barcoding primers

(dH_2O=distilled water, µM=micromolar, mM=millimolar)

Reagent	**Amount per sample**
Pool with adapter sequence	5 µl
Index Primer i500 (0,2 µM)	1 µl
Index Primer i700 (0,2 µM)	1 µl
dNTPs (10 mM)	1 µl
FastStart Taq DNA polymerase	0,5 µl
10x PCR Buffer with MgCl2	5 µl
dH_2O	36,5 µl

Table 17: Cycler programme for touchdown PCR

*(min=minute, dH_2O=distilled water, *decreased by -1,2°C each cycle)*

95°C	**95°C**	**68°C***	**72°C**	**72°C**	**8°C**
15 min	30s	30s	1 min	10 min	hold
		14 cycles			

***Figure 2**: Illustration of the two successive PCRs*

The sequence of interest (blue) is targeted with two previously designed primers (green) that are supplied with a predetermined overhang. The whole sequence is finally tagged with a multiplex identifier (MID - yellow) that allows correct assignment of each sample after the DBS run.

Sequencing of the final pool with Miseq

To obtain optimal sequencing results, the final pool should have to a total volume of 800 µl and a concentration not higher than 8 pM to avoid the potential risk of over-clustering. Therefore, the final pool was measured three times in the Bioanalyzer and the average concentration of all three measurements was used for further elution. Now, 5 ul of this pooled pool was denatured in 5 µl of 0.2 N NaOH at room temperature for 5 minutes and subsequently diluted to 8000 pM with pre-chilled HT1 buffer. In a final step 560 µl of this solution was mixed with 240 µl of 8 pM PhiX control, giving the 30% ratio of PhiX control required for low diversity libraries. The whole mixture was finally run in the Miseq Sequencer using the Illumina MiSeq Reagent Kit v2 (500 cycles) cartridge after performing a pre-run wash.

Table 18: DBS sample organization and index primer combinations

Detailed information on each sample is provided in the appendix (FCB=foetal cord blood sample, WI=sperm sample, D=index primer)

	BEGAIN	EEF1A2	SPIB	i7 index	i5 index
1	FCB 47	FCB 18	FCB 21	D701	D501
2	FCB 49	FCB 85	FCB 46	D701	D502
3	FCB 59	FCB 103	FCB 47	D701	D503
4	FCB 79	FCB 129	FCB 74	D701	D504
5	FCB 106	FCB 139	FCB 80	D701	D505
6	FCB 126	FCB 141	FCB 104	D701	D506

7	FCB 128	FCB 157	FCB 126	D701	D507
8	FCB 129	FCB 158	FCB 134	D701	D508
9	FCB 142	FCB 160	FCB 159	D702	D501
10	FCB 143	FCB 161	FCB 173	D702	D502
11	FCB 145	FCB 163	FCB 176	D702	D503
12	FCB 146	FCB 171	FCB 180	D702	D504
13	FCB 147	FCB 185	FCB 184	D702	D505
14	FCB 174	FCB 191	FCB 193	D702	D506
15	FCB 175	FCB 193	FCB 196	D702	D507
16	FCB 177	FCB 205	FCB 206	D702	D508
17	FCB 178	FCB 210	FCB 207	D703	D501
18	FCB 182	FCB 222	FCB 212	D703	D502
19	FCB 189	FCB 223	FCB 217	D703	D503
20	FCB 190	FCB 227	FCB 218	D703	D504
21	FCB 200	FCB 230	FCB 223	D703	D505
22	FCB 201	FCB 231	FCB 235	D703	D506
23	FCB 203	FCB 232	FCB 261	D703	D507
24	FCB 205	FCB 252	FCB 275	D703	D508
25	FCB 209	FCB 275	WI 050	D704	D501
26	FCB 210	FCB 276	WI 091	D704	D502
27	FCB 230	FCB 280	WI 265	D704	D503
28	FCB 232	FCB 286	WI 272	D704	D504
29	FCB 233	FCB 287	WI 281	D704	D505
30	FCB 234	WI 034	WI 291	D704	D506
31	FCB 240	WI 195	WI 398	D704	D507
32	FCB 252	WI 294	WI 474	D704	D508
33	FCB 256	WI 484	WI 488	D705	D501
34	FCB 268	WI 547	WI 493	D705	D502
35	FCB 280	WI 580	WI 597	D705	D503
36	FCB 282	WI 683	WI 683	D705	D504
37	FCB 285	WI 745	WI 750	D705	D505
38	FCB 287	WI 758	WI 900	D705	D506
39	WI 034	WI 769	WI 962	D705	D507
40	WI 077	WI 815	WI 967	D705	D508
41	WI 291	WI 887	WI 1097	D706	D501
42	WI 305	WI 900	WI 1131	D706	D502
43	WI 484	WI 1169	WI 1133	D706	D503
44	WI 580	WI 1211	WI 1236	D706	D504
45	WI 671	WI 1348	WI 1315	D706	D505
46	WI 745	WI 1396	WI 1396	D706	D506
47	WI 963	WI 1458	WI 1458	D706	D507
48				D706	D508

Table 19*:* Index primer sequence

Primer	MID
D501	TATAGCCT
D502	ATAGAGGC
D503	CCTATCCT
D504	GGCTCTGA
D505	AGGCGAAG
D506	TAATCTTA
D507	CAGGACGT
D508	GTACTGAC
D701	ATTACTCG
D702	TCCGGAGA
D703	CGCTCATT
D704	GAGATTCC
D705	ATTCAGAA
D706	GAATTCGT

2.2.10 Data processing and analysis

With the run completed, the Illumina Genome Analyzer processed the generated sequencing reads. Data was acquired in the form of FastQ files and processed further with the publicly available Amplikyzer2 software developed by Sven Rahmann (https://bitbucket.org/svenrahmann/amplikyzer/wiki/Home). Therefore, in the first instance, all FastQ. files were converted to one akzr.gz which in a second step was converted into text files for each allele and sample containing information on read numbers and methylation of every single CpG and read. To identify methylation levels of the corresponding allele, the analysed amplicon sequences were aligned with the reference genomic sequence for the respective assay. Finally, the alleles were split according to the genetic variant within the target region. Solely reads with an overall bisulphite conversion rate of >95% were used for further analysis. All other options in the Amplikyzer menu were left as default.

For DBS as well as for Pyrosequencing further statistical analysis was performed with SPSS Version 26. As all datasets proved not to be normally distributed in the Shapiro-Wilk test, a 2-tailed Spearman correlation was used for detecting methylation changes upon advancing sample age in the bovine cohort. As several studies report an association between human DNA methylation patterns and semen parameters such as decreased sperm count, motility[216], and morphological defects[217], mostly samples classified as

normozoospermia according to WHO criteria were used. Pearson's partial correlation was applied to adjust for the possible confounding factors of donor's BMI and sperm concentration. Generally, a p-value of <0,05 was considered statistically significant.

3 Results

3.1 Pyrosequencing results of 10 human and 4 bovine candidate loci

10 different amplicons were analysed in 94 human sperm samples and 4 amplicons in 36 bovine sperm samples from 15 bulls at different ages of their lifespan. All amplicons had previously been shown to correlate with age in RRBS experiments conducted in this lab and were selected to be validated with a different methodical approach on a larger scale and in an independent cohort. Selection of the genes relied on the location of the CpG sites in regulatory units (promoter, CTCF binding), the p-value in RRBS, the presence of a SNP (*BEGAIN*, *EEF1A2*, *SPIB*), and evolutionary conservation between humans and bulls (*CHD7*, *HDAC11*, *PAK1*, *PTK2B*, *RPL6*). Table 20 gives an overview of the genomic regions of the analysed amplicons. For bovine results, Spearman's r was applied to correlate methylation with age, while for the human cohort two-tailed Pearson's partial correlation was used to adjust for the potential confounding factors of donor's BMI and sperm concentration. For all 4 bovine regions, a significant age effect could be replicated in Pyrosequencing. Equally, in human sperm all 10 selected regions showed significant methylation changes with ageing. In human samples, the correlation coefficients proved generally moderate and uniquely negative (-,220 to -,423), whereas bovine correlation coefficients turned out to be more extensive and exclusively positive (,467 to ,768). Table 21 shows the main results in the form of the average methylation of all analysed CpGs as well as the correlation coefficients with age and the corresponding p-value for each amplicon. Figures 3 and 4 give a graphical impression of the results in the form of scatter plots. Bovine samples are indicated by blue colour, human samples are red.

Table 20: Information about the location of the selected amplicons

Genomic locations refer to GRCh38 in human and to ARS-UCD1.2 in bovine genome.

Amplicon	Species	Region	Genomic location
BEGAIN	Homo sapiens	Promoter	14: 100569917 – 100569985
EEF1A2		Promoter	20: 63498370 – 63498381
LMNA		Promoter	1: 156083727 – 156083734
MBD3		Promoter	19: 1583845 – 1583914
NFKB2		Promoter	10: 102398797 – 102398849
PRAM1		Protein coding	19: 8499697 – 8499727
PRKAR2A		Promoter	3: 48846377 – 48846496
RASGEF1C		CTCF binding	5: 180128402 – 180128452
RPL6		Promoter	12: 112408247 – 112408263
SPIB		Protein Coding	19: 50427290 – 50427353
CHD7	Bos taurus	Promoter	14: 26361261 – 26361323
HDAC11		Promoter	22: 58440641 – 58440645
PAK1		Promoter	29: 18586586 – 18586667
PTK2B		Promoter	8: 74490924 – 74490972

Table 21: Mean methylation and correlation with age for each amplicon

All datasets not normally distributed. For human amplicons Pearson's partial correlation adjusted for BMI and Sperm concentration was applied. Statistically significant results are shaded green.

	Gene	Methylation (%): Mean±SD [range]	Spearman's ρ/ Pearsons r	
			Correlation	p-value
Homo sapiens	*BEGAIN*	37,16±10,9 [13,35-60,03]	-,305	,035
	EEF1A2	14.7±7.7 [1.9-41.6]	-,230	,040
	LMNA	10,4±2,87 [4,73-18,4]	-,423	,003
	MBD3	55.3±8.7 [34.3-77.6]	-,250	,003
	NFKB2	44.5±10.0 [22.3–64.0]	-,370	,002
	PRAM1	61.4±9.3 [32.3-79.1]	-,220	,040
	PRKAR2A	21.2±5.3 [8.0-36.7]	-,340	,001
	RASGEF1C	60.1±9.1 [37.0–81.2]	-,280	,030
	RPL6	36.8±11.5 [15.8–66.5]	-,249	,049
	SPIB	40,25±7,12 [25,09-70,03]	-,334	,007
Bos taurus	*CHD7*	53,03±18,43[18,28-83,45]	,768	,000
	HDAC11	89,28±3,09 [78,65-92,94]	,476	,004
	PAK1	47,6±12,3 [18,34-83,45]	,604	,000
	PTK2B	66,63±8,78 [48,13-80,43]	,527	,001

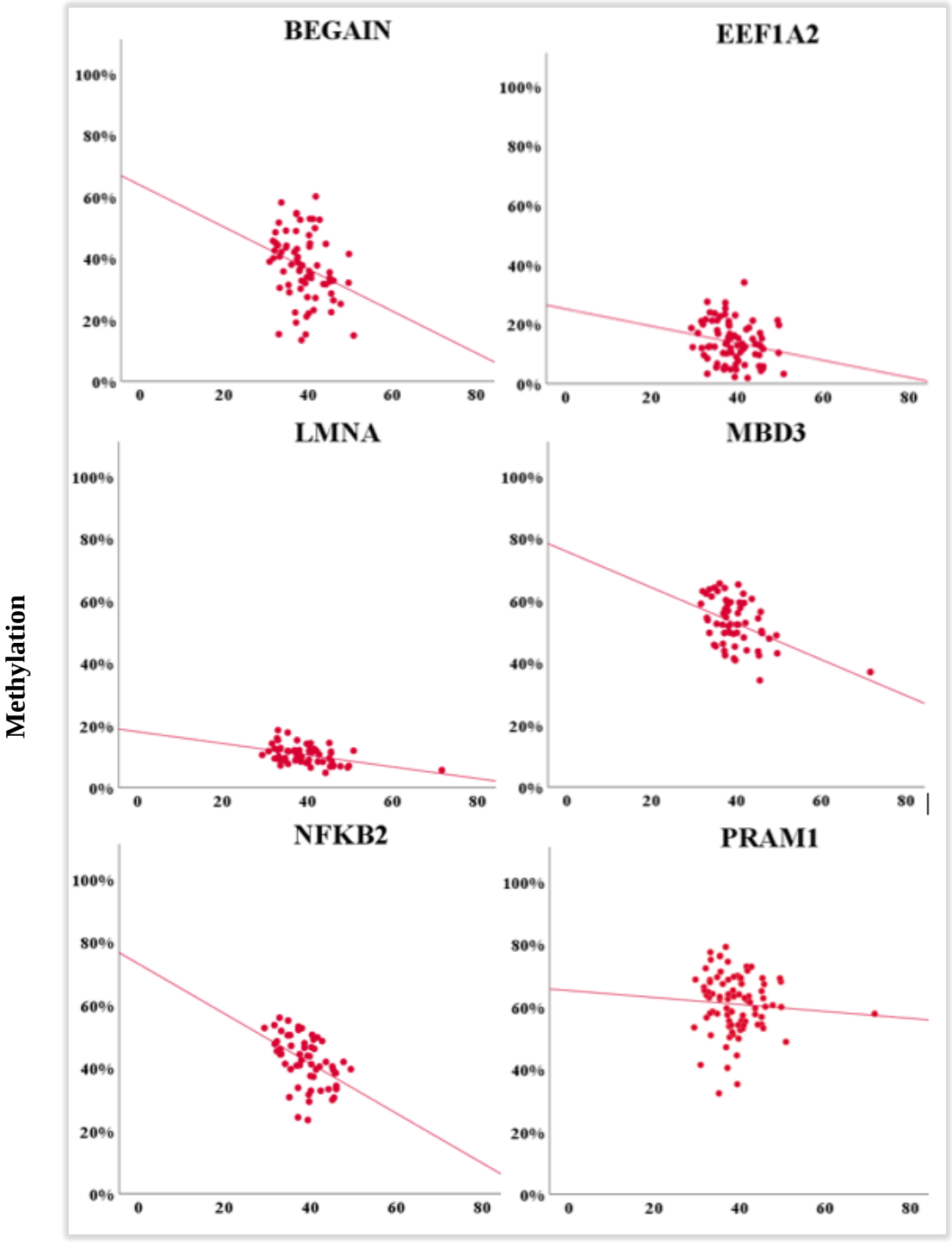
BEGAIN
EEF1A2
LMNA
MBD3
NFKB2
PRAM1
100%
80%
60%
40%
20%
0%
0
20
40
60
80
Methylation
Age (yr.)

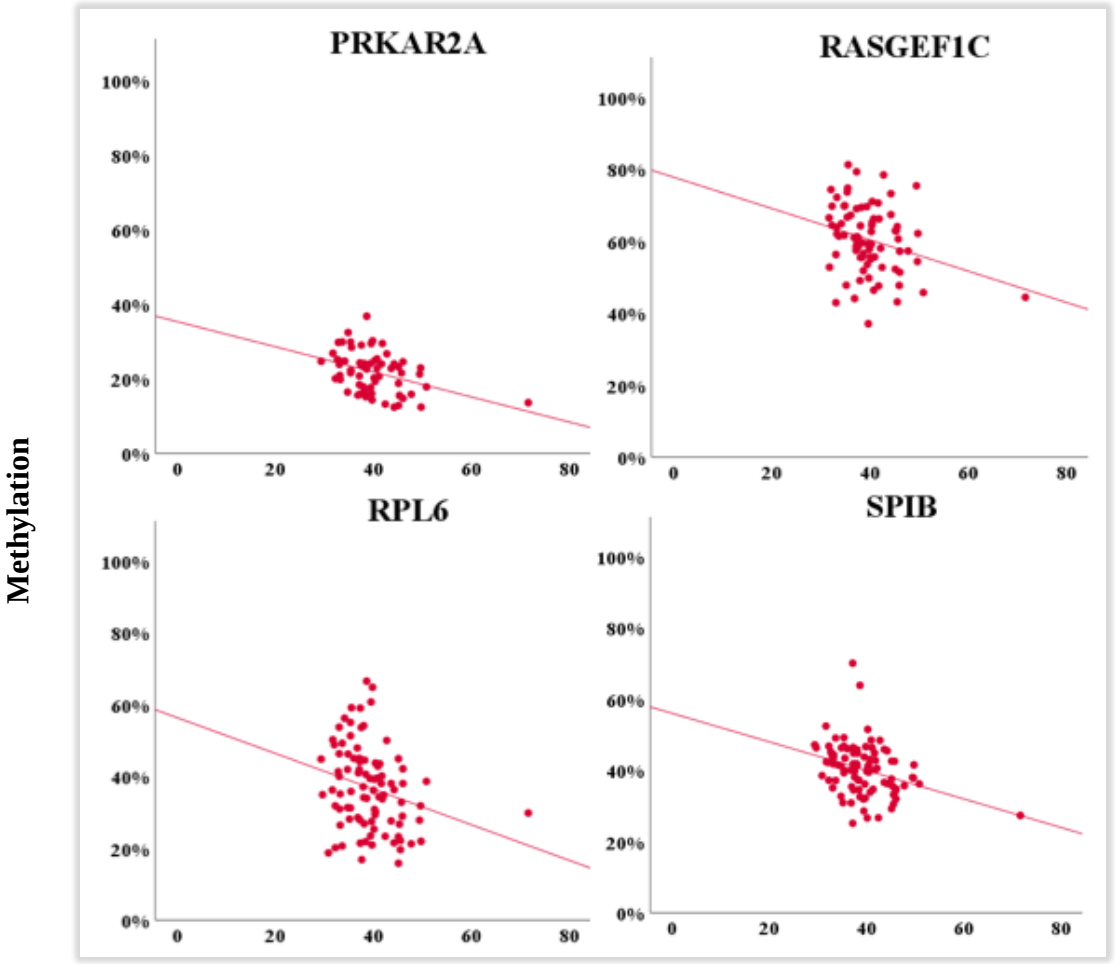

Figure 3: Average methylation in human sperm as a function of the donor's age for 10 different amplicons (modified from: *Species-Specific Paternal Age Effects and Sperm Methylation Levels of Developmentally Important Genes - Cells. 2022*).

Mean methylation is given on the y-axis as a function of the donor's age in years on the x-axis.

Remark: Please note the exclusively negative correlation coefficients for all amplicons in human sperm.

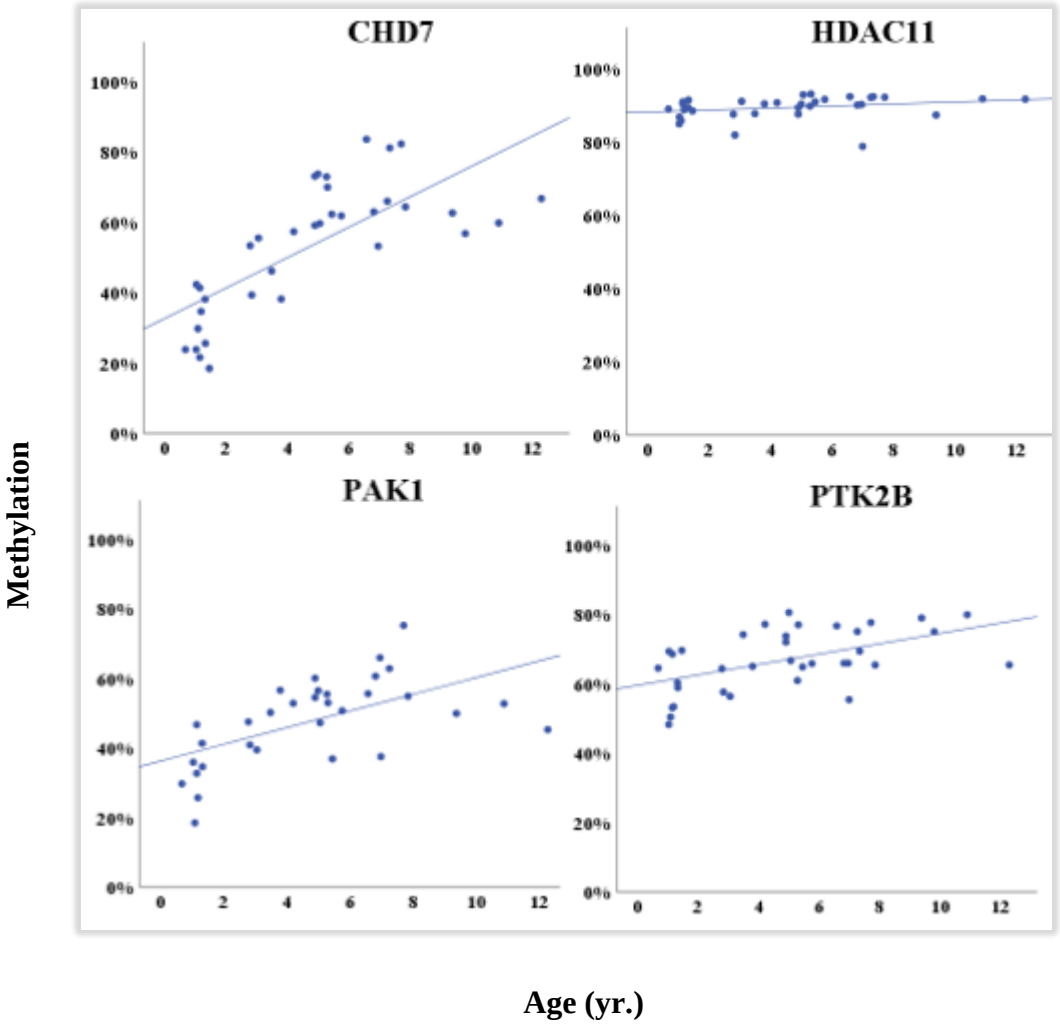

Figure 4: Average methylation in bovine sperm as function of the donor's age for 4 different amplicons (modified from: *Species-Specific Paternal Age Effects and Sperm Methylation Levels of Developmentally Important Genes - Cells. 2022*).

Mean methylation is given on the y-axis as a function of the donor's age in years on the x-axis.

Remark: Please note the exclusively positive correlation coefficients for all amplicons in bovine sperm.

3.2 Comparison of conserved CpG sites between human and bovine sperm

In the past decade, an increasing number of studies in the mammalian sperm epigenome has located numerous regions that are subject to paternal age effects in several species, including the human and bovine genomes. Nonetheless, there appears to be only a minor overlap between the data sets of different species. Therefore, we investigated if paternal age effects on the sperm methylome are shared between different mammalian species by comparing methylation patterns at orthologous CpG sites in human and bovine sperm. Here, we focused on deciphering whether the previously described sperm DNA methylation signatures underlying male germ cell ageing are maintained between humans and bulls in evolutionarily conserved regions.

3.2.1 Identification of conserved CpG sites between human and bovine sperm

Four bovine candidate genes (*CHD7, HDAC11, PAK1,* and *PTK2B*) and one human candidate gene (*RPL6*) that showed high sequence homology between the two species and that had shown an age effect in Pyrosequencing were searched for orthologous regions and conserved CpG sites between humans and bulls. Therefore, the Ensembl "BLASTN" tool and the Genome Reference Consortium Human Build 38 (GRCh38) or hg38, ARS-UCD1.2 or bosTau9, were used as references for mapping and comparing human and bovine CpG sites. Pyrosequencing assays were designed to target the evolutionarily conserved CpGs in the respective species. Table 22 gives an impression of the sequence homology and the conserved CpGs between humans and bulls for all analysed amplicons.

Comparison of conserved CpG sites between human and bovine sperm

Table 22: Conserved CpGs between Bos taurus and Homo sapiens (modified from: *Species-Specific Paternal Age Effects and Sperm Methylation Levels of Developmentally Important Genes - Cells. 2022*).

Conserved CpGs are marked with individual colour codes, non-conserved CpGs are portrayed grey. Overall, sequences of the selected amplicons are homologous (>80% sequence identity) between the two species. Genomic locations refer to GRCh38 in humans and to ARS-UCD1.2 in the bovine genome.

Species	Start	Sequence	End
CHD7			
Bos taurus	*14:26361243*	CTAGGCGGTTACCTGGCCCGGGGGGACTTCTCCATGCCGCAGCATG	*14:26361288*
Homo sapiens	*8:60741997*	ATGGGCAGCTATATGGCACGTGGGGATTTTTCCATGCAGCAGCATG	*8:60742042*
HDAC11			
Bos taurus	*22:58440641*	CGGCGTC[…]AGCGCGGCGAGTACACGATGGGCCAGCG	*22:58440716*
Homo sapiens	*3:13481361*	CGGCATC[…]AGCGCGGCGAGTACACG ATTGGCCAGCG	*3:13481287*
PAK1			
Bos taurus	*29:18586633*	CGGCTCTGCGACAGAAACCGCAGGCAGAGATGCCG	*29:18586667*
Homo sapiens	*11:77411828*	CGGCTCTGCGACGGAAACAATCGCCAGAGATGCCG	*11:77411794*
PTK2B			
Bos taurus	*8:74491018*	CGACGTAATGTGCCCACCTTCACTCG	*8:74490993*
Homo sapiens	*8:27397637*	CGGCGTAACGTGCCCAACTTTACTCG	*8:27397612*
RPL6			
Bos taurus	*12:112408273*	CGGCGGTACCCGGGTGGTTAAACTTCG	*12:112408247*
Homo sapiens	*17:61838759*	TGGTGGTACCCGAGTGGTCAAACTTCG	*17:61838785*

3.2.2 Comparison of human and bovine sperm methylation in conserved regions

The sperm methylation analysis of 5 selected amplicons was performed in human and bovine sperm on an individual CpG level, including conserved as well as non-conserved CpGs. Here, human and bovine sperm diverged largely in the methylation levels of the orthologous regions. Specifically, the CpGs determined by BLASTN in the complementary species regularly showed extreme methylation levels (<10% or >90%) whereas the methylation levels in the species where the age effect was originally observed proved medium methylated (10%-90%). For example, although the *PAK1* amplicon showed hypomethylation (1-5%) in sperm samples from humans, bovine sperm revealed moderate methylation levels and a strong age effect. Conversely, *RPL6* exhibited hypermethylation (90-100%) in bovine sperm but displayed moderate methylation values and a significant age effect in human sperm. Table 23 shows the average methylation levels for all analysed CpGs in the respective species. Figure 5 gives a more intuitive impression of the methylation differences between human and bovine sperm.

Table 23: Average methylation levels between bos taurus and homo sapiens for 5 conserved amplicons

(SD=standard deviation, the first four genes are endowed with bovine age-DMRs, RPL6 with human age-DMRs)

Gene	**Methylation (%) ±SD [range]**	
	Homo sapiens	Bos taurus
CHD7	93,78±1,1 [90,69-96,23]	53,03±18,43[18,28-83,45]
HDAC11	4,73±1,17 [2,5-8,04]	89,28±3,09 [78,65-92,94]
PAK1	1,06±0,19 [0,62-1,72]	47,6±12,3 [18,34-83,45]
PTK2B	92,31±1,37 [90,26-94,90]	66,63±8,78 [48,13-80,43]
RPL6	36.8±11.5 [15.8–66.5]	95,19±2,3 [89,8-99,61]

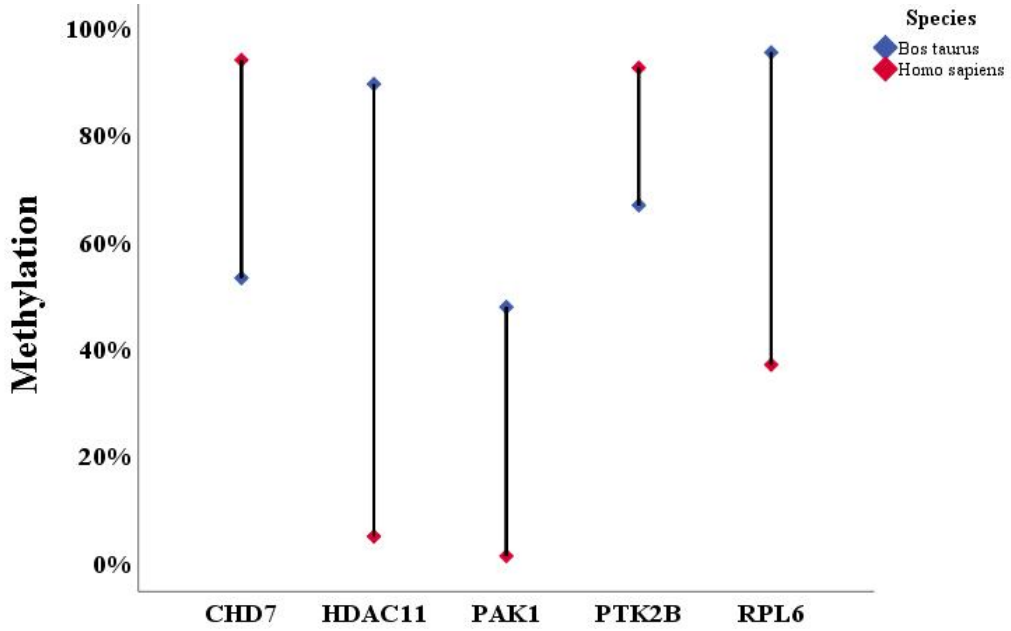

Figure 5: Average methylation for all analysed CpGs in the 5 different amplicons (modified from: *Species-Specific Paternal Age Effects and Sperm Methylation Levels of Developmentally Important Genes - Cells. 2022*).

Methylation is portrayed on the y-axis for each amplicon and split into bovine (blue quadrangle) and human (red quadrangle) results. The black lines illustrate the extent of the methylation difference between the two species. The first four genes are endowed with bovine age-DMRs, RPL6 has a human age-DMR.

3.2.3 Age effects on human and bovine sperm methylation in conserved regions

To decipher if the age-related DNA methylation marks in five selected single-copy genes are conserved between humans and bulls, the average methylation of all analysed CpGs for each amplicon was correlated with the donor's age. Spearman's correlation was used for the bovine cohort, whereas in the human cohort Pearson's partial correlation adjusted for the donor's body mass index and sperm concentration was applied. Table 24 shows the main results, including the correlation coefficients and the corresponding p-value. Here, none of the age effects on sperm methylation observed in one species was preserved in the other species. Interestingly, the direction of correlation with age was again different in the two species. Sperm DNA methylation in bovine samples increased with age whereas it decreased with age in humans. Although there was a significant age effect on both human and bovine *RPL6* sperm methylation, it tended in opposite directions. Figure 6 gives a graphical summary of the results in the form of scatter plots. Age is given as a percentage of the lifespan. For humans, 80 years, and for bulls 20 years are considered 100%.

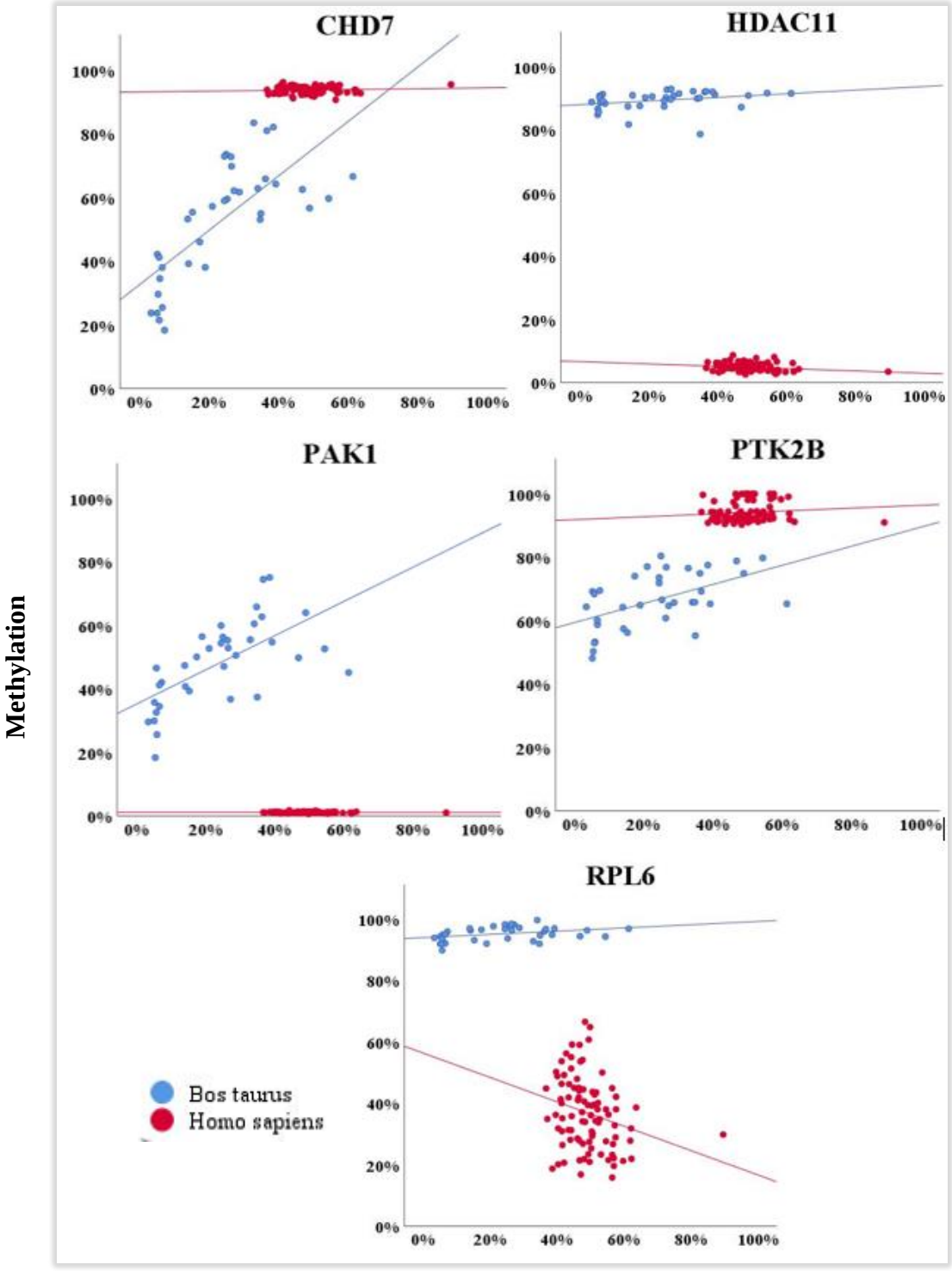

Figure 6: Average methylation in human and bovine sperm as a function of the donor's age for 5 different amplicons

The donor's age is given in percent of the expected lifespan on the x-axis. Bovine samples are marked by blue colour codes, human samples are portayed red.

Table 24: Age effects on the sperm methylome in conserved CpG sites between humans and bulls

Pearson's r partial correlation adjusted for the donor's BMI and sperm concentration was applied for human results. Bovine results were correlated with Spearman's ρ.

Gene	Homo sapiens		Bos taurus	
	Pearson's r		Spearman's ρ	
	Corr.	p-value	Corr.	p-value
CHD7	,138	,287	,768	,000
HDAC11	-,211	,097	,476	,004
PAK1	-,024	,853	,604	,000
PTK2B	-,112	,481	,527	,001
RPL6	-,249	,049	,363	,030

3.3 Transgenerational epigenetic inheritance

In the last few years, evidence has emerged that not only the methylation patterns of imprinted genes and repetitive elements but also those of single-copy genes can escape epigenetic reprogramming[142] and therefore potentially impact the offspring's DNA methylation landscape. The aim of this experiment was to identify whether the observed age effects on human sperm methylation in the above-mentioned genes are transmitted to the next generation, that is to say if the offspring of older fathers show lower methylation levels in foetal cord blood (FCB) than those conceived by younger fathers. However, since somatic cells are endowed with one paternal and one maternal genome copy, it is necessary to identify the methylation of both parental alleles separately. Given that Pyrosequencing results represent the mean methylation of both alleles, a method gaining methylation information on a single allele level, namely Deep Bisulphite Sequencing (DBS), had to be applied. Before performing DBS, it is indispensable to genotype the foetal cord blood samples to differentiate between maternal and paternal alleles. Therefore, Pyrosequencing of an informative SNP nearby the sequence of interest was conducted in a cohort of 185 FCB samples and the sperm of the respective father. Subsequently, only heterozygous FCB samples with homozygous fathers for the analysed SNP that allowed a correct mapping of maternal and paternal alleles were selected for DBS. Only 3 of the previously validated genes, namely *BEGAIN*, *EEF1A2*, and *SPIB* fulfilled the criteria of an informative SNP with high minor allele frequency in the central European population in direct proximity to the CpGs of interest. Primers were designed with the Pyromark Q CpG software including the SNP in the periphery of the amplicon

for prospective allele differentiation. The assays comprised 14 CpGs for *BEGAIN*, 15 CpGs for *EEF1A2*, and 16 CpGs for *SPIB*.

3.3.1 Genotyping results of FCB samples

Genotypes for 185 FCB and the corresponding paternal sperm samples were identified by Pyrosequencing. They corresponded largely to the expected frequency in the Central European population (ensemble.org). Out of 185 genotyped FCB samples, 38 samples proved eligible for *BEGAIN*, 29 for *EEF1A2* and as few as 24 for *SPIB* (Table 25). Clearly arranged information is provided in Table 26, detailed information on the genotype of individual samples is provided in Supplementary Table 2 in the appendix.

Table 25: Genotyping results for FCB

(SNP=single nucleotide polymorphism)

Gene	SNP	Genotypes	Selected samples
BEGAIN	rs7141087	CC: 14% CT: 53% TT: 33%	38
EEF1A2	rs1757693	AA: 43% AG: 62% GG: 4%	29
SPIB	rs11084013	AA: 37% AG: 53% GG: 9%	24

Table 26: Heterozygous FCB samples and corresponding sperm used for DBS

Heterozygous foetal cord blood samples with homozygous fathers and the allele distribution for the respective SNP. For BEGAIN 38, for EEF1A2 34, and for SPIB 24 samples fulfilled these criteria and were therefore selected for Deep Bisulphite Sequencing (detailed information provided in the appendix).

	BEGAIN				**EEF1A2**				**SPIB**			
	FCB		Paternal Sperm		FCB		Paternal Sperm		FCB		Paternal Sperm	
	ID	Geno-type	ID	Geno-type	ID	Geno-type	ID	Geno-type	ID	Geno-type	ID	Geno-type
1	FCB 47	CT	WI 153	TT	FCB 18	AG	WI 050	GG	FCB 21	AG	WI 059	AA
2	FCB 49	CT	WI 145	TT	FCB 85	AG	WI 373	GG	FCB 46	AG	WI 153	GG
3	FCB 59	CT	WI 272	TT	FCB 103	AG	WI 297	GG	FCB 47	AG	WI 153	GG
4	FCB 79	CT	WI 317	CC	FCB 129	AG	WI 493	GG	FCB 74	AG	WI 339	AA
5	FCB 106	CT	WI 360	TT	FCB 139	AG	WI 293	AA	FCB 80	AG	WI 282	AA
6	FCB 126	CT	WI 472	TT	FCB 141	AG	WI 579	GG	FCB 104	AG	WI 375	AA
7	FCB 128	CT	WI 109	TT	FCB 157	AG	WI 313	GG	FCB 126	AG	WI 472	AA
8	FCB 129	CT	WI 493	TT	FCB 158	AG	WI 648	GG	FCB 134	AG	WI 537	GG
9	FCB 142	CT	WI 597	TT	FCB 160	AG	WI 291	GG	FCB 159	AG	WI 637	GG
10	FCB 143	CT	WI 588	TT	FCB 161	AG	WI 291	GG	FCB 173	AG	WI 723	AA
11	FCB 145	CT	WI 622	TT	FCB 163	AG	WI 659	GG	FCB 176	AG	WI 464	GG
12	FCB 146	CT	WI 587	CC	FCB 171	AG	WI 684	GG	FCB 180	AG	WI 820	GG
13	FCB 147	CT	WI 599	CC	FCB 185	AG	WI 756	GG	FCB 184	AG	WI 233	GG
14	FCB 174	CT	WI 750	TT	FCB 191	AG	WI 790	GG	FCB 193	AG	WI 851	AA
15	FCB 175	CT	WI_775	CC	FCB 193	AG	WI 851	AA	FCB 196	AG	WI 888	GG
16	FCB 177	CT	WI 767	TT	FCB 205	AG	WI 777	GG	FCB 206	AG	WI 926	AA
17	FCB 178	CT	WI 736	TT	FCB 210	AG	WI 962	AA	FCB 207	AG	WI 670	AA
18	FCB 182	CT	WI 842	TT	FCB 222	AG	WI 494	GG	FCB 212	AG	WI 963	GG

19	FCB 189	CT	WI 398	TT	FCB 223	AG	WI 893	GG	FCB 217	AG	WI 747	GG
20	FCB 190	CT	WI 398	TT	FCB 227	AG	WI 476	GG	FCB 218	AG	WI 1012	AA
21	FCB 200	CT	WI 031	CC	FCB 230	AG	WI 1133	GG	FCB 223	AG	WI 893	GG
22	FCB 201	CT	WI 897	CC	FCB 231	AG	WI 1161	GG	FCB 235	AG	WI 1169	GG
23	FCB 203	CT	WI 900	TT	FCB 232	AG	WI 1156	GG	FCB 261	AG	WI 1430	AA
24	FCB 205	CT	WI 777	TT	FCB 252	AG	WI_911	GG	FCB 275	AG	WI_2024	GG
25	FCB 209	CT	WI 449	CC	FCB 275	AG	WI 2024	GG				
26	FCB 210	CT	WI 962	TT	FCB 276	AG	WI 2024	GG				
27	FCB 230	CT	WI 1133	CC	FCB 280	AG	WI 2043	GG				
28	FCB 232	CT	WI 1156	CC	FCB 286	AG	WI 771	GG				
29	FCB 233	CT	WI 1131	CC	FCB 287	AG	WI 2076	AA				
30	FCB 234	CT	WI 601	TT								
31	FCB 240	CT	WI 1224	CC								
32	FCB 252	CT	WI 911	TT								
33	FCB 256	CT	WI 1396	TT								
34	FCB 268	CT	WI 1463	TT								
35	FCB 280	CT	WI 2043	CC								
36	FCB 282	CT	WI 2082	TT								
37	FCB 285	CT	WI 2064	TT								
38	FCB 287	CT	WI 2076	CC								

3.3.2 DNA Methylation levels in FCB

During an individual's development, the DNA methylation landscape of differentiated cells is modified by dynamic processes involving *de novo* DNA methylation as well as demethylation to meet the specific demands of the respective tissue. Accordingly, the methylation levels of individual CpGs in foetal cord blood are not necessarily alike to those of sperm DNA. To portray these differences, Table 27 shows a confrontation of the mean methylation levels for sperm and foetal cord blood in DBS. Here, notably *SPIB* showed a clear hypermethylation in FCB compared to human sperm, whereas *BEGAIN* and *EEF1A2* revealed similar methylation levels in both tissues.

Table 27: Comparison of average methylation levels between FCB and sperm

Gene	**Methylation (%): Mean±SD [range]**	
	Sperm (DBS)	FCB (DBS)
BEGAIN	19,98±5,36 [8,86-27,25]	33,9±4,4 [21,3-47,3]
EEF1A2	8,64±5,3 [2,4-24,5]	3,93±1,12 [2-7,6]
SPIB	37,33±8,93 [23,96-69,9]	93,79±2,04 [87-95,7]

3.3.3 Parental influence on FCB DNA methylation

To determine whether for any of the three genes the age-dependent methylation changes observed in human sperm are transmitted to the next generation, the FCB methylation level of an individual CpG was correlated with the age of the respective parent using Spearman's correlation. Results of the correlation analysis are shown in Table 28 for the paternal allele and in Table 29 for the maternal allele. Here, two single CpGs in *SPIB* revealed a borderline significant decrease in methylation upon advancing paternal age. This indicates that there is no transmission of the observed age effects in human sperm to the next generation for the CpG loci. In the same manner, there is no influence of maternal age on the offspring's maternal allele's methylation level.

Table 28: Paternal allele methylation in FCB is correlated with paternal age

BEGAIN			***EEF1A2***			***SPIB***		
Spearman's ρ			**Spearman's ρ**			**Spearman's ρ**		
CpG	Corr.	p-value	CpG	Corr.	p-value	CpG	Corr.	p-value
1	-0,014	0,932	1	0,127	0,511	1	-0,099	0,652
2	0,135	0,42	2	0,035	0,855	2	-0,225	0,302
3	0,021	0,899	3	-0,16	0,406	3	-0,132	0,549
4	0,02	0,904	4	-0,101	0,604	4	0,132	0,547
5	-0,004	0,98	5	-0,317	0,094	5	-0,095	0,667
6	0,055	0,745	6	-0,329	0,081	6	-0,479	0,021
7	-0,078	0,643	7	0,13	0,503	7	0,017	0,938
8	-0,047	0,777	8	-0,127	0,512	8	-0,152	0,489
9	0,181	0,276	9	0,208	0,279	9	-0,088	0,691
10	0,105	0,531	10	-0,031	0,875	10	0,025	0,911
11	0,11	0,511	11	-0,123	0,526	11	0,045	0,837
12	0,188	0,259	12	-0,112	0,562	12	-0,414	0,05
13	0,05	0,768	13	0,084	0,664	13	-0,033	0,883
14	-0,056	0,741	14	0,17	0,377	14	0,053	0,81
Mean	0,071	0,67	15	-0,002	0,991	15	-0,302	0,161
			Mean	-,015	0,942	16	0,147	0,504
						Mean	-0,198	0,366

Table 29: Maternal allele methylation in FCB is correlated with maternal age

BEGAIN			***EEF1A2***			***SPIB***		
Spearman's ρ			**Spearman's ρ**			**Spearman's ρ**		
CpG	Corr.	p-value	CpG	Corr.	p-value	CpG	Corr.	p-value
1	-0,083	0,623	1	0,242	0,224	1	-0,031	-0,888
2	0,09	0,597	2	0,086	0,668	2	-0,138	0,53
3	-0,12	0,48	3	0,208	0,298	3	-0,203	0,352
4	-0,085	0,615	4	0,015	0,942	4	-0,178	0,417
5	-0,068	0,69	5	-0,158	0,431	5	-0,093	0,671
6	-0,228	0,175	6	-0,158	0,432	6	0,007	0,974
7	-0,029	0,864	7	-0,172	0,391	7	-0,218	0,318
8	-0,023	0,892	8	0,187	0,349	8	-0,255	0,241
9	0,036	0,834	9	0,521	0,005	9	-0,215	0,325
10	-0,016	0,926	10	-0,159	0,43	10	-0,286	0,186
11	-0,117	0,49	11	0,079	0,697	11	-0,205	0,349
12	-0,034	0,841	12	0,399	0,039	12	-0,463	0,026
13	-0,136	0,421	13	0,075	0,711	13	-0,283	0,191
14	-0,08	0,636	14	0,005	0,98	14	-0,062	0,778
Mean	-0,086	0,615	15	0,034	0,867	15	-0,274	0,206
			Mean	-0,006	0,977	16	-0,195	0,374
						Mean	-0,160	0,465

3.4 Haplotype-dependent allele specific DNA methylation

Recent research has elucidated that allele-specific methylation (ASM) is a widespread phenomenon across the human genome[218]. In heterozygous genomes, allele-specific studies could potentially uncover biologically relevant differences in DNA methylation levels between alleles based on local changes within the genetic sequence[219,220]. Therefore, for each amplicon and tissue (sperm and FCB), the DBS methylation data was compared between the A and the G alleles at a single CpG level. In FCB samples, especially *BEGAIN* displayed huge methylation differences between both alleles (Table 30). In sperm, *SPIB* showed the greatest disparity in methylation levels between the A and the G alleles (Table 31). As one could assume, the greatest methylation differences between both alleles were found in the CpGs directly adjacent to the polymorphism.

Table 30: *BEGAIN* allele specific methylation in FCB

Methylation differences between the A allele (blue) and the G allele (red) for BEGAIN in FCB. "N" marks the location of the polymorphism. On grounds of clarity, only adjacent CpGs are shown (diff=difference).

CpG	9	10	11		12	13	14
A	47%	46%	33%	***N***	25%	43%	37%
G	41%	34%	24%		20%	36%	30%
Diff	6%	12%	9%		5%	7%	7%

Table 31: *SPIB* allele specific methylation in sperm

Methylation differences between A allele (blue) an G allele (red) for SPIB in sperm. "N" marks the location of the polymorphism. On grounds of clarity, only adjacent CpGs are shown (diff=difference).

CpG	1		2	3
A	70%	***N***	42%	82%
G	59%		29%	80%
Diff	11%		13%	2%

4 Discussion

4.1 Validation of candidate loci via Pyrosequencing

In recent years, several lists of age-associated DMRs in a variety of tissues and species have been published, comprising extensive studies of paternal age effects in human[13,14] and bovine sperm[221]. These studies were based on different techniques, including Illumina methylation arrays[8,222], reduced representation bisulphite sequencing[120], whole genome bisulphite sequencing[13], and methyl capture sequencing[223]. Multiple epigenetic clocks have successfully been established based on linear regression algorithms on different methylation data. However, the similarity of the age-DMR lists in these studies is rather low: For example, Bernhardt *et al.* compared a set of 2,357 gene symbols known to contain sperm age-DMRs to seven published studies and found 90% of these genes to be reported in only one study. Conversely, only 10% of the genes associated with age-DMRs were present in more than one study. We aimed to replicate a few loci of human and bovine age-DMRs from our RRBS analysis. Validation was done through an independent and reliable high throughput method: Pyrosequencing.

For all ten selected human amplicons (*BEGAIN*, *EEF1A2*, *LMNA*, *MBD3*, *NFKB2*, *PRAM1*, *PRKAR2A*, *RASGEF1C*, *RPL6* and *SPIB*) and for all four bovine genes (*CHD7*, *HDAC11*, *PAK1* and *PTK2B*), a significant effect of advancing age on sperm DNA methylation could be replicated via Pyrosequencing in a larger independent cohort. This, on the one hand, confirms the aptitude of RRBS to screen for genomic regions that are subject to age-associated methylation changes, allowing high CpG coverage in an unbiased way. In the same way, it emphasizes the strength of amplicon-based Pyrosequencing as a dependable high throughput method in shorter target regions.

Notably, the strength of the correlation between age and DNA methylation level was lower for the human target regions (correlation coefficients from -0,220 to -0,423) than for the bovine candidate loci (0,476 to 0,768). Generally, CpG sites used to predict age in the context of already established epigenetic clocks on human sperm exhibit a stronger correlation with age (Pearson's r≈0,7)[14]. The low coefficients in human sperm might derive from the small age range of the contributors. Still, this and the sample size (94) of the cohort increase the informative value and robustness of the obtained results and support the assumption that the paternal age effect is mediated by several changes of

minor extent rather than extremely penetrant epimutations in a few genes. Moreover, most donated sperm samples were classified as normozoospermia according to WHO criteria and therefore enabled the elimination of any potential bias caused by the quality of sperm parameters. This proves that the observed DMRs are largely independent of the reproductive status of the contributor. The same was achieved by the application of Pearson's partial correlation, adjusting for the donor's BMI and sperm concentration. As for the bovine cohort, the contributor's age range was larger as samples were obtained from individual bulls at different points of their lifespan. This, and the fact that individual bulls contributed more than one sample, might explain why the observed age effects in bovine sperm were often more impressive than those observed in human sperm despite the substantially lower sample size. Furthermore, as all bull sperm samples were derived from high-performing bulls maintained in the same animal farm, the cohort appears more homogenous with little interference from external factors other than age influencing methylation results. Interestingly, when comparing the DMRs validated in this study to publicly available datasets of age-associated DMRs in human sperm, only 1 out of 10 genes, namely *BEGAIN*, matches with a previously reported list[8]. To our knowledge, none of the bovine sperm DMRs in this study overlaps with pre-existing published datasets. Differences between the selected methodologies, cohorts, and sample size might explain the little overlap between age-DMR sets reported in various studies.

4.1.1 Direction of age-associated methylation changes

Beyond the possible use of the analysed loci as age predictors in linear regression models, they could provide deeper insights into the DNA methylation machinery. As already mentioned, DNA is tautly packed with protamines during spermiogenesis and therefore inapproachable to TET enzymes and DNA methyltransferases, evolving the question of at what stage the observed methylation changes can at all be enacted[13]. A likely source is the spermatogonial stem cell, which, as already discussed, is 10-100-fold more prone to epigenetic errors than to genetic errors[12,100] leading to a germ cell-specific pattern of age-dependent epigenetic alterations. A remarkable finding in this study was the fact that bovine DMRs exclusively exhibited increasing methylation with age, whereas human CpGs were solely submitted to demethylation with ageing. The observation of a regional decrease in human sperm methylation is consistent with the findings of other researchers: In fact, out of 148 age-DMRs identified by Jenkins *et al.* 140 displayed a decline in

methylation with age whereas only eight regions exhibited increasing methylation. Contrarily, Cao *et al.* found more hypermethylated (62%) than hypomethylated (38%) CpG sites during ageing. However, they discovered that age-associated hypermethylation occurs more frequently distant from gene coding regions, whereas age-associated hypomethylation is a feature of proximity to genes[223], which again is compatible with the results of this study. Conversely, the opposite trend was observed in bovine sperm which exhibits exclusively increasing methylation with advancing age on a single CpG level. This observation conforms with the findings of Takeda *et al.* in 2019[15]. Although the cause and the biological impact of this opposite trend between humans and bulls are very difficult to interpret, it is obvious to seek their origins in the DNA methylation machineries, especially those responsible for the maintenance of DNA methylation patterns. Therefore, it could be revealing to identify if the local decrease of DNA methylation in human sperm goes along with a reduced activity of DNMT1. However, this would contrast with the finding that global methylation levels in human sperm tend to increase with age. Interestingly, the finding of a local increase in DNA methylation in bovine sperm is analogous to findings in human somatic tissues.

4.1.2 Putative functional consequences of age-associated methylation changes

Consistent with the findings of previous reviewers, age-dependent methylation changes appear to be a primary feature of medium methylated CpG sites. It has been repeatedly reported that especially loci of intermediary DNA methylation are subject to well-coordinated methylation changes often induced by external environmental conditions[224] and the ageing process. Therefore, they are considered an epigenetic hallmark of many complex disorders. Age-related human DMRs are not arbitrarily distributed throughout the genome but appear clustered nearby genes exerting crucial functions in embryogenesis and neuronal development[8,13]. Out of all the genes analysed in this study, two have known functions in embryogenesis (*LMNA*[225], *PTK2B*[226]) and two are implicated in neurodevelopment (*HDAC11*[227], *PAK1*[228]) in a broader sense. Most of the DMRs detected in this study are located in the promoter region of the respective gene. Generally, a decline in methylation of CpG islands as observed for all human DMRs is supposed to enhance transcription, whereas hypermethylation as observed for the bovine candidate genes is linked to reduced gene expression. Provided that these epigenetic marks are transmitted to the next generation, one might deduce that advanced paternal

age could enhance gene activation in humans and lead to gene silencing in bovines. A couple of examples from literature research shall emphasize the idea that altered DNA methylation in the analysed genes indeed has functional consequences for the individual: *RASGEF1C* was found to be differentially methylated at single positions in the temporal gyrus between Alzheimer patients and controls[204]. Peripheral blood promoter methylation of *NFKB2*, a gene crucial for immunoactivities, was reported to increase after physical activity[229,230] and tofu diet[231] so that these regimens might attenuate the proinflammatory response.

4.2 Species comparison

To fathom if the observed effects are a mere epiphenomenon or part of a species-specific adaptation process, we compared age effects between human and bovine sperm DNA methylation in five different conserved amplicons. Although sperm DNA methylation is a well-studied epigenetic feature, not much focus has been brought on the conservation of age effects on DNA methylation between the male germlines of different mammals. Previous reports claim evolutionary conservation of the paternal age effect on sperm methylation of orthologous rDNA regions between several different mammalian species[22]. This study narrowed down to human and bovine sperm samples. Cattle (*Bos taurus*) and humans deviated from a shared ancestor approximately 90 million years ago. Still, around 80% of the cattle genome is shared with humans[232]. Consequentially, the human genome is more similar to those of cows, although they share a more recent common ancestor with other orders such as rodents[233]. All five analyzed amplicons are located in the promoter region of the respective gene. As recently reported, CpG islands, particularly those linked with promoters, are highly conserved among mammalian species[234]. Since methylated as well as some non-methylated CpGs represent mutational hotspots[235], most CpG sites have undergone mutational changes over an evolutionary time period. Still, a total of ~400,000 CpG sites, predominantly located in coding regions, have been preserved across mammalian evolution[236], potentially shaping gene expression by controlling the chromatin structure and accessibility for transcription factors. We therefore aimed to decipher if the same applies to their methylation status and the paternal age effect.

4.2.1 Species-specific DNA methylation levels in conserved regions

When comparing the average methylation of all analysed CpGs per amplicon, methylation differences between humans and cattle turned out to be surprisingly huge (for example *HDAC11* had >90% methylation for cattle and <10% for humans). Furthermore, the species what was not subject to a paternal age effect in the respective region often showed extreme methylation values, with more than 90% (human CHD7) or less than 5% (human *PAK1*) of the CpGs being methylated. Hereby, hyper- and hypomethylated regions exhibited considerably less methylation variation than moderately methylated CpG sites. Some of our observations are inconsistent with recent findings by Fang *et al.*, who, while comparing WGBS data of human and bovine sperm, found that methylation levels of promoters in orthologous genes are fractionally correlated (Pearson's r = 0,44-0,53) between the human and bovine epigenomes. They concluded that a decent fraction of the epigenome has been conserved across the evolution in mammals[237]. Nonetheless, they also observed orthologous regions revealing opposite methylation levels in bovine and human sperm analogous to the findings of this study, suggesting that these genes might be implicated in sundry pathways that have functional relevance for the particular species.

Within humans, differences in methylation levels are known to account not only for differences between individuals but also for phenotypic differences between different human populations[238] as a response to environmental agents. Here, the interrelation of DNA methylation with the developed phenotype is mediated through only minor differences in the methylation level of <10 % or even 1–5 %[239]. Therefore, it seems verisimilar that the huge methylation differences observed in this study also reflect phenotypic differences between distinct species. Epigenetic phenotypes are not necessarily restricted to the exposed individual but can also be transmitted to the offspring[224]. Hence, it seems plausible to assume that species-specifically hypomethylated sperm promoters reflect lineage-specific phenotypic adaptation to the environmental conditions of each species. Human-specific hypomethylated promoters are associated with neurodevelopmental and brain-related traits[237]. Conversely, it appears plausible that for bovine development, genes linked with immune functions are of particular importance as ruminants have multiple stomachs and therefore are exposed to many more microorganisms than humans generally are. Importantly, species-specific

DNA methylation patterns may be based on differences in the underlying DNA sequence as well as dissimilar epigenetic reprogramming mechanisms in the germline. Vice versa, differences in DNA methylation might also be a driver for differences in the underlying genomic sequence between different species, functioning as mutational hotspots[235,240].

4.2.2 Species-specific age effects on DNA methylation in conserved regions

A major goal of this study was to verify whether paternal age effects that are observed in one species are also conserved in the corresponding region of another mammalian species. However, a conservation of paternal age effects on sperm age-DMRs between humans and bovines could not be observed in any of the candidate regions. As expected, CpGs revealing low (<10%) or considerably high average methylation values (>90%) are rarely subject to methylation changes with advancing age. Hence, contrary to findings in rDNA, age effects on sperm methylation in single-copy genes appear to be species-specific and not to be conserved between male mammalian germlines. If these age-related methylation changes are passed on to the next generation, one might deduce that advanced paternal age could enhance gene activation in humans, and lead to gene silencing in bovines. We furthermore observed that paternal age effects are driven on a regional level and not by individual CpGs, that is to say there was no detectable difference between conserved and non-conserved CpGs in terms of methylation level and paternal age effect. This is insofar not surprising, as the methylation of neighbouring CpGs is generally interdependent and phenotypic consequences through modified gene activation often result from changes at a regional level[241].

As the functional meaning of age-related methylation changes remains an enigma, it is elusive to speculate about the meaning of the observed species-specific character of the paternal age effect. However, the observations made in this study emphasize the idea that genes whose regulatory regions are subject to paternal age effects in the sperm epigenome may be involved in species-specific environmental adaptation. Overall, species differences in mammalian sperm epigenomes (methylation levels and paternal age effect) may be an important propulsive element in forming lineage-specific complex phenotypes[237].

4.3 DNA methylation on a single allele level

4.3.1 Transmission to the next generation

In humans, CpGs affected by the paternal age effect are enriched near genes exerting a critical role in embryogenesis and neuronal development, hinting at an important role of the ageing sperm methylome in influencing the development potential and life-long disease risk in the progeny of older fathers[8,13]. Still, transgenerational epigenetic inheritance requires the condition that certain epigenetic marks escape the genome-wide reprogramming in the germline as well as in the newly formed zygote. Besides some imprinted genes, a mounting number of CpG sites located in regulatory genetic elements are considered candidates for transgenerational epigenetic inheritance[120]. Indeed, several studies indicate that the erasure of the epigenetic landscape is patchy not only at imprinted loci or repetitive elements but also at single-copy genes[7,92,141]. Interestingly, age-associated methylation alterations in the male germline are significantly enriched in regions escaping histone replacement[8]. Indeed, up to 15% of the human sperm histones[242] escape replacement by protamines. In 2016, Atsem and Reichenbach found that increasing paternal age goes along with *FOXK1* hypomethylation in human sperm and is associated with lower methylation levels of the paternal allele in somatic cells (FCB) of the progeny, concluding that epigenetic alterations in sperm can be transmitted to differentiated somatic cells of the next generation. In this study, we investigated if the same effect exists for three selected genes, namely *BEGAIN*, *EEF1A2*, and *SPIB*. Here, FCB average methylation analysis revealed hypermethylation for *SPIB* (>90%) and hypomethylation for *EEF1A2* (<10%) with only low interindividual variation, making a transgenerational inheritance very unlikely. Only *BEGAIN* methylation values in FCB proved similar to sperm methylation levels and exhibited broader interindividual variation (standard deviation ±4,4%). However, when performing Spearman correlations, neither the paternal allele nor the maternal allele showed significant methylation alterations upon advancing parental age on a regional level for any of the genes. Only two individual CpGs for *SPIB* showed persistent hypomethylation in foetal cord blood upon advancing paternal age at a significant level. As generally the density of methylated CpGs on a regional level rather than a single CpG is responsible for activating transcription, one can deduce that none of the paternal age effects observed in human sperm for those three genes is transmitted to the next generation on a functional level. One possible explanation for the

obtained results might be the fact that none of the genes that were searched for transmission to the next generation is known to be involved in neurodevelopmental pathways that are considered primary candidates of transgenerational epigenetic inheritance[120]. Moreover, it is essential to realize that notwithstanding the paternal age effect being detectable in a large proportion of the sperm ejaculate, only one single sperm will contribute its methylation pattern to the embryo, which can either be fully methylated or fully unmethylated on a single CpG level. Hence, one would expect a greater chance for elder fathers to contribute an unmethylated allele for the analysed CpG sites to the newly formed zygote. To date, it remains an enigma to what extent the methylation pattern in differentiated somatic cells can resemble the original methylation profile of the transmitting sperm.

4.3.2 Haplotype-dependent DNA methylation

Allele specific methylation (ASM) is a common phenomenon occurring at >35,000 sites across the human genome[243]. Although allele specific methylation is a well-known feature of imprinted genes, it also occurs in a non-imprinted context, referred to as a so-called cis-regulatory effect. Indeed, methylation differences of CpG sites in direct proximity to a SNP can amount to 85% between the alleles[244] in non-imprinted regions and can be proportionally associated with gene expression[243]. This is insofar interesting as it provides a possible link by which even noncoding sequences could exert phenotypic effects[243].

As in this study only FCB and sperm samples that were heterozygous for a respective SNP were considered for DBS, it was possible to compare the methylation level between A and G alleles (haplotype-dependent methylation) and for FCB additionally according to the parent of origin (imprinting). Therefore, for each gene, the mean methylation of all samples was calculated and compared between the two alleles (A vs. G, maternal vs. paternal allele). For all three genes, maternal and paternal alleles were equally methylated in FCB. However, *BEGAIN* (FCB) and *SPIB* (sperm) methylation levels diverged between the SNP haplotypes. For *BEGAIN*, FCB methylation values of the CpGs adjacent to the SNP rs7141087 were 9-12% higher for the A-allele than for the G-allele, while both alleles were equally methylated in sperm. Conversely, CpGs in direct vicinity to SNP rs11084013 for *SPIB* showed 12-14% higher methylation levels for the A-allele than for the G-allele in sperm, but no differences in FCB methylation. In both cases, only the most proximate CpGs to the SNP were affected by this phenomenon. Such heterogeneity

of ASM across tissues (sperm and FCB) is a feature already known from previous research[243].

Conclusively, the DNA sequence and epigenome are strongly interlaced. Even the exchange of one nucleotide can significantly amend the methylation level at a neighbouring CpG site. Importantly, this phenomenon can bedevil data interpretation if a sample shows polymorphisms near the targeted methylation site[245] and should therefore be taken into account in comparative DNA methylation studies[244].

4.4 Strengths and limitations

Somatic contamination

To exclude any potential contamination of sperm DNA by bacteria or somatic remnants, methylation data for one paternally and one maternally expressed gene was analysed for each sample of the human and bovine sperm cohorts. Samples with unusual methylation levels of >20% for paternally and <70% for maternally expressed genes were considered somatically contaminated and excluded from further analysis. As a consequence, the finally acquired methylation levels are the result of pure sperm analysis.

Confounding factors

Abnormal semen parameters are related to changes in DNA methylation patterns[246]. To exclude any possible fertility assessed confounding factors, mostly (>90%) sperm classified as normozoospermia according to WHO criteria were used in the human sperm cohort. Furthermore, Pearson's partial correlations were applied to adjust for BMI and sperm concentration. Within the FCB cohort, we did not exclude the issue that the type of assisted reproductive technology (IVF or ICSI) functions as a confounding factor.

Selection of conserved CpG sites for species comparison

Probably the most crucial part of such a study straddling two different species is the selection of orthologous regions. Obviously, the use of nucleotide BLAST as conducted in this study implies the selection of orthologous regions based on their sequence homology and not on the functional concordance between the two species. For instance, the presence of multiple processed pseudogenes for *RPL6* inherits the risk of targeting a structurally similar but functionally unimportant amplicon. We addressed this issue by

verifying if the location of the selected amplicon was in a functionally identical region (mainly promoter) for both species.

Sample size

One definite strength of this study relies on the high sample numbers, especially for the human cohort. However, it must be stated that the total number of 11 analysed amplicons might provide enough information to deduce that sperm methylation signatures upon ageing are species-specific in single-copy genes, but robust statements on a larger scale concerning the direction of correlation within each species cannot be made. Here, Pyrosequencing simply cannot compete with the power of whole genome approaches. Another weak point of this study is the fact that the inevitable presence of an informative SNP nearby the sequence of interest to differentiate between maternal and paternal alleles severely limited the selection of potential candidate loci for transgenerational inheritance. Finally, none of the investigated genes was implicated in neurodevelopmental pathways that are the most promising candidates for transgenerational epigenetic inheritance. For DBS experiments, the FCB sample size was limited due to the need for heterozygous FCB samples with homozygous fathers for an informative SNP (38 FCB samples for *BEGAIN*, 29 for *EEF1A2*, and 24 for *SPIB*). Moreover, due to the provenance of the samples from a fertility centre, the age range (30-51.46 years) and standard deviation (±5.01 years) were generally low.

5hmC

For the sake of completeness, it shall be mentioned that bisulphite Pyrosequencing is not able to distinguish hydroxymethylated from methylated cytosines, so that theoretically 5hmC contribution might have biased methylation results. However, this appears very unlikely considering that sperm 5hmC levels are generally insignificantly low compared to somatic tissues such as brain[247].

4.5 Future perspectives

As extrapolating results from only a few candidate genes to the epigenome as a whole is risky, a promising approach to further address the origins of sperm age-DMRs on a larger scale are genome-wide methylation studies (Illumina methylation arrays, reduced representation bisulphite sequencing, whole genome bisulphite sequencing, and methyl

capture sequencing). First, bundling the already available information based on different techniques by comparing already existing sperm age-DMRs from different research groups and scanning for overlaps between the different datasets would help to assess the credibility and replicability of the results. Comparisons of gene symbols associated with age-DMRs between different datasets already exist, however, to date, no composition proceedings on a single CpG level have been made. Second, an epigenome-wide comparison over species boundaries (for example between humans and bulls) could give further insights into the role of DNA methylation as a driver of evolutionary processes on a far larger scale than this study could do. Therefore, it would be interesting to decipher whether or not sperm age-DMRs are enriched in genes that participate in biological processes that are of particular importance for the respective species. Finally, future studies in embryonic, foetal and adult tissues from the progeny of old and young fathers could reveal if the observed methylation changes are transmitted to the offspring. Functional analyses (for example luciferase assays) could then demonstrate if these methylation changes go along with an altered transcriptional activity of the respective genes, representing a direct link between sperm age-DMRs and the development potential of the next generation.

5 Summary

Western societies are steadily becoming older undergoing a clear trend of delayed parenthood. Children of older fathers have an undeniably higher risk for certain neurodevelopmental disorders and other medical conditions. Changes in the epigenetic landscape and especially in DNA methylation patterns are likely to account for a portion of this inherited disease susceptibility. DNA methylation changes during the ageing process are a well-known epigenetic feature. These so-called age-DMRs exist in developmentally important genes in the methylome of several mammalian species. However, there is only a minor overlap between the age-DMR datasets of different studies. We therefore replicated age-DMRs (which were obtained from a genome wide technique) by applying a different technical approach in a larger sample number. Here, this study confirmed 10 age-DMRs in the human and 4 in the bovine sperm epigenome from a preliminary candidate list based on RRBS. For this purpose, we used bisulphite Pyrosequencing in 94 human and 36 bovine sperm samples. These Pyrosequencing results confirm RRBS as an effective and reliable method to screen for age-DMRs in the vertebrate genome. To decipher whether paternal age effects are an evolutionary conserved feature of mammalian development, we compared methylation patterns between human and bovine sperm in orthologous regulatory regions. We discovered that the level of methylation and the age effect are both species-specific and speculate that these methylation marks reflect the lineage-specific development of each species to hit evolutionary requirements and adaptation processes. Different methylation levels between species in developmentally important genes also imply a differing mutational burden, representing a potential driver for point mutations and consequently deviations in the underlying DNA sequence of different species. Using the example of different haplotypes, this study showed the great effect of single base variations on the methylation of adjacent CpGs. Nonetheless, this study could not provide further evidence or a mechanism for the transfer of epigenetic marks to future generations. Therefore, further research in tissues from the progeny of old and young fathers is required to determine if the observed methylation changes are transmitted to the next generation and if they are associated with altered transcriptional activity of the respective genes. This could provide a direct link between the methylome of sperm from elderly fathers and the development potential of the next generation.

Zusammenfassung

Unsere westliche Gesellschaft wird immer älter und unterliegt einem eindeutigen Trend zur verzögerten Elternschaft. Kinder von älteren Vätern haben ein unbestreitbar höheres Risiko für bestimmte neurologische Entwicklungsstörungen und andere Erkrankungen. Epigenetische Veränderungen insbesondere im DNA-Methylierungsmuster sind wahrscheinlich für einen Teil dieser vererbten Krankheitsanfälligkeit verantwortlich. Altersbedingte Veränderungen im DNA-Methylierungsmuster sind ein bekanntes und gut erforschtes Phänomen in der Epigenetik. Diese so genannten Alters-DMRs konnten im Methylom mehrerer Säugetierarten nachgewiesen werden, insbesondere in entwicklungsrelevanten Genen. Allerdings gibt es nur geringe Überschneidungen zwischen den Alters-DMR-Datensätzen verschiedener Studien. Unser Ziel war es daher, die Vertrauenswürdigkeit eines laborinternen Datensatzes, der auf Reduced Representation Bisulphite Sequencing (RRBS) basierte, zu erhöhen, indem wir einen anderen technischen Ansatz in einer unabhängigen Kohorte anwenden. Mit der Methode des Bisulphite Pyrosequencing konnten wir in dieser Studie 10 Alters-DMRs im menschlichen und 4 im Rinder-Spermienepigenom aus einer vorläufigen Kandidatenliste basierend auf RRBS validieren. Diese Ergebnisse bestätigen, dass RRBS eine wirksame und zuverlässige Methode ist, um neue Alters-DMRs im Wirbeltiergenom zu finden. Um festzustellen, ob väterliche Alterseffekte in der Evolution verschiedener Säugetierarten konserviert wurden, verglichen wir die Methylierungsmuster orthologer Regionen zwischen dem menschlichem und dem Rinderspermienepigenom. Es zeigte sich, dass sowohl der Methylierungsgrad als auch der Alterseffekt artspezifisch sind. Daher vermuten wir, dass diese Methylierungsmuster die artspezifische Entwicklung als Antwort auf evolutionäre Anforderungen und durchlebte Anpassungsprozesse darstellen. Diese unterschiedlichen Methylierungslevel zwischen verschiedenen Arten in entwicklungswichtigen Genen implizieren auch eine unterschiedliche Mutationslast, die einen potenziellen Treiber für Punktmutationen und folglich Abweichungen in der zugrunde liegenden DNA-Sequenz der verschiedenen Arten darstellt. Am Beispiel verschiedener Haplotypen konnten wir exemplarisch den ausgeprägten Einfluss bereits einzelner DANN-Basenvariationen auf die Methylierung benachbarter CpGs demonstrieren. Allerdings konnte diese Studie keinen weiteren Beweis oder einen Mechanismus für die Übertragung von epigenetischen Markierungen auf künftige

Generationen liefern. Daher sind weitere Untersuchungen an embryonalen, fötalen und adulten Geweben von Nachkommen alter bzw. junger Väter unabdingbar, um festzustellen, ob die beobachteten Methylierungsveränderungen auch auf die nächste Generation übertragen werden. Ferner ist festzustellen, ob sie die Transkriptionsaktivität der betroffenen Gene beeinflussen. Dies könnte einen direkten Einfluss des Spermienmethyloms älterer Väter auf das Entwicklungspotenzial der nächsten Generation belegen.

6 References

1 Peterson, B. D., Pirritano, M., Tucker, L. & Lampic, C. Fertility awareness and parenting attitudes among American male and female undergraduate university students. *Hum Reprod* **27**, 1375-1382, doi:10.1093/humrep/des011 (2012).

2 Cardwell, C. R., Carson, D. J. & Patterson, C. C. Parental age at delivery, birth order, birth weight and gestational age are associated with the risk of childhood Type 1 diabetes: a UK regional retrospective cohort study. *Diabet Med* **22**, 200-206, doi:10.1111/j.1464-5491.2005.01369.x (2005).

3 Comings, D. E. & MacMurray, J. P. Maternal age at the birth of the first child as an epistatic factor in polygenic disorders. *Am J Med Genet B Neuropsychiatr Genet* **141B**, 1-6, doi:10.1002/ajmg.b.30026 (2006).

4 Sipos, A. *et al.* Paternal age and schizophrenia: a population based cohort study. *BMJ* **329**, 1070, doi:10.1136/bmj.38243.672396.55 (2004).

5 Johnson, K. J. *et al.* Parental age and risk of childhood cancer: a pooled analysis. *Epidemiology* **20**, 475-483, doi:10.1097/EDE.0b013e3181a5a332 (2009).

6 Nelson Goff, B. S. *et al.* Receiving the initial Down syndrome diagnosis: a comparison of prenatal and postnatal parent group experiences. *Intellect Dev Disabil* **51**, 446-457, doi:10.1352/1934-9556-51.6.446 (2013).

7 Atsem, S. *et al.* Paternal age effects on sperm FOXK1 and KCNA7 methylation and transmission into the next generation. *Hum Mol Genet* **25**, 4996-5005, doi:10.1093/hmg/ddw328 (2016).

8 Jenkins, T. G., Aston, K. I., Pflueger, C., Cairns, B. R. & Carrell, D. T. Age-associated sperm DNA methylation alterations: possible implications in offspring disease susceptibility. *PLoS Genet* **10**, e1004458, doi:10.1371/journal.pgen.1004458 (2014).

9 Aston, K. I. *et al.* Aberrant sperm DNA methylation predicts male fertility status and embryo quality. *Fertil Steril* **104**, 1388-1397 e1381-1385, doi:10.1016/j.fertnstert.2015.08.019 (2015).

10 Crow, J. F. The origins, patterns and implications of human spontaneous mutation. *Nat Rev Genet* **1**, 40-47, doi:10.1038/35049558 (2000).

11 de Kluiver, H., Buizer-Voskamp, J. E., Dolan, C. V. & Boomsma, D. I. Paternal age and psychiatric disorders: A review. *Am J Med Genet B Neuropsychiatr Genet* **174**, 202-213, doi:10.1002/ajmg.b.32508 (2017).

12 Bennett-Baker, P. E., Wilkowski, J. & Burke, D. T. Age-associated activation of epigenetically repressed genes in the mouse. *Genetics* **165**, 2055-2062, doi:10.1093/genetics/165.4.2055 (2003).

13 Laurentino, S. *et al.* A germ cell-specific ageing pattern in otherwise healthy men. *Aging Cell* **19**, e13242, doi:10.1111/acel.13242 (2020).

14 Pisarek, A. *et al.* Epigenetic age prediction in semen - marker selection and model development. *Aging (Albany NY)* **13**, 19145-19164, doi:10.18632/aging.203399 (2021).

15 Takeda, K. *et al.* Age-related changes in DNA methylation levels at CpG sites in bull spermatozoa and in vitro fertilization-derived blastocyst-stage embryos revealed by combined bisulfite restriction analysis. *J Reprod Dev* **65**, 305-312, doi:10.1262/jrd.2018-146 (2019).

16 Lambert, S. *et al.* Spermatozoa DNA methylation patterns differ due to peripubertal age in bulls. *Theriogenology* **106**, 21-29, doi:10.1016/j.theriogenology.2017.10.006 (2018).

17 Jenkins, T. G., Aston, K. I., Cairns, B., Smith, A. & Carrell, D. T. Paternal germ line aging: DNA methylation age prediction from human sperm. *BMC Genomics* **19**, 763, doi:10.1186/s12864-018-5153-4 (2018).
18 Milekic, M. H. *et al.* Age-related sperm DNA methylation changes are transmitted to offspring and associated with abnormal behavior and dysregulated gene expression. *Mol Psychiatry* **20**, 995-1001, doi:10.1038/mp.2014.84 (2015).
19 Adkins, R. M., Thomas, F., Tylavsky, F. A. & Krushkal, J. Parental ages and levels of DNA methylation in the newborn are correlated. *BMC Med Genet* **12**, 47, doi:10.1186/1471-2350-12-47 (2011).
20 Curley, J. P., Mashoodh, R. & Champagne, F. A. Epigenetics and the origins of paternal effects. *Horm Behav* **59**, 306-314, doi:10.1016/j.yhbeh.2010.06.018 (2011).
21 Field, A. E. *et al.* DNA Methylation Clocks in Aging: Categories, Causes, and Consequences. *Mol Cell* **71**, 882-895, doi:10.1016/j.molcel.2018.08.008 (2018).
22 Potabattula, R. *et al.* Increasing methylation of sperm rDNA and other repetitive elements in the aging male mammalian germline. *Aging Cell* **19**, e13181, doi:10.1111/acel.13181 (2020).
23 Colwell, M. *et al.* Evolutionary conservation of DNA methylation in CpG sites within ultraconserved noncoding elements. *Epigenetics* **13**, 49-60, doi:10.1080/15592294.2017.1411447 (2018).
24 Pertea, M. The human transcriptome: an unfinished story. *Genes (Basel)* **3**, 344-360, doi:10.3390/genes3030344 (2012).
25 Palazzo, A. F. & Lee, E. S. Non-coding RNA: what is functional and what is junk? *Front Genet* **6**, 2, doi:10.3389/fgene.2015.00002 (2015).
26 Inbar-Feigenberg, M., Choufani, S., Butcher, D. T., Roifman, M. & Weksberg, R. Basic concepts of epigenetics. *Fertil Steril* **99**, 607-615, doi:10.1016/j.fertnstert.2013.01.117 (2013).
27 Horak, M., Novak, J. & Bienertova-Vasku, J. Muscle-specific microRNAs in skeletal muscle development. *Dev Biol* **410**, 1-13, doi:10.1016/j.ydbio.2015.12.013 (2016).
28 Lee, Y. S. & Dutta, A. MicroRNAs in cancer. *Annu Rev Pathol* **4**, 199-227, doi:10.1146/annurev.pathol.4.110807.092222 (2009).
29 Mishra, S., Yadav, T. & Rani, V. Exploring miRNA based approaches in cancer diagnostics and therapeutics. *Crit Rev Oncol Hematol* **98**, 12-23, doi:10.1016/j.critrevonc.2015.10.003 (2016).
30 Consortium, E. P. An integrated encyclopedia of DNA elements in the human genome. *Nature* **489**, 57-74, doi:10.1038/nature11247 (2012).
31 Jin, B. & Robertson, K. D. DNA methyltransferases, DNA damage repair, and cancer. *Adv Exp Med Biol* **754**, 3-29, doi:10.1007/978-1-4419-9967-2_1 (2013).
32 Lister, R. *et al.* Human DNA methylomes at base resolution show widespread epigenomic differences. *Nature* **462**, 315-322, doi:10.1038/nature08514 (2009).
33 Bird, A. P. Functions for DNA methylation in vertebrates. *Cold Spring Harb Symp Quant Biol* **58**, 281-285, doi:10.1101/sqb.1993.058.01.033 (1993).
34 Lander, E. S. *et al.* Initial sequencing and analysis of the human genome. *Nature* **409**, 860-921, doi:10.1038/35057062 (2001).
35 Gardiner-Garden, M. & Frommer, M. CpG islands in vertebrate genomes. *J Mol Biol* **196**, 261-282, doi:10.1016/0022-2836(87)90689-9 (1987).
36 Deaton, A. M. & Bird, A. CpG islands and the regulation of transcription. *Genes Dev* **25**, 1010-1022, doi:10.1101/gad.2037511 (2011).
37 Saxonov, S., Berg, P. & Brutlag, D. L. A genome-wide analysis of CpG dinucleotides in the human genome distinguishes two distinct classes of promoters. *Proc Natl Acad Sci U S A* **103**, 1412-1417, doi:10.1073/pnas.0510310103 (2006).

38 Li, E., Bestor, T. H. & Jaenisch, R. Targeted mutation of the DNA methyltransferase gene results in embryonic lethality. *Cell* **69**, 915-926, doi:10.1016/0092-8674(92)90611-f (1992).
39 Yoder, J. A., Soman, N. S., Verdine, G. L. & Bestor, T. H. DNA (cytosine-5)-methyltransferases in mouse cells and tissues. Studies with a mechanism-based probe. *J Mol Biol* **270**, 385-395, doi:10.1006/jmbi.1997.1125 (1997).
40 Cheng, X. & Blumenthal, R. M. Mammalian DNA methyltransferases: a structural perspective. *Structure* **16**, 341-350, doi:10.1016/j.str.2008.01.004 (2008).
41 Yen, R. W. *et al.* Isolation and characterization of the cDNA encoding human DNA methyltransferase. *Nucleic Acids Res* **20**, 2287-2291, doi:10.1093/nar/20.9.2287 (1992).
42 Xie, S. *et al.* Cloning, expression and chromosome locations of the human DNMT3 gene family. *Gene* **236**, 87-95, doi:10.1016/s0378-1119(99)00252-8 (1999).
43 Probst, A. V., Dunleavy, E. & Almouzni, G. Epigenetic inheritance during the cell cycle. *Nat Rev Mol Cell Biol* **10**, 192-206, doi:10.1038/nrm2640 (2009).
44 Law, J. A. & Jacobsen, S. E. Establishing, maintaining and modifying DNA methylation patterns in plants and animals. *Nat Rev Genet* **11**, 204-220, doi:10.1038/nrg2719 (2010).
45 Jin, B., Li, Y. & Robertson, K. D. DNA methylation: superior or subordinate in the epigenetic hierarchy? *Genes Cancer* **2**, 607-617, doi:10.1177/1947601910393957 (2011).
46 Xu, X. DNA methylation and cognitive aging. *Oncotarget* **6**, 13922-13932, doi:10.18632/oncotarget.4215 (2015).
47 Kareta, M. S., Botello, Z. M., Ennis, J. J., Chou, C. & Chedin, F. Reconstitution and mechanism of the stimulation of de novo methylation by human DNMT3L. *J Biol Chem* **281**, 25893-25902, doi:10.1074/jbc.M603140200 (2006).
48 Suetake, I., Shinozaki, F., Miyagawa, J., Takeshima, H. & Tajima, S. DNMT3L stimulates the DNA methylation activity of Dnmt3a and Dnmt3b through a direct interaction. *J Biol Chem* **279**, 27816-27823, doi:10.1074/jbc.M400181200 (2004).
49 Moore, L. D., Le, T. & Fan, G. DNA methylation and its basic function. *Neuropsychopharmacology* **38**, 23-38, doi:10.1038/npp.2012.112 (2013).
50 Mayer, W., Niveleau, A., Walter, J., Fundele, R. & Haaf, T. Demethylation of the zygotic paternal genome. *Nature* **403**, 501-502, doi:10.1038/35000656 (2000).
51 Paroush, Z., Keshet, I., Yisraeli, J. & Cedar, H. Dynamics of demethylation and activation of the alpha-actin gene in myoblasts. *Cell* **63**, 1229-1237, doi:10.1016/0092-8674(90)90418-e (1990).
52 Morgan, H. D., Dean, W., Coker, H. A., Reik, W. & Petersen-Mahrt, S. K. Activation-induced cytidine deaminase deaminates 5-methylcytosine in DNA and is expressed in pluripotent tissues: implications for epigenetic reprogrammeming. *J Biol Chem* **279**, 52353-52360, doi:10.1074/jbc.M407695200 (2004).
53 Tahiliani, M. *et al.* Conversion of 5-methylcytosine to 5-hydroxymethylcytosine in mammalian DNA by MLL partner TET1. *Science* **324**, 930-935, doi:10.1126/science.1170116 (2009).
54 Ito, S. *et al.* Tet proteins can convert 5-methylcytosine to 5-formylcytosine and 5-carboxylcytosine. *Science* **333**, 1300-1303, doi:10.1126/science.1210597 (2011).
55 Hackett, J. A. *et al.* Germline DNA demethylation dynamics and imprint erasure through 5-hydroxymethylcytosine. *Science* **339**, 448-452, doi:10.1126/science.1229277 (2013).

56 Cortellino, S. *et al.* Thymine DNA glycosylase is essential for active DNA demethylation by linked deamination-base excision repair. *Cell* **146**, 67-79, doi:10.1016/j.cell.2011.06.020 (2011).
57 Mellen, M., Ayata, P., Dewell, S., Kriaucionis, S. & Heintz, N. MeCP2 binds to 5hmC enriched within active genes and accessible chromatin in the nervous system. *Cell* **151**, 1417-1430, doi:10.1016/j.cell.2012.11.022 (2012).
58 Pfeifer, G. P., Kadam, S. & Jin, S. G. 5-hydroxymethylcytosine and its potential roles in development and cancer. *Epigenetics Chromatin* **6**, 10, doi:10.1186/1756-8935-6-10 (2013).
59 Lin, I. H., Chen, Y. F. & Hsu, M. T. Correlated 5-Hydroxymethylcytosine (5hmC) and Gene Expression Profiles Underpin Gene and Organ-Specific Epigenetic Regulation in Adult Mouse Brain and Liver. *PLoS One* **12**, e0170779, doi:10.1371/journal.pone.0170779 (2017).
60 Cimmino, L., Abdel-Wahab, O., Levine, R. L. & Aifantis, I. TET family proteins and their role in stem cell differentiation and transformation. *Cell Stem Cell* **9**, 193-204, doi:10.1016/j.stem.2011.08.007 (2011).
61 Choy, J. S. *et al.* DNA methylation increases nucleosome compaction and rigidity. *J Am Chem Soc* **132**, 1782-1783, doi:10.1021/ja910264z (2010).
62 Deng, G. X. *et al.* Association between promoter DNA methylation and gene expression in the pathogenesis of ischemic stroke. *Aging (Albany NY)* **11**, 7663-7677, doi:10.18632/aging.102278 (2019).
63 Shen, L. *et al.* Genome-wide profiling of DNA methylation reveals a class of normally methylated CpG island promoters. *PLoS Genet* **3**, 2023-2036, doi:10.1371/journal.pgen.0030181 (2007).
64 Hsieh, C. L. Dependence of transcriptional repression on CpG methylation density. *Mol Cell Biol* **14**, 5487-5494, doi:10.1128/mcb.14.8.5487-5494.1994 (1994).
65 Jones, P. A. & Takai, D. The role of DNA methylation in mammalian epigenetics. *Science* **293**, 1068-1070, doi:10.1126/science.1063852 (2001).
66 Varley, K. E. *et al.* Dynamic DNA methylation across diverse human cell lines and tissues. *Genome Res* **23**, 555-567, doi:10.1101/gr.147942.112 (2013).
67 Yang, X. *et al.* Gene body methylation can alter gene expression and is a therapeutic target in cancer. *Cancer Cell* **26**, 577-590, doi:10.1016/j.ccr.2014.07.028 (2014).
68 Hellman, A. & Chess, A. Gene body-specific methylation on the active X chromosome. *Science* **315**, 1141-1143, doi:10.1126/science.1136352 (2007).
69 Aran, D., Toperoff, G., Rosenberg, M. & Hellman, A. Replication timing-related and gene body-specific methylation of active human genes. *Hum Mol Genet* **20**, 670-680, doi:10.1093/hmg/ddq513 (2011).
70 Xie, X. *et al.* Silencer-delimited transgenesis: NRSE/RE1 sequences promote neural-specific transgene expression in a NRSF/REST-dependent manner. *BMC Biol* **10**, 93, doi:10.1186/1741-7007-10-93 (2012).
71 Bestor, T. H. DNA methylation: evolution of a bacterial immune function into a regulator of gene expression and genome structure in higher eukaryotes. *Philos Trans R Soc Lond B Biol Sci* **326**, 179-187, doi:10.1098/rstb.1990.0002 (1990).
72 Michaud, E. J. *et al.* Differential expression of a new dominant agouti allele (Aiapy) is correlated with methylation state and is influenced by parental lineage. *Genes Dev* **8**, 1463-1472, doi:10.1101/gad.8.12.1463 (1994).
73 Schulz, W. A., Steinhoff, C. & Florl, A. R. Methylation of endogenous human retroelements in health and disease. *Curr Top Microbiol Immunol* **310**, 211-250, doi:10.1007/3-540-31181-5_11 (2006).

74 Walsh, C. P., Chaillet, J. R. & Bestor, T. H. Transcription of IAP endogenous retroviruses is constrained by cytosine methylation. *Nat Genet* **20**, 116-117, doi:10.1038/2413 (1998).
75 Yuen, R. K., Jiang, R., Penaherrera, M. S., McFadden, D. E. & Robinson, W. P. Genome-wide mapping of imprinted differentially methylated regions by DNA methylation profiling of human placentas from triploidies. *Epigenetics Chromatin* **4**, 10, doi:10.1186/1756-8935-4-10 (2011).
76 Tucci, V., Isles, A. R., Kelsey, G., Ferguson-Smith, A. C. & Erice Imprinting, G. Genomic Imprinting and Physiological Processes in Mammals. *Cell* **176**, 952-965, doi:10.1016/j.cell.2019.01.043 (2019).
77 Moulton, T. *et al.* Epigenetic lesions at the H19 locus in Wilms' tumour patients. *Nat Genet* **7**, 440-447, doi:10.1038/ng0794-440 (1994).
78 Soejima, H. & Higashimoto, K. Epigenetic and genetic alterations of the imprinting disorder Beckwith-Wiedemann syndrome and related disorders. *J Hum Genet* **58**, 402-409, doi:10.1038/jhg.2013.51 (2013).
79 Borsani, G. *et al.* Characterization of a murine gene expressed from the inactive X chromosome. *Nature* **351**, 325-329, doi:10.1038/351325a0 (1991).
80 Brockdorff, N. *et al.* Conservation of position and exclusive expression of mouse Xist from the inactive X chromosome. *Nature* **351**, 329-331, doi:10.1038/351329a0 (1991).
81 Okamoto, I. & Heard, E. Lessons from comparative analysis of X-chromosome inactivation in mammals. *Chromosome Res* **17**, 659-669, doi:10.1007/s10577-009-9057-7 (2009).
82 Boumil, R. M., Ogawa, Y., Sun, B. K., Huynh, K. D. & Lee, J. T. Differential methylation of Xite and CTCF sites in Tsix mirrors the pattern of X-inactivation choice in mice. *Mol Cell Biol* **26**, 2109-2117, doi:10.1128/MCB.26.6.2109-2117.2006 (2006).
83 Cruz, C. *et al.* Tri-methylation of histone H3 lysine 4 facilitates gene expression in ageing cells. *Elife* **7**, doi:10.7554/eLife.34081 (2018).
84 Otani, J. *et al.* Structural basis for recognition of H3K4 methylation status by the DNA methyltransferase 3A ATRX-DNMT3-DNMT3L domain. *EMBO Rep* **10**, 1235-1241, doi:10.1038/embor.2009.218 (2009).
85 Ooi, S. K. *et al.* DNMT3L connects unmethylated lysine 4 of histone H3 to de novo methylation of DNA. *Nature* **448**, 714-717, doi:10.1038/nature05987 (2007).
86 Hashimoto, H., Vertino, P. M. & Cheng, X. Molecular coupling of DNA methylation and histone methylation. *Epigenomics* **2**, 657-669, doi:10.2217/epi.10.44 (2010).
87 Okitsu, C. Y. & Hsieh, C. L. DNA methylation dictates histone H3K4 methylation. *Mol Cell Biol* **27**, 2746-2757, doi:10.1128/MCB.02291-06 (2007).
88 Meissner, A. *et al.* Genome-scale DNA methylation maps of pluripotent and differentiated cells. *Nature* **454**, 766-770, doi:10.1038/nature07107 (2008).
89 Mohn, F. *et al.* Lineage-specific polycomb targets and de novo DNA methylation define restriction and potential of neuronal progenitors. *Mol Cell* **30**, 755-766, doi:10.1016/j.molcel.2008.05.007 (2008).
90 Mikkelsen, T. S. *et al.* Genome-wide maps of chromatin state in pluripotent and lineage-committed cells. *Nature* **448**, 553-560, doi:10.1038/nature06008 (2007).
91 Lee, J. H. & Skalnik, D. G. CpG-binding protein (CXXC finger protein 1) is a component of the mammalian Set1 histone H3-Lys4 methyltransferase complex, the analogue of the yeast Set1/COMPASS complex. *J Biol Chem* **280**, 41725-41731, doi:10.1074/jbc.M508312200 (2005).
92 Messerschmidt, D. M., Knowles, B. B. & Solter, D. DNA methylation dynamics during epigenetic reprogramming in the germline and preimplantation embryos. *Genes Dev* **28**, 812-828, doi:10.1101/gad.234294.113 (2014).

93 Yamaguchi, S. *et al.* Dynamics of 5-methylcytosine and 5-hydroxymethylcytosine during germ cell reprogramming. *Cell Res* **23**, 329-339, doi:10.1038/cr.2013.22 (2013).
94 Zeng, Y. & Chen, T. DNA Methylation Reprogramming during Mammalian Development. *Genes (Basel)* **10**, doi:10.3390/genes10040257 (2019).
95 Rougier, N. *et al.* Chromosome methylation patterns during mammalian preimplantation development. *Genes Dev* **12**, 2108-2113, doi:10.1101/gad.12.14.2108 (1998).
96 Bundesamt, S. (2022).
97 Petridou, E. T. *et al.* Advanced parental age as risk factor for childhood acute lymphoblastic leukaemia: results from studies of the Childhood Leukaemia International Consortium. *Eur J Epidemiol* **33**, 965-976, doi:10.1007/s10654-018-0402-z (2018).
98 Shi, Q. & Martin, R. H. Aneuploidy in human sperm: a review of the frequency and distribution of aneuploidy, effects of donor age and lifestyle factors. *Cytogenet Cell Genet* **90**, 219-226, doi:10.1159/000056773 (2000).
99 Momand, J. R., Xu, G. & Walter, C. A. The paternal age effect: a multifaceted phenomenon. *Biol Reprod* **88**, 108, doi:10.1095/biolreprod.112.103440 (2013).
100 Goriely, A. & Wilkie, A. O. Paternal age effect mutations and selfish spermatogonial selection: causes and consequences for human disease. *Am J Hum Genet* **90**, 175-200, doi:10.1016/j.ajhg.2011.12.017 (2012).
101 Malaspina, D., Gilman, C. & Kranz, T. M. Paternal age and mental health of offspring. *Fertil Steril* **103**, 1392-1396, doi:10.1016/j.fertnstert.2015.04.015 (2015).
102 Kong, A. *et al.* Rate of de novo mutations and the importance of father's age to disease risk. *Nature* **488**, 471-475, doi:10.1038/nature11396 (2012).
103 Yatsenko, A. N. & Turek, P. J. Reproductive genetics and the aging male. *J Assist Reprod Genet* **35**, 933-941, doi:10.1007/s10815-018-1148-y (2018).
104 Ucar, D. *et al.* The chromatin accessibility signature of human immune aging stems from CD8(+) T cells. *J Exp Med* **214**, 3123-3144, doi:10.1084/jem.20170416 (2017).
105 Mattson, M. P. & Arumugam, T. V. Hallmarks of Brain Aging: Adaptive and Pathological Modification by Metabolic States. *Cell Metab* **27**, 1176-1199, doi:10.1016/j.cmet.2018.05.011 (2018).
106 Booth, L. N. & Brunet, A. The Aging Epigenome. *Mol Cell* **62**, 728-744, doi:10.1016/j.molcel.2016.05.013 (2016).
107 Villeponteau, B. The heterochromatin loss model of aging. *Exp Gerontol* **32**, 383-394, doi:10.1016/s0531-5565(96)00155-6 (1997).
108 Jung, H. J. & Suh, Y. MicroRNA in Aging: From Discovery to Biology. *Curr Genomics* **13**, 548-557, doi:10.2174/138920212803251436 (2012).
109 Ibanez-Ventoso, C. & Driscoll, M. MicroRNAs in C. elegans Aging: Molecular Insurance for Robustness? *Curr Genomics* **10**, 144-153, doi:10.2174/138920209788185243 (2009).
110 Bocklandt, S. *et al.* Epigenetic predictor of age. *PLoS One* **6**, e14821, doi:10.1371/journal.pone.0014821 (2011).
111 Horvath, S. DNA methylation age of human tissues and cell types. *Genome Biol* **14**, R115, doi:10.1186/gb-2013-14-10-r115 (2013).
112 Fraga, M. F. *et al.* Epigenetic differences arise during the lifetime of monozygotic twins. *Proc Natl Acad Sci U S A* **102**, 10604-10609, doi:10.1073/pnas.0500398102 (2005).
113 Poulsen, P., Esteller, M., Vaag, A. & Fraga, M. F. The epigenetic basis of twin discordance in age-related diseases. *Pediatr Res* **61**, 38R-42R, doi:10.1203/pdr.0b013e31803c7b98 (2007).

114 Issa, J. P. Aging and epigenetic drift: a vicious cycle. *J Clin Invest* **124**, 24-29, doi:10.1172/JCI69735 (2014).
115 Horvath, S. & Raj, K. DNA methylation-based biomarkers and the epigenetic clock theory of ageing. *Nat Rev Genet* **19**, 371-384, doi:10.1038/s41576-018-0004-3 (2018).
116 Hannum, G. *et al.* Genome-wide methylation profiles reveal quantitative views of human aging rates. *Mol Cell* **49**, 359-367, doi:10.1016/j.molcel.2012.10.016 (2013).
117 Bell, C. G. *et al.* DNA methylation aging clocks: challenges and recommendations. *Genome Biol* **20**, 249, doi:10.1186/s13059-019-1824-y (2019).
118 Bollati, V. *et al.* Decline in genomic DNA methylation through aging in a cohort of elderly subjects. *Mech Ageing Dev* **130**, 234-239, doi:10.1016/j.mad.2008.12.003 (2009).
119 Richardson, B. Impact of aging on DNA methylation. *Ageing Res Rev* **2**, 245-261, doi:10.1016/s1568-1637(03)00010-2 (2003).
120 Denomme, M. M., Haywood, M. E., Parks, J. C., Schoolcraft, W. B. & Katz-Jaffe, M. G. The inherited methylome landscape is directly altered with paternal aging and associated with offspring neurodevelopmental disorders. *Aging Cell* **19**, e13178, doi:10.1111/acel.13178 (2020).
121 Hilker, R. *et al.* Heritability of Schizophrenia and Schizophrenia Spectrum Based on the Nationwide Danish Twin Register. *Biol Psychiatry* **83**, 492-498, doi:10.1016/j.biopsych.2017.08.017 (2018).
122 Maher, B. Personal genomes: The case of the missing heritability. *Nature* **456**, 18-21, doi:10.1038/456018a (2008).
123 Zuk, O., Hechter, E., Sunyaev, S. R. & Lander, E. S. The mystery of missing heritability: Genetic interactions create phantom heritability. *Proc Natl Acad Sci U S A* **109**, 1193-1198, doi:10.1073/pnas.1119675109 (2012).
124 Manolio, T. A. *et al.* Finding the missing heritability of complex diseases. *Nature* **461**, 747-753, doi:10.1038/nature08494 (2009).
125 Eichler, E. E. *et al.* Missing heritability and strategies for finding the underlying causes of complex disease. *Nat Rev Genet* **11**, 446-450, doi:10.1038/nrg2809 (2010).
126 Altshuler, D., Daly, M. J. & Lander, E. S. Genetic mapping in human disease. *Science* **322**, 881-888, doi:10.1126/science.1156409 (2008).
127 Hirschhorn, J. N. Genomewide association studies--illuminating biologic pathways. *N Engl J Med* **360**, 1699-1701, doi:10.1056/NEJMp0808934 (2009).
128 Simeone, P. & Alberti, S. Epigenetic heredity of human height. *Physiol Rep* **2**, doi:10.14814/phy2.12047 (2014).
129 Hasselquist, D. & Nilsson, J. A. Maternal transfer of antibodies in vertebrates: trans-generational effects on offspring immunity. *Philos Trans R Soc Lond B Biol Sci* **364**, 51-60, doi:10.1098/rstb.2008.0137 (2009).
130 Stein, A. D. & Lumey, L. H. The relationship between maternal and offspring birth weights after maternal prenatal famine exposure: the Dutch Famine Birth Cohort Study. *Hum Biol* **72**, 641-654 (2000).
131 Gluckman, P. D., Hanson, M. A. & Beedle, A. S. Non-genomic transgenerational inheritance of disease risk. *Bioessays* **29**, 145-154, doi:10.1002/bies.20522 (2007).
132 Jirtle, R. L. & Skinner, M. K. Environmental epigenomics and disease susceptibility. *Nat Rev Genet* **8**, 253-262, doi:10.1038/nrg2045 (2007).
133 Blatt, J., Van Le, L., Weiner, T. & Sailer, S. Ovarian carcinoma in an adolescent with transgenerational exposure to diethylstilbestrol. *J Pediatr Hematol Oncol* **25**, 635-636, doi:10.1097/00043426-200308000-00009 (2003).

134 Anway, M. D., Cupp, A. S., Uzumcu, M. & Skinner, M. K. Epigenetic transgenerational actions of endocrine disruptors and male fertility. *Science* **308**, 1466-1469, doi:10.1126/science.1108190 (2005).
135 Weaver, I. C. *et al.* Epigenetic programmeming by maternal behavior. *Nat Neurosci* **7**, 847-854, doi:10.1038/nn1276 (2004).
136 Ferrari, R., Berk, A. J. & Kurdistani, S. K. Viral manipulation of the host epigenome for oncogenic transformation. *Nat Rev Genet* **10**, 290-294, doi:10.1038/nrg2539 (2009).
137 Ravelli, A. C., van Der Meulen, J. H., Osmond, C., Barker, D. J. & Bleker, O. P. Obesity at the age of 50 y in men and women exposed to famine prenatally. *Am J Clin Nutr* **70**, 811-816, doi:10.1093/ajcn/70.5.811 (1999).
138 Potabattula, R. S. K. Male aging and obesity effects on sperm methylome and consequences for the next generation. (2018).
139 Jenkins, T. G. & Carrell, D. T. The sperm epigenome and potential implications for the developing embryo. *Reproduction* **143**, 727-734, doi:10.1530/REP-11-0450 (2012).
140 Hammoud, S. S. *et al.* Distinctive chromatin in human sperm packages genes for embryo development. *Nature* **460**, 473-478, doi:10.1038/nature08162 (2009).
141 Lane, N. *et al.* Resistance of IAPs to methylation reprogramming may provide a mechanism for epigenetic inheritance in the mouse. *Genesis* **35**, 88-93, doi:10.1002/gene.10168 (2003).
142 Tang, W. W. *et al.* A Unique Gene Regulatory Network Resets the Human Germline Epigenome for Development. *Cell* **161**, 1453-1467, doi:10.1016/j.cell.2015.04.053 (2015).
143 Chen, Q., Yan, W. & Duan, E. Epigenetic inheritance of acquired traits through sperm RNAs and sperm RNA modifications. *Nat Rev Genet* **17**, 733-743, doi:10.1038/nrg.2016.106 (2016).
144 Miller, D., Ostermeier, G. C. & Krawetz, S. A. The controversy, potential and roles of spermatozoal RNA. *Trends Mol Med* **11**, 156-163, doi:10.1016/j.molmed.2005.02.006 (2005).
145 Hultman, C. M., Sandin, S., Levine, S. Z., Lichtenstein, P. & Reichenberg, A. Advancing paternal age and risk of autism: new evidence from a population-based study and a meta-analysis of epidemiological studies. *Mol Psychiatry* **16**, 1203-1212, doi:10.1038/mp.2010.121 (2011).
146 genecards.org, uniprot.org and the National Library of Medicine (last access: 22.07.2022).
147 Yao, I., Iida, J., Nishimura, W. & Hata, Y. Synaptic and nuclear localization of brain-enriched guanylate kinase-associated protein. *J Neurosci* **22**, 5354-5364, doi:20026505 (2002).
148 Deguchi, M. *et al.* BEGAIN (brain-enriched guanylate kinase-associated protein), a novel neuronal PSD-95/SAP90-binding protein. *J Biol Chem* **273**, 26269-26272, doi:10.1074/jbc.273.41.26269 (1998).
149 Kennedy, M. B. The postsynaptic density at glutamatergic synapses. *Trends Neurosci* **20**, 264-268, doi:10.1016/s0166-2236(96)01033-8 (1997).
150], E. A. e. t. e. f. a. H. s. h., Gene ID: 1915, u. o.-J.-. & Datasets, D.
151 in *GeneCards - The Human Gene Database* (Updated: Jan 10, 2023).
152 Condeelis, J. Elongation factor 1 alpha, translation and the cytoskeleton. *Trends Biochem Sci* **20**, 169-170, doi:10.1016/s0968-0004(00)88998-7 (1995).
153 Soares, D. C., Barlow, P. N., Newbery, H. J., Porteous, D. J. & Abbott, C. M. Structural models of human eEF1A1 and eEF1A2 reveal two distinct surface clusters of sequence

variation and potential differences in phosphorylation. *PLoS One* **4**, e6315, doi:10.1371/journal.pone.0006315 (2009).
154 Tomlinson, V. A. *et al.* Translation elongation factor eEF1A2 is a potential oncoprotein that is overexpressed in two-thirds of breast tumours. *BMC Cancer* **5**, 113, doi:10.1186/1471-2407-5-113 (2005).
155 Lee, M. H. & Surh, Y. J. eEF1A2 as a putative oncogene. *Ann N Y Acad Sci* **1171**, 87-93, doi:10.1111/j.1749-6632.2009.04909.x (2009).
156 Newbery, H. J. *et al.* Translation elongation factor eEF1A2 is essential for post-weaning survival in mice. *J Biol Chem* **282**, 28951-28959, doi:10.1074/jbc.M703962200 (2007).
157 Mateyak, M. K. & Kinzy, T. G. eEF1A: thinking outside the ribosome. *J Biol Chem* **285**, 21209-21213, doi:10.1074/jbc.R110.113795 (2010).
158 Hotokezaka, Y. *et al.* Interaction of the eukaryotic elongation factor 1A with newly synthesized polypeptides. *J Biol Chem* **277**, 18545-18551, doi:10.1074/jbc.M201022200 (2002).
159 Gonen, H., Dickman, D., Schwartz, A. L. & Ciechanover, A. Protein synthesis elongation factor EF-1 alpha is an isopeptidase essential for ubiquitin-dependent degradation of certain proteolytic substrates. *Adv Exp Med Biol* **389**, 209-219, doi:10.1007/978-1-4613-0335-0_26 (1996).
160 Ruest, L. B., Marcotte, R. & Wang, E. Peptide elongation factor eEF1A-2/S1 expression in cultured differentiated myotubes and its protective effect against caspase-3-mediated apoptosis. *J Biol Chem* **277**, 5418-5425, doi:10.1074/jbc.M110685200 (2002).
161 Khacho, M. *et al.* eEF1A is a novel component of the mammalian nuclear protein export machinery. *Mol Biol Cell* **19**, 5296-5308, doi:10.1091/mbc.E08-06-0562 (2008).
162 Vlasenko, D. O., Novosylna, O. V., Negrutskii, B. S. & El'skaya, A. V. Truncation of the A,A(*),A' helices segment impairs the actin bundling activity of mammalian eEF1A1. *FEBS Lett* **589**, 1187-1193, doi:10.1016/j.febslet.2015.03.030 (2015).
163 Sun, Y. *et al.* Up-regulation of eEF1A2 promotes proliferation and inhibits apoptosis in prostate cancer. *Biochem Biophys Res Commun* **450**, 1-6, doi:10.1016/j.bbrc.2014.05.045 (2014).
164 De Rinaldis, M., Giorda, R. & Trabacca, A. Mild epileptic phenotype associates with de novo eef1a2 mutation: Case report and review. *Brain Dev* **42**, 77-82, doi:10.1016/j.braindev.2019.08.001 (2020).
165 Cao, S. *et al.* Homozygous EEF1A2 mutation causes dilated cardiomyopathy, failure to thrive, global developmental delay, epilepsy and early death. *Hum Mol Genet* **26**, 3545-3552, doi:10.1093/hmg/ddx239 (2017).
166 HDAC11 Gene - Histone Deacetylase 11. *GeneCards - The Human Gene Database* (Updated: Jan 10, 2023).
167 Liu, S. S., Wu, F., Jin, Y. M., Chang, W. Q. & Xu, T. M. HDAC11: a rising star in epigenetics. *Biomed Pharmacother* **131**, 110607, doi:10.1016/j.biopha.2020.110607 (2020).
168 Klieser, E. *et al.* Comprehensive immunohistochemical analysis of histone deacetylases in pancreatic neuroendocrine tumors: HDAC5 as a predictor of poor clinical outcome. *Hum Pathol* **65**, 41-52, doi:10.1016/j.humpath.2017.02.009 (2017).
169 LMNA Gene - Lamin A/C. *GeneCards - The Human Gene Database* (Updated: Jan 10, 2023).
170 Bonne, G. & Quijano-Roy, S. Emery-Dreifuss muscular dystrophy, laminopathies, and other nuclear envelopathies. *Handb Clin Neurol* **113**, 1367-1376, doi:10.1016/B978-0-444-59565-2.00007-1 (2013).

171 Boyes, J. & Bird, A. Repression of genes by DNA methylation depends on CpG density and promoter strength: evidence for involvement of a methyl-CpG binding protein. *EMBO J* **11**, 327-333 (1992).
172 Prendergast, G. C. & Ziff, E. B. Methylation-sensitive sequence-specific DNA binding by the c-Myc basic region. *Science* **251**, 186-189, doi:10.1126/science.1987636 (1991).
173 Bednarik, D. P. *et al.* DNA CpG methylation inhibits binding of NF-kappa B proteins to the HIV-1 long terminal repeat cognate DNA motifs. *New Biol* **3**, 969-976 (1991).
174 Iguchi-Ariga, S. M. & Schaffner, W. CpG methylation of the cAMP-responsive enhancer/promoter sequence TGACGTCA abolishes specific factor binding as well as transcriptional activation. *Genes Dev* **3**, 612-619, doi:10.1101/gad.3.5.612 (1989).
175 Nan, X., Meehan, R. R. & Bird, A. Dissection of the methyl-CpG binding domain from the chromosomal protein MeCP2. *Nucleic Acids Res* **21**, 4886-4892, doi:10.1093/nar/21.21.4886 (1993).
176 Yildirim, O. *et al.* Mbd3/NURD complex regulates expression of 5-hydroxymethylcytosine marked genes in embryonic stem cells. *Cell* **147**, 1498-1510, doi:10.1016/j.cell.2011.11.054 (2011).
177 Zhang, Y. *et al.* Analysis of the NuRD subunits reveals a histone deacetylase core complex and a connection with DNA methylation. *Genes Dev* **13**, 1924-1935, doi:10.1101/gad.13.15.1924 (1999).
178 Xu, M. *et al.* Methyl-CpG-binding domain 3 inhibits epithelial-mesenchymal transition in pancreatic cancer cells via TGF-beta/Smad signalling. *Br J Cancer* **116**, 91-99, doi:10.1038/bjc.2016.397 (2017).
179 NFKB2 nuclear factor kappa B subunit 2. *NIH - National Library of Medicine* (updated on 8-Dec-2022).
180 Sun, S. C. The noncanonical NF-kappaB pathway. *Immunol Rev* **246**, 125-140, doi:10.1111/j.1600-065X.2011.01088.x (2012).
181 Manuel Sanchez-Maldonado, J. *et al.* NFKB2 polymorphisms associate with the risk of developing rheumatoid arthritis and response to TNF inhibitors: Results from the REPAIR consortium. *Sci Rep* **10**, 4316, doi:10.1038/s41598-020-61331-5 (2020).
182 Marta, Z. N. *et al.* NFKB2 gene expression in patients with peptic ulcer diseases and gastric cancer. *Mol Biol Rep* **47**, 2015-2021, doi:10.1007/s11033-020-05299-5 (2020).
183 Morris, G. F. An alternative to lung inflammation and fibrosis. *Am J Pathol* **176**, 2595-2598, doi:10.2353/ajpath.2010.100272 (2010).
184 Zhang, Y., Tong, L., Chen, S., Wu, W. & Wang, L. Analysis of NFKB2mediated regulation of mechanisms underlying the development of Hodgkin's lymphoma. *Mol Med Rep* **17**, 8129-8136, doi:10.3892/mmr.2018.8911 (2018).
185 Liu, Y. *et al.* Novel NFKB2 mutation in early-onset CVID. *J Clin Immunol* **34**, 686-690, doi:10.1007/s10875-014-0064-x (2014).
186 Shi, C. *et al.* NFKB2 mutation in common variable immunodeficiency and isolated adrenocorticotropic hormone deficiency: A case report and review of literature. *Medicine (Baltimore)* **95**, e5081, doi:10.1097/MD.0000000000005081 (2016).
187 PAK1 Gene - P21 (RAC1) Activated Kinase 1. *GeneCards - The Human Gene Database* (Updated: Jan 10, 2023).
188 Rane, C. K. & Minden, A. P21 activated kinase signaling in cancer. *Semin Cancer Biol* **54**, 40-49, doi:10.1016/j.semcancer.2018.01.006 (2019).
189 Wang, K. *et al.* Inhibition of PAK1 suppresses pancreatic cancer by stimulation of anti-tumour immunity through down-regulation of PD-L1. *Cancer Lett* **472**, 8-18, doi:10.1016/j.canlet.2019.12.020 (2020).

190 Frick, A. *et al.* A Novel PAK1-Notch1 Axis Regulates Crypt Homeostasis in Intestinal Inflammation. *Cell Mol Gastroenterol Hepatol* **11**, 892-907 e891, doi:10.1016/j.jcmgh.2020.11.001 (2021).
191 Maruta, H. & He, H. PAK1-blockers: Potential Therapeutics against COVID-19. *Med Drug Discov* **6**, 100039, doi:10.1016/j.medidd.2020.100039 (2020).
192 PRKAR2A protein kinase cAMP-dependent type II regulatory subunit alpha. *NIH - National Library of Medicine* (updated on 8-Dec-2022).
193 PRKAR2A Gene - Protein Kinase CAMP-Dependent Type II Regulatory Subunit Alpha. *GeneCards - The Human Gene Database* (Updated: Jan 10, 2023).
194 Saloustros, E. *et al.* Hematopoietic neoplasms in Prkar2a-deficient mice. *J Exp Clin Cancer Res* **34**, 143, doi:10.1186/s13046-015-0257-z (2015).
195 PML-RARA regulated adaptor molecule 1. *NIH- National Library of Medicine* (updated on 4-Dec-2022).
196 in *NIH - National Library of Medicine* (updated on 4-Dec-2022).
197 Clemens, R. A. *et al.* PRAM-1 is required for optimal integrin-dependent neutrophil function. *Mol Cell Biol* **24**, 10923-10932, doi:10.1128/MCB.24.24.10923-10932.2004 (2004).
198 Moog-Lutz, C. *et al.* PRAM-1 is a novel adaptor protein regulated by retinoic acid (RA) and promyelocytic leukaemia (PML)-RA receptor alpha in acute promyelocytic leukaemia cells. *J Biol Chem* **276**, 22375-22381, doi:10.1074/jbc.M011683200 (2001).
199 Medicine, N. L. o. Gene ID: 2185, updated on 21-Jun-2023.
200 Q14289 · FAK2_HUMAN. *www.uniprot.org* (Retrieved: 22.01.2023).
201 Batissoco, A. C. *et al.* A Cell Junctional Protein Network Associated with Connexin-26. *Int J Mol Sci* **19**, doi:10.3390/ijms19092535 (2018).
202 Karch, C. M. & Goate, A. M. Alzheimer's disease risk genes and mechanisms of disease pathogenesis. *Biol Psychiatry* **77**, 43-51, doi:10.1016/j.biopsych.2014.05.006 (2015).
203 RASGEF1C Gene - RasGEF Domain Family Member 1C. *GeneCards - The Human Gene Database* (Updated: Jan 10, 2023).
204 Li, Q. S., Sun, Y. & Wang, T. Epigenome-wide association study of Alzheimer's disease replicates 22 differentially methylated positions and 30 differentially methylated regions. *Clin Epigenetics* **12**, 149, doi:10.1186/s13148-020-00944-z (2020).
205 RPL6 Gene - Ribosomal Protein L6. *GeneCards - The Human Gene Database* (Updated: Jan 10, 2023).
206 Yang, C. *et al.* Ribosomal protein L6 (RPL6) is recruited to DNA damage sites in a poly(ADP-ribose) polymerase-dependent manner and regulates the DNA damage response. *J Biol Chem* **294**, 2827-2838, doi:10.1074/jbc.RA118.007009 (2019).
207 Wei, J. *et al.* Ribosomal Proteins Regulate MHC Class I Peptide Generation for Immunosurveillance. *Mol Cell* **73**, 1162-1173 e1165, doi:10.1016/j.molcel.2018.12.020 (2019).
208 Gou, Y. *et al.* Ribosomal protein L6 promotes growth and cell cycle progression through upregulating cyclin E in gastric cancer cells. *Biochem Biophys Res Commun* **393**, 788-793, doi:10.1016/j.bbrc.2010.02.083 (2010).
209 Anirudhan, A. *et al.* RPL6: A Key Molecule Regulating Zinc- and Magnesium-Bound Metalloproteins of Parkinson's Disease. *Front Neurosci* **15**, 631892, doi:10.3389/fnins.2021.631892 (2021).
210 SPIB Gene - Spi-B Transcription Factor. *GeneCards - The Human Gene Database* (Updated: Jan 10, 2023).
211 Schotte, R., Nagasawa, M., Weijer, K., Spits, H. & Blom, B. The ETS transcription factor Spi-B is required for human plasmacytoid dendritic cell development. *J Exp Med* **200**, 1503-1509, doi:10.1084/jem.20041231 (2004).

212 Montes-Moreno, S. *et al.* SPIB, a novel immunohistochemical marker for human blastic plasmacytoid dendritic cell neoplasms: characterization of its expression in major hematolymphoid neoplasms. *Blood* **121**, 643-647, doi:10.1182/blood-2012-08-447599 (2013).
213 Cooper, T. G. *et al.* World Health Organization reference values for human semen characteristics. *Hum Reprod Update* **16**, 231-245, doi:10.1093/humupd/dmp048 (2010).
214 www.qiagen.com. (Last access: 20.06.2023).
215 Bernstein, D. L., Kameswaran, V., Le Lay, J. E., Sheaffer, K. L. & Kaestner, K. H. The BisPCR(2) method for targeted bisulfite sequencing. *Epigenetics Chromatin* **8**, 27, doi:10.1186/s13072-015-0020-x (2015).
216 Laqqan, M., Tierling, S., Alkhaled, Y., LoPorto, C. & Hammadeh, M. E. Alterations in sperm DNA methylation patterns of oligospermic males. *Reprod Biol* **17**, 396-400, doi:10.1016/j.repbio.2017.10.007 (2017).
217 Boissonnas, C. C., Jouannet, P. & Jammes, H. Epigenetic disorders and male subfertility. *Fertil Steril* **99**, 624-631, doi:10.1016/j.fertnstert.2013.01.124 (2013).
218 Meaburn, E. L., Schalkwyk, L. C. & Mill, J. Allele-specific methylation in the human genome: implications for genetic studies of complex disease. *Epigenetics* **5**, 578-582, doi:10.4161/epi.5.7.12960 (2010).
219 Shoemaker, R., Deng, J., Wang, W. & Zhang, K. Allele-specific methylation is prevalent and is contributed by CpG-SNPs in the human genome. *Genome Res* **20**, 883-889, doi:10.1101/gr.104695.109 (2010).
220 Abante, J., Fang, Y., Feinberg, A. P. & Goutsias, J. Detection of haplotype-dependent allele-specific DNA methylation in WGBS data. *Nat Commun* **11**, 5238, doi:10.1038/s41467-020-19077-1 (2020).
221 Stiavnicka, M. *et al.* Sperm DNA methylation patterns at discrete CpGs and genes involved in embryonic development are related to bull fertility. *BMC Genomics* **23**, 379, doi:10.1186/s12864-022-08614-5 (2022).
222 Oluwayiose, O. A. *et al.* Sperm DNA methylation mediates the association of male age on reproductive outcomes among couples undergoing infertility treatment. *Sci Rep* **11**, 3216, doi:10.1038/s41598-020-80857-2 (2021).
223 Cao, M. *et al.* High-resolution analyses of human sperm dynamic methylome reveal thousands of novel age-related epigenetic alterations. *Clin Epigenetics* **12**, 192, doi:10.1186/s13148-020-00988-1 (2020).
224 Leenen, F. A., Muller, C. P. & Turner, J. D. DNA methylation: conducting the orchestra from exposure to phenotype? *Clin Epigenetics* **8**, 92, doi:10.1186/s13148-016-0256-8 (2016).
225 Sehgal, P., Chaturvedi, P., Kumaran, R. I., Kumar, S. & Parnaik, V. K. Lamin A/C haploinsufficiency modulates the differentiation potential of mouse embryonic stem cells. *PLoS One* **8**, e57891, doi:10.1371/journal.pone.0057891 (2013).
226 Luo, J., McGinnis, L. K., Carlton, C., Beggs, H. E. & Kinsey, W. H. PTK2b function during fertilization of the mouse oocyte. *Biochem Biophys Res Commun* **450**, 1212-1217, doi:10.1016/j.bbrc.2014.03.083 (2014).
227 D'Mello, S. R. Regulation of Central Nervous System Development by Class I Histone Deacetylases. *Dev Neurosci* **41**, 149-165, doi:10.1159/000505535 (2019).
228 Ohori, S. *et al.* A novel PAK1 variant causative of neurodevelopmental disorder with postnatal macrocephaly. *J Hum Genet* **65**, 481-485, doi:10.1038/s10038-020-0728-8 (2020).

229 Zhang, Y. *et al.* NFkappaB2 Gene as a Novel Candidate that Epigenetically Responds to Interval Walking Training. *Int J Sports Med* **36**, 769-775, doi:10.1055/s-0035-1547221 (2015).
230 Masuki, S. *et al.* Effects of milk product intake on thigh muscle strength and NFKB gene methylation during home-based interval walking training in older women: A randomized, controlled pilot study. *PLoS One* **12**, e0176757, doi:10.1371/journal.pone.0176757 (2017).
231 Morikawa, M. *et al.* Effects of dried tofu supplementation during interval walking training on the methylation of the NFKB2 gene in the whole blood of older women. *J Physiol Sci* **68**, 749-757, doi:10.1007/s12576-017-0589-x (2018).
232 Bovine Genome, S. *et al.* The genome sequence of taurine cattle: a window to ruminant biology and evolution. *Science* **324**, 522-528, doi:10.1126/science.1169588 (2009).
233 Mooove Over Humans, the Cow Genome is Here. *Science - JENNIFER COUZIN-FRANKEL* (23 APR 2009).
234 Illingworth, R. S. *et al.* Orphan CpG islands identify numerous conserved promoters in the mammalian genome. *PLoS Genet* **6**, e1001134, doi:10.1371/journal.pgen.1001134 (2010).
235 Behringer, M. G. & Hall, D. W. Genome-Wide Estimates of Mutation Rates and Spectrum in Schizosaccharomyces pombe Indicate CpG Sites are Highly Mutagenic Despite the Absence of DNA Methylation. *G3 (Bethesda)* **6**, 149-160, doi:10.1534/g3.115.022129 (2015).
236 Qu, J. *et al.* Evolutionary expansion of DNA hypomethylation in the mammalian germline genome. *Genome Res* **28**, 145-158, doi:10.1101/gr.225896.117 (2018).
237 Fang, L. *et al.* Comparative analyses of sperm DNA methylomes among human, mouse and cattle provide insights into epigenomic evolution and complex traits. *Epigenetics* **14**, 260-276, doi:10.1080/15592294.2019.1582217 (2019).
238 Heyn, H. *et al.* DNA methylation contributes to natural human variation. *Genome Res* **23**, 1363-1372, doi:10.1101/gr.154187.112 (2013).
239 Levenson, V. V. DNA methylation as a universal biomarker. *Expert Rev Mol Diagn* **10**, 481-488, doi:10.1586/erm.10.17 (2010).
240 Pfeifer, G. P. Mutagenesis at methylated CpG sequences. *Curr Top Microbiol Immunol* **301**, 259-281, doi:10.1007/3-540-31390-7_10 (2006).
241 Weber, M. *et al.* Distribution, silencing potential and evolutionary impact of promoter DNA methylation in the human genome. *Nat Genet* **39**, 457-466, doi:10.1038/ng1990 (2007).
242 Gatewood, J. M., Cook, G. R., Balhorn, R., Schmid, C. W. & Bradbury, E. M. Isolation of four core histones from human sperm chromatin representing a minor subset of somatic histones. *J Biol Chem* **265**, 20662-20666 (1990).
243 Schalkwyk, L. C. *et al.* Allelic skewing of DNA methylation is widespread across the genome. *Am J Hum Genet* **86**, 196-212, doi:10.1016/j.ajhg.2010.01.014 (2010).
244 Zhang, Y., Rohde, C., Reinhardt, R., Voelcker-Rehage, C. & Jeltsch, A. Non-imprinted allele-specific DNA methylation on human autosomes. *Genome Biol* **10**, R138, doi:10.1186/gb-2009-10-12-r138 (2009).
245 LaBarre, B. A. *et al.* MethylToSNP: identifying SNPs in Illumina DNA methylation array data. *Epigenetics Chromatin* **12**, 79, doi:10.1186/s13072-019-0321-6 (2019).
246 Laqqan, M., Ahmed, I., Yasin, M., Hammadeh, M. E. & Yassin, M. Influence of variation in global sperm DNA methylation level on the expression level of protamine genes and human semen parameters. *Andrologia* **52**, e13484, doi:10.1111/and.13484 (2020).

247 Jenkins, T. G., Aston, K. I., Cairns, B. R. & Carrell, D. T. Paternal aging and associated intraindividual alterations of global sperm 5-methylcytosine and 5-hydroxymethylcytosine levels. *Fertil Steril* **100**, 945-951, doi:10.1016/j.fertnstert.2013.05.039 (2013).

Appendix

I Abbreviations and acronyms

A	
A	Adenosine
AID/APOBEC	Activation-induced cytidine deaminase/apolipoprotein B mRNA-editing enzyme complex
ATP	Adenosine triphosphate
ART	Assisted reproductive technology
B	
BER	Base excision repair
bp	Base pairs
C	
°C	Degree Celsius
cAMP	Cyclic adenosine monophosphate
CpG	Cytosine-phosphate-guanine dinucleotides
D	
DBS	Deep Bisulphite Sequencing
DMR	Differentially methylated region
DNA	Deoxyribonucleic acid
dH_20	Distilled water
DNMT	DNA methyltransferases
dNTP	Nucleoside triphosphate
E	
EDTA	Ethylenediaminetetraacetic acid
EtOH	Ethanol
ESC	Embryonic stem cell
ETS	Erythroblast transformation specific
F	
FCB	Foetal cord blood
G	
g	Gram
G	Guanine
GTP	Guanine triphosphate
GWAS	Genome wide association studies
H	
H3K4me3	Histone 3 Lysine 4 trimethylation
I	
ICSI	Intracytoplasmic sperm injection
IGF2	Insulin-like growth factor 2
IVF	In-vitro fertilization
K	
kg	Kilogram
L	
lncRNA	Long non-coding RNA
M	
M	Molar
$MgCl_2$	Magnesium chloride

MID	Multiplex identifier
miRNA	microRNA
ml	Milliliter
mm	Millimetre
mM	Millimolar
mRNA	Messenger RNA
N	
NaCL	Sodium chloride
NaOH	Sodium hydroxide
ncRNA	Non-coding RNA
ng	Nanogram
NGS	Next generation sequencing
nr	Number
P	
PCR	Polymerase chain reaction
PGC	Primordial germ cell
piRNA	Piwi-interacting RNA
Ppi	Pyrophosphate
PSD	Postsynaptic density
p-value	Probability value
R	
Rho	Spearman’s rank correlation coefficient
RNA	Ribonucleic acid
Rpm	Revolutions per minute
Rs	Reference SNP
S	
SAM	S-Adenosyl methionine
SDS	Sodium dodecyl sulfate
siRNA	Small interfering RNA
sncRNA	Small non-coding RNA
SNP	Single nucleotide polymorphism
SPRI	Solid phase reversible immobilization
T	
T	Thymine
Te	Tris-EDTA buffer
Tet	Ten-eleven translocation dioxygenase
TDG	Thymine-DNA glycosylase
tsRNA	tRNA-derived small RNA
V	
Vs	Versus
W	
WHO	World health organization
%	Percentage
Mg	Microgram
µL	Microliter
µM	Micromolar
mM	Millimolar
5-mC	5-Methylcytosine

5-hmC	5-Hydroxymethylcytosine
5-fC	5-Formylcytosine
5-hmU	5-Hydroxymethyluracil
X	
Xist	X inactivate specific transcript

II Index of figures

Figure 1: Illustration of the constructive approach of the study subdivided into three successive main experiments:..... 19
Figure 2: Illustration of the two successive PCRs..... 37
Figure 3: Average methylation in human sperm as a function of the donor's age for 10 different amplicons (modified from: Species-Specific Paternal Age Effects and Sperm Methylation Levels of Developmentally Important Genes - Cells. 2022). 44
Figure 4: Average methylation in bovine sperm as function of the donor's age for 4 different amplicons (modified from: Species-Specific Paternal Age Effects and Sperm Methylation Levels of Developmentally Important Genes - Cells. 2022). 45
Figure 5: Average methylation for all analysed CpGs in the 5 different amplicons (modified from: Species-Specific Paternal Age Effects and Sperm Methylation Levels of Developmentally Important Genes - Cells. 2022)..... 49
Figure 6: Average methylation in human and bovine sperm as a function of the donor's age for 5 different amplicons..... 50

III Index of tables

Table 1: Reagents and equipment..... 20
Table 2: Human sperm cohort parameters for Pyrosequencing..... 22
Table 3: Human FCB cohort parameters..... 23
Table 4: Human sperm cohort parameters for DBS..... 24
Table 5: Characteristics of the bovine sperm cohort..... 24
Table 6[214]: Reaction setup for bisulphite conversion according to the manufacturer's manual (www.qiagen.com)..... 27
Table 7: Thermal cycler programme for bisulphite conversion..... 27
Table 8: Reagent setup for standard PCR..... 28
Table 9: Thermal cycler conditions for standard PCR..... 28
Table 10: Reagent setup for Pyrosequencing..... 31
Table 11: PCR and Pyrosequencing primers for 10 different human amplicons..... 31
Table 12: PCR and Pyrosequencing primers for 4 different bovine amplicons..... 32
Table 13: Checking for evolutionary conservation; PCR and Pyrosequencing primers..... 33
Table 14: Genotyping primers for 3 different amplicons..... 33
Table 15: DBS primers for 3 different amplicons..... 35
Table 16: Reagent setup for PCR with barcoding primers..... 36
Table 17: Cycler programme for touchdown PCR..... 36
Table 18: DBS sample organization and index primer combinations..... 37
Table 19: Index primer sequence..... 39
Table 20: Information about the location of the selected amplicons..... 42

Table 21: Mean methylation and correlation with age for each amplicon 42
Table 22: Conserved CpGs between Bos taurus and Homo sapiens (modified from: Species-Specific Paternal Age Effects and Sperm Methylation Levels of Developmentally Important Genes - Cells. 2022). 47
Table 23: Average methylation levels between bos taurus and homo sapiens for 5 conserved amplicons 48
Table 24: Age effects on the sperm methylome in conserved CpG sites between humans and bulls 51
Table 25: Genotyping results for FCB 52
Table 26: Heterozygous FCB samples and corresponding sperm used for DBS 53
Table 27: Comparison of average methylation levels between FCB and sperm 55
Table 28: Paternal allele methylation in FCB is correlated with paternal age 56
Table 29: Maternal allele methylation in FCB is correlated with maternal age 56
Table 30: BEGAIN allele specific methylation in FCB 57
Table 31: SPIB allele specific methylation in sperm 57

V Publications

1) Prell A, Sen MO, Potabattula R, Bernhardt L, Dittrich M, Hahn T, Schorsch M, Zacchini F, Ptak GE, Niemann H, Haaf T. **Species-Specific Paternal Age Effects and Sperm Methylation Levels of Developmentally Important Genes**. Cells. 2022 Feb 19;11

2) Bernhardt L, Dittrich M, Prell A, Potabattula R, Drummer C, Behr R, Hahn T, Schorsch M, Müller T, Haaf T. **Age-related methylation changes in the human sperm epigenome**. Aging (Albany NY). 2023 Feb 27

Appendix

Supplementary Table 1: Human sperm samples for bisulphite pyrosequencing

	Sample ID	Age	Conc	Mrphlgy	Motility	BMI	Spermiogramm
1	WI_101	50.9	26	5	10		keine Angaben
2	WI_931	45.6	150	17	60	22.2	Normozoospermia
3	WI_1041	37.7	120	10	35	24.2	Normozoospermia
4	WI_1227	38.5	150	12	50	23.5	Normozoospermia
5	WI_1321	49.8	31	9	39		keine Angaben
6	WI_2011	49.7	110	8	55	23.2	keine Angaben
7	WI_2037	38.5	88	12	72	25.3	Normozoospermia
8	WI_2044	34.8	125	14	70	21.9	Normozoospermia
9	WI_2053	45.2	65	9	53	25.2	Normozoospermia
10	WI_2054	45.6	120	12	55	23.4	Normozoospermia
11	WI_2067	35.4	92	8	60	24.2	Normozoospermia
12	WI_2068	45.2	128	9	75	25.9	Normozoospermia
13	WI_2069	39.5	88	6	63	25.2	Normozoospermia
14	WI_2078	33.7	80	12	70	24.5	Normozoospermia
15	WI_2081	38.3	94	18	64	23.4	Normozoospermia
16	WI_2089	40.4	120	6	38	23.4	Normozoospermia
17	WI_2090	29.7	80	4	60	25.5	Normozoospermia
18	WI_2091	32.9	95	6	52	31.8	Normozoospermia
19	WI_2093	37.2	75	6	40	24.8	Normozoospermia
20	WI_2098	49.5	130	5	35	24.5	Normozoospermia
21	WI_2106	45.4	150	6	60	25.1	Normozoospermia
22	WI_2114	46.1	100	4	45	27.5	Normozoospermia
23	WI_2115	45.8	120	6	50	22.8	Normozoospermia

24	WI_2116	37.3	100	4	40	23.4	Normozoospermia
25	WI_2121	39.6	54	5	83	23.4	Normozoospermia
26	WI_2131	36.9	98	8	65		Normozoospermia
27	WI_2135	41.7	190	5	58	29	Normozoospermia
28	WI_2137	40.2	100	4	62	23.4	Normozoospermia
29	WI_2143	33.3	100	6	50	23.4	Normozoospermia
30	WI_2145	33.3	70	6	55	29.6	Normozoospermia
31	WI_2148	47.8	120	5	55	23.4	Normozoospermia
32	WI_2149	45.2	40	5	70	25.2	Normozoospermia
33	WI_2155	30.9	78	4	59	26.8	Normozoospermia
34	WI_2160	37.2	160	6	50		Normozoospermia
35	WI_2163	44.3	61	8	43		Normozoospermia
36	WI_2165	35.5	59	9	42		Normozoospermia
37	WI_2168	35.4	61	8	43		Normozoospermia
38	WI_2173	40.8	45	4	42		Normozoospermia
39	WI_2175	33.1	55	8	46		Normozoospermia
40	WI_2187	41.8	45	10	48		Normozoospermia
41	WI_2193	40.1	95	8	50		Normozoospermia
42	WI_2198	32.1	95	4	50		Normozoospermia
43	WI_2199	40.5	78	6	59		Normozoospermia
44	WI_2208	34.2	52	6	75		Normozoospermia
45	WI_2213	38.0	260	6	50		Normozoospermia
46	WI_2215	36.8	55	9	84		Normozoospermia
47	WI_2223	36.1	86	6	79		Normozoospermia
48	WI_2231	37.6	62	8	56		Normozoospermia
49	WI_2240	37.0	80	6	62		Normozoospermia
50	WI_2241	31.7	79	9	84		Normozoospermia
51	WI_2243	42.8	106	12	55		Normozoospermia

52	WI_2244	39.4	78	6	44		Normozoospermia
53	WI_2256	39.8	31	4	67		Normozoospermia
54	WI_2265	37.4	92	6	59		Normozoospermia
55	WI_2270	38.2	61	6	72		Normozoospermia
56	WI_2292	37.6	190	8	68	23.7	Normozoospermia
57	WI_2304	41.4	180	5	55	30.7	Normozoospermia
58	WI_2308	32.3	90	5	50	18.9	Normozoospermia
59	WI_2319	46.1	250	6	70	27.8	Normozoospermia
60	WI_2340	38.1	42	6	52		Normozoospermia
61	WI_2352	42.5	15	12	56	30.2	Normozoospermia
62	WI_2353	34.8	20	4	48	23.4	Normozoospermia
63	WI_2383	37.4	120	11	50	25	Normozoospermia
64	WI_2395	33.2	95	6	55	21.9	Normozoospermia
65	WI_2399	32.7	50	6	60	27.4	Normozoospermia
66	WI_2407	41.9	64	8	52	25.7	Normozoospermia
67	WI_2408	71.7	70	8	10	26.2	Asthenozoospermia. Teratozoospermia
68	WI_2416	40.5	31	5	42	21.2	Normozoospermia
69	WI_2419	34.9	85	15	50	23.7	Normozoospermia
70	WI_2446	35.6	81	6	77	30.4	Normozoospermia
71	WI_2447	39.7	84	11	71	30.4	Normozoospermia
72	WI_2449	33.7	110	6	70	30.2	Normozoospermia
73	WI_2452	35.4	100	6	60	21.6	Normozoospermia
74	WI_2456	33.1	45	7	50	27.4	Normozoospermia
75	WI_2457	32.3	109	6	66	24.3	Normozoospermia
76	WI_2461	38.1	90	6	60	31.1	Normozoospermia
77	WI_2470	44.3	35	4	46		Normozoospermia
78	WI_2471	38.7	50	5	51	27.7	Normozoospermia

79	WI_2485	42.2	80	10	45	26.1	Normozoospermia
80	WI_2495	33.1	60	4	44	22.5	Normozoospermia
81	WI_2499	39.9	34	6	47	30	Normozoospermia
82	WI_2505	41.2	50	5	60	28.1	Normozoospermia
83	WI_2519	43.7	17	4	71	25.7	Normozoospermia
84	WI_2531	31.8	55	6	46	28.7	Normozoospermia
85	WI_2544	40.3	118	5	40	22.1	Normozoospermia
86	WI_2551	29.4	98	7	49	25.1	Normozoospermia
87	WI_2565	40.3	68	9	66	24.2	Normozoospermia
88	WI_2569	40.8	50	5	65	23.5	Normozoospermia
89	WI_2576	38.7	20	4	50		Normozoospermia
90	WI_2589	37.3	45	4	51	27.8	Normozoospermia
91	WI_2602	35.2	22	10	55	31.8	Normozoospermia
92	WI_2630	46.0	52	10	84	24.4	Normozoospermia
93	WI_2632	43.7	40	12	85	25.1	Normozoospermia
94	WI_2642	41.0	47	7	50	29.7	Normozoospermia

Supplementary Table 2: Heterozygous FCB samples and corresponding sperm

	BEGAIN				EEF1A2				SPIB			
	FCB		Paternal Sperm		FCB		Paternal Sperm		FCB		Paternal Sperm	
	ID	Genotype	ID	Genotype	ID	Genotype	ID	Genotype	ID	Genotype	ID	Genotype
1	FCB 47	CT	WI 153	TT	FCB 18	AG	WI 050	GG	FCB 21	AG	WI 059	AA
2	FCB 49	CT	WI 145	TT	FCB 85	AG	WI 373	GG	FCB 46	AG	WI 153	GG
3	FCB 59	CT	WI 272	TT	FCB 103	AG	WI 297	GG	FCB 47	AG	WI 153	GG
4	FCB 79	CT	WI 317	CC	FCB 129	AG	WI 493	GG	FCB 74	AG		
5	FCB 106	CT	WI 360	TT	FCB 139	AG	WI 293	AA	FCB 80	AG	WI 282	AA
6	FCB 126	CT	WI 472	TT	FCB 141	AG	WI 579	GG	FCB 104	AG	WI 375	AA
7	FCB 128	CT	WI 109	TT	FCB 157	AG	WI 313	GG	FCB 126	AG	WI 472	AA
8	FCB 129	CT	WI 493	TT	FCB 158	AG	WI 648	GG	FCB 134	AG	WI 537	GG
9	FCB 142	CT	WI 597	TT	FCB 160	AG	WI 291	GG	FCB 159	AG	WI 637	GG
10	FCB 143	CT	WI 588	TT	FCB 161	AG	WI 291	GG	FCB 173	AG	WI 723	AA
11	FCB 145	CT	WI 622	TT	FCB 163	AG	WI 659	GG	FCB 176	AG	WI 464	GG
12	FCB 146	CT	WI 587	CC	FCB 171	AG	WI 684	GG	FCB 180	AG	WI 820	GG
13	FCB 147	CT	WI 599	CC	FCB 185	AG	WI 756	GG	FCB 184	AG	WI 233	GG
14	FCB 174	CT	WI 750	TT	FCB 191	AG	WI 790	GG	FCB 193	AG	WI 851	AA
15	FCB 175	CT	WI_775	CC	FCB 193	AG	WI 851	AA	FCB 196	AG	WI 888	GG
16	FCB 177	CT	WI 767	TT	FCB 205	AG	WI 777	GG	FCB 206	AG	WI 926	AA
17	FCB 178	CT	WI 736	TT	FCB 210	AG	WI 962	AA	FCB 207	AG	WI 670	AA
18	FCB 182	CT	WI 842	TT	FCB 222	AG	WI 494	GG	FCB 212	AG	WI 963	GG
19	FCB 189	CT	WI 398	TT	FCB 223	AG	WI 893	GG	FCB 217	AG	WI 747	GG
20	FCB 190	CT	WI 398	TT	FCB 227	AG	WI 476	GG	FCB 218	AG	WI 1012	AA

21	FCB 200	CT	WI 031	CC	FCB 230	AG	WI 1133	GG	FCB 223	AG	WI 893	GG
22	FCB 201	CT	WI 897	CC	FCB 231	AG	WI 1161	GG	FCB 235	AG	WI 1169	GG
23	FCB 203	CT	WI 900	TT	FCB 232	AG	WI 1156	GG	FCB 261	AG	WI_1430	AA
24	FCB 205	CT	WI 777	TT	FCB 252	AG	WI_911	GG	FCB 275	AG	WI_2024	GG
25	FCB 209	CT	WI 449	CC	FCB 275	AG	WI_2024	GG				
26	FCB 210	CT	WI 962	TT	FCB 276	AG	WI_2024	GG				
27	FCB 230	CT	WI 1133	CC	FCB 280	AG	WI_2043	GG				
28	FCB 232	CT	WI 1156	CC	FCB 286	AG	WI_771	GG				
29	FCB 233	CT	WI 1131	CC	FCB 287	AG	WI_2076	AA				
30	FCB 234	CT	WI 601	TT								
31	FCB 240	CT	WI_1224	CC								
32	FCB 252	CT	WI_911	TT								
33	FCB 256	CT	WI_1396	TT								
34	FCB 268	CT	WI_1463	TT								
35	FCB 280	CT	WI_2043	CC								
36	FCB 282	CT	WI_2082	TT								
37	FCB 285	CT	WI_2064	TT								
38	FCB 287	CT	WI_2076	CC								

Supplementary Table 3: FCB samples for DBS

	FCB Number	Birth weight (g)	Length (cms)	FCB pH	Gender	Father ID	Age mother	treatment	birth mode
1	FCB 18	2410	52	7.36	Male	WI 050	33	ICSI	spontan
2	FCB 21	2570	50	7.30	Female	WI 059	28	IVF	prim. sectio
3	FCB 46	2510	48	7.15	Male	WI 153	33	ICSI	vacuum
4	FCB 47	2770	48	7.00	Male	WI 153	33	ICSI	sek. sectio
5	FCB 49					WI 145	37	IVF	
6	FCB 59	2090	48.5	7.19	Male	WI 272	34	ICSI	spontan
7	FCB 60	2200	49	7.16	Female	WI 272	34	ICSI	spontan
8	FCB 74	2200			Female	WI_339	42		
9	FCB 79	2550	51	7.22	Male	WI 317	30	ICSI	spontan
10	FCB 80	3410	53	7.23	Male	WI 282	35	IVF	spontan
11	FCB 85	2490	47		Female	WI 373	30	ICSI	prim. sectio
12	FCB 103	4020	53	7.28	Female	WI 297	34	IVF	sek. sectio
13	FCB 104					WI 375	35	IVF	
14	FCB 106	3925	51	7.21	Female	WI 360	36	ICSI	spontan
15	FCB 126	2910	49	6.90	Male	WI 472	37	ICSI	spontan
16	FCB 128	3310	54		Female	WI 109	39	IVF	spontan
17	FCB 129	2920	52		Male	WI 493	38	ICSI	prim. sectio
18	FCB 134	3400	51		Male	WI 537	30	ICSI	prim. sectio
19	FCB 139	3760	52	7.43	Male	WI 293	34	ICSI	spontan
20	FCB 141	2835	51		Female	WI 579	40	ICSI	spontan
21	FCB 142	2580	48		Female	WI 597	30	IVF	prim. sectio
22	FCB 143	3280	52	7.26		WI 588	39	IVF	vacuum
23	FCB 145	3610	53	7.33		WI 622	33	ICSI	sek. sectio
24	FCB 146	4118	54	7.26	Female	WI 587	34	IVF	sek. sectio
25	FCB 147	3780	52		Female	WI 599	37	IVF	spontan
26	FCB 157	3200	51		Male	WI 313	36	ICSI	sek. sectio

27	FCB 158	3130	51		Female	WI 648	38	IVF	spontan
28	FCB 159	3325	51	7.26	Male	WI 637	35	IVF	sek. sectio
29	FCB 160	3500	52		Male	WI 291	40	M/T	spontan
30	FCB 161					WI 291	40	M/T	spontan
31	FCB 162	3495	51	7.35		WI 683	25	IVF	prim. sectio
32	FCB 163	3260	51	7.21	Male	WI 659	39	ICSI	spontan
33	FCB 171	3030	50		Female	WI 684	32	ICSI	vacuum
34	FCB 173	3320	50		Female	WI 723	37	IVF	spontan
35	FCB 174	3540	54	7.32	Male	WI 750	39	IVF	prim. sectio
36	FCB 175	2680			Male	WI_775	34		
37	FCB 176	4220	52		Female	WI 464	39	ICSI	spontan
38	FCB 177	3920	52		Male	WI 767	35	ICSI	spontan
39	FCB 178	3460	54	7.32	Male	WI 736	36	ICSI	sek. sectio
40	FCB 180	2140	49	7.34	Female	WI 820	34	ICSI	prim. sectio
41	FCB 182	2650	48	7.32	Female	WI 842	33	IVF	sek. sectio
42	FCB 184	3215	52		Female	WI 233	33	ICSI	spontan
43	FCB 185	4100	55	7.34	Male	WI 756	34	ICSI	sek. sectio
44	FCB 189	2340	46	7.32	Female	WI 398	32	ICSI	spontan
45	FCB 190	2240	45	7.33	Female	WI 398	32	ICSI	prim. sectio
46	FCB 191	3650	52		Male	WI 790	32	M/T. Kryo	vacuum
47	FCB 193	4950	57	7.32	Female	WI 851	31	ICSI	sek. sectio
48	FCB 196	2930	49		Female	WI 888	34	IVF	spontan
49	FCB 200	3790	54	7.23	Male	WI 031	33	ICSI	vacuum
50	FCB 201	2690	47	7.20	Male	WI 897	38	ICSI	spontan
51	FCB 203	3470	52	7.19	Male	WI 900	37	IVF	vacuum
52	FCB 205	2815	48		Male	WI 777	37	ICSI	spontan
53	FCB 206	2990	52		Male	WI 926	37	ICSI	spontan
54	FCB 207	3440	54		Male	WI 670	36	ICSI	spontan
55	FCB 209	3630	54	7.26	Male	WI 449	31	ICSI	spontan

56	FCB 210	3050	51		Male	WI 962	34	ICSI	spontan
57	FCB 212	3720	52		Female	WI 963	34	ICSI	sek. sectio
58	FCB 217	2720	49	7.27	Female	WI 747	42	ICSI	sek. sectio
59	FCB 218	3410	50	7.25	Female	WI 1012	32	ICSI	vacuum
60	FCB 222	2700	51	7.31	Female	WI 494	36	ICSI	spontan
61	FCB 223			7.26	Male	WI 893	31	ICSI	prim. sectio
62	FCB 227	3620	52		Female	WI 476	27	ICSI	vacuum
63	FCB 230	3450	52	7.38	Female	WI_1133	30	ICSI	sek. sectio
64	FCB 231	3330	54	7.23	Male	WI 1161	34	M/T	spontan
65	FCB 232	3135	50	7.33	Female	WI 1156	30	ICSI	spontan
66	FCB 233	4540	52	7.322	Male	WI 1131	33	IVF	vacuum
67	FCB 234	3540	56		Female	WI 601	41	ICSI	sek. sectio
68	FCB 235	3060	50	7.09	Female	WI 1169	37	IVF	spontan
69	FCB 240	2830			Male	WI_1224	34		
70	FCB 252	3720			Female	WI_911	32		
71	FCB 256	3350			Male	WI_1396	40		
72	FCB 261	3605			Female	WI_1430	39		
73	FCB 268	3020			Female	WI_1463	31		
74	FCB 275	2785			Male	WI_2024	32		
75	FCB 276	2880			Male	WI_2024	32		
76	FCB 280					WI_2043			
77	FCB 282	2970			Male	WI_2082	38		
78	FCB 285	3760			Male	WI_2064	38		
79	FCB 286					WI_771			
80	FCB 287	3040			Female	WI_2076	34		

Supplementary Table 4: Corresponding paternal sperm

	Father ID	Age father	BMI Father	Volume	Concentration	Morphology	Motility	Remark
1	WI 050	34		2	9	3	29	OAT-Syndrome
2	WI 059	34.49		5	80	15	50	-
3	WI 153	33.33		3	95	8	38	Asthenozoospermia
4	WI 153	33.33		3	95	8	38	Asthenozoospermia
5	WI 145	39.96		5.2	69	8	40	-
6	WI 272	47.92	25.70	8.5	11	1	7	OAT-Syndrome
7	WI 272	47.92	25.70	8.5	11	1	7	OAT-Syndrome
8	WI 339	40.19	28.40		70	10	40	
9	WI 317	36.64	24.70	3.2	162	15	25	-
10	WI 282	35.17	24.50	3.7	32	9	73	-
11	WI 373	36.20	24.30	3.5	12	7	29	OAT-Syndrome
12	WI 297	36.88		1.9	112	10	44	-
13	WI 375	35.30	23.40	A: 0.8. B: 1	87	10	53	-
14	WI 360	32.57		2.5	5	4	54	OAT-Syndrome
15	WI 472	44.31		8	16	5	40	-
16	WI 109	47.49			A:23. B:42	A:10. B:10	A:30. B:41	S
17	WI 493	41.73		4.1	14	7	41	OAT-Syndrome
18	WI 537	38.06		2	30	6	50	Asthenozoospermia-
19	WI 293	37.72		3.6	3.4	2	40	-
20	WI 579	39.46	29.10	5.2	10	8	41	-
21	WI 597	33.05	26.60	A:0.8; B:0.6	27	9	51	Asthenozoospermia
22	WI 588	37.98		3	25	8	65	-
23	WI 622	34.20		3.5	65	8	37	Asthenozoospermia
24	WI 587	36.95	25.10	2.5	70	15	55	-
25	WI 599	40.32		3.5	31	13	39	Asthenozoospermia

26	WI 313	39.47	30.10	A: 2.6; B: 1.5	10	5	33	Oligozoospermie
27	WI 648	39.02	23.40	6.5	38	11	58	-
28	WI 637	40.40	28.40	4	80	15	55	-
29	WI 291	45.56		0.75	2/BF			Kryptozoospermie
30	WI 291	45.56		0.75	2/BF			Kryptozoospermie
31	WI 683	30.99		2.5	81	10	37	Asthenozoospermia-
32	WI 659	42.59	40.30	5.5	8	5	40	OAT-Syndrome
33	WI 684	46.56		1	2	1	14	Oligozoospermie
34	WI 723	34.75	27.50	2.5	49	7	59	-
35	WI 750	49.83		3.5	52	9	50	-
36	WI 775	34.52	22.70		22	12	38	
37	WI 464	40.54		2	15	5	43	OAT-Syndrome
38	WI 767	35.36		3.8	3	8	38	OAT-Syndrome
39	WI 736	35.28	25.80	9.5	31	3	10	Asthenozoospermia
40	WI 820	32.51		2	85	5	26	Asthenozoospermia
41	WI 842	34.20	25.40	1	60	10	50	Hyposemie
42	WI 233	38.07		2.1	4.6	5	12	-
43	WI 756	38.03	24.10	0.5	23	2	16	Asthenozoospermia
44	WI 398	41.94		2.3	20	2	45	OAT-Syndrome
45	WI 398	41.94		2.3	20	2	45	OAT-Syndrome
46	WI 790	51.46	22.70	0.8				-
47	WI 851	33.63	23.90	2	50	5	41	-
48	WI 888	34.05	29.10	A:2.5; B:2	9	4	31	OAT-Syndrome
49	WI 031	39.37		2.5				OAT-Syndrome
50	WI 897	48.62	28.70	2.5	61	6	18	-
51	WI 900	40.49	25.10	2.5	105	8	59	-
52	WI 777	43.32	25.70	3.5	22	7	12	Asthenozoospermia
53	WI 926	47.43	22.40	A:2.5; B:2	3			Kryptozoospermie

54	WI 670	37.27	29.50	3	75	9	32	Asthenozoospermia
55	WI 449	35.57		2.5	5	4	31	OAT-Syndrome
56	WI 962							
57	WI 963	47.67	23.40	3	100	5	20	Asthenozoospermia
58	WI 747	43.25		3.6	17	5	52	-
59	WI 1012	31.91	22.7	4	32	3	28	Asthenozoospermia
60	WI 1012	31.91	22.70	4	50	7	40	Asthenozoospermia
61	WI 893	40.10	26.20	3	9	5	26	-
62	WI 476	39.15	23.80		12	8	60	OAT-Syndrome
63	WI 1133	32.97	23.50		110	10	40	Asthenozoospermia
64	WI 1161	34.86	24.50	0.5 (TESE 2 Straws)				-
65	WI 1156	36.82	30.00	7	61	1	43	Asthenozoospermia
66	WI 1131	30.00	24.90	3	52	10	45	Asthenozoospermia-
67	WI 601	39.80		3	32	10	31	Asthenozoospermia-
68	WI 1169	48.28	23.40	2.5	130	12	70	-
69	WI_1224	36.64	23.30		75	6	40	-
70	WI_911	39.33	23.40		2	4	16	
71	WI_1396	41.10	29.90		19	4	26	
72	WI_1430	38.59	27.70		8	1	62	
73	WI_1463	35.93	23.40		81	3	50	
74	WI_2024	35.91	25.00		58	8	46	
75	WI_2024	35.91	25.00		58	8	46	
76	WI_2043	36.50	21.9		30	6	24	
77	WI_2082	32.54	24.7		50	7	60	
78	WI_2064	38.63	23.4		52	2	53	
79	WI_771	43.46	26.90		36	6	27	
80	WI_2076	37.49	21.8		24		75	

Supplementary Table 5: Heterozygous Sperm samples for DBS

	Father ID	Age father	BMI Father	Volume	Concentration	Morphology	Motility	Remark	Gene
1	WI 034	30.57		3	29	5	13	-	BEGAIN
2	WI 034	30.57		3	29	5	13	-	EEF1A2
3	WI 050	34		2	9	3	29	OAT-Syndrome	SPIB
4	WI 077	26.80		3.5	11	16	36	OAT-Syndrome	BEGAIN
5	WI 091	32.26		1.2	26	4	12	-	SPIB
6	WI 195	34.15		2.5	85	7	13	Asthenozoospermia	EEF1A2
7	WI 265	35.14	23.40	3.4	52	5	48	Asthenozoospermia	SPIB
8	WI 272	47.92	25.70	8.5	11	1	7	OAT-Syndrome	SPIB
9	WI 281	43.17	24	3.5	22	15	55	Asthenozoospermia	SPIB
10	WI 291	45.56		0.75	2			Kryptozoospermie	BEGAIN
11	WI 291	45.56		0.75	2			Kryptozoospermie	SPIB
12	WI 294	39.98	23.10	2.1	22	3	62	Asthenozoospermia	EEF1A2
13	WI 305	47.56		3.5	24	1	16	Asthenozoospermia	BEGAIN
14	WI 398	41.94		2.3	20	2	45	OAT-Syndrome	SPIB
15	WI 474	39.80	26.60	4	17	2	20	-	SPIB
16	WI 484	29.36	27.30	3.5	16	4	12	OAT-Syndrome	BEGAIN
17	WI 484	29.36	27.30	3.5	16	4	12	OAT-Syndrome	EEF1A2
18	WI 488	43.87		4	32	3	28	Asthenozoospermia	SPIB
19	WI 493	41.73		4.1	14	7	41	OAT-Syndrome	SPIB
20	WI 547	42.67	27.7	4.5	14	7	30	Oligozoospermie	EEF1A2
21	WI 580	47.00	23.40	3	101	7	48	-	BEGAIN
22	WI 580	47.00	23.40	3	101	7	48	-	EEF1A2
23	WI 597	33.05	26.60	A:0.8; B:0.6	27	9	51	Asthenozoospermia	SPIB
24	WI 671	48.59		1.5	21	3	7	-	BEGAIN
25	WI 683	30.99		2.5	81	10	37	Asthenozoospermia-	SPIB

26	WI 683	30.99		2.5	81	10	37	Asthenozoospermia-	EEF1A2
27	WI 745	28.08	24.80	2.9	4	11	54	-	BEGAIN
28	WI 745	28.08	24.80	2.9	40	11	54	-	EEF1A2
29	WI 750	49.83		3.5	52	9	50	-	SPIB
30	WI 758	40.25	24.30	3.5	46	5	40	-	EEF1A2
31	WI 769	33.29		kein	0	1.9	361	-	EEF1A2
32	WI 815	33.85	23.40	A:4;B:2	9	5	57	-	EEF1A2
33	WI 887	38.86	30.40	5.5	41	13	60	-	EEF1A2
34	WI 900	40.49	25.10	2.5	105	8	59	-	SPIB
35	WI 900	40.49	25.10	2.5	105	8	59	-	EEF1A2
36	WI 962	40.53	24.20	5.5	6	1	4	OAT-Syndrome	SPIB
37	WI 963	47.67	23.40	3	100	5	20	Asthenozoospermia	BEGAIN
38	WI 967	32.95	23.10		5			Kryptozoospermie	SPIB
39	WI 1097	44.45	29.10		0.20				SPIB
40	WI 1131	30.00	24.90	3	52	10	45	Asthenozoospermia-	SPIB
41	WI 1133	32.97	23.50		110	10	40	Asthenozoospermia	SPIB
42	WI 1169	48.28	23.40	2.5	130	12	70	-	EEF1A2
43	WI 1211	39.74	24.20		0.5				EEF1A2
44	WI 1236	44.38	24.30		68	13	53		SPIB
45	WI 1315	33.54	17.30		19	8	67		SPIB
46	WI 1348	32.70	21.40		2	6	27.00		EEF1A2
47	WI 1396	41.10	29.90		19	4	26		SPIB
48	WI 1396	41.10	29.90		19	4	26		EEF1A2
49	WI 1458	42.54	23.40		45	10	13		SPIB
50	WI 1458	42.54	23.40		45	10	13		EEF1A2

Supplementary Table 6: Bull sperm samples

	Bull name	Age (years)		
1	Blomdahl	1.1	5.0	6.6
2	Bowers	1.1	3.1	5.4
3	Mowambo	1.2	5.3	7.3
4	Puki	1.1	3.8	7.0
5	X-man	1.3	2.8	4.9
6	Armor Red	1.5	3.5	4.2
7	Bahrain	1.3	5.1	5.8
8	Elwood	2.8	6.8	7.8
9	Mergim	0.7	9.4	10.9
10	Benstrup	1.0	-	7.0
11	Bengal	1.0	-	5.3
12	Emidio	-	4.9	7.3
13	Truman	-	-	7.7
14	Mavid	-	-	9.8
15	Stylist	-	-	12.3